COMMISSION ON POWDER DIFFRACTION

INTERNATIONAL UNION OF CRYSTALLOGRAPHY

http://www.mpi-stuttgart.mpg.de/cpd/index.html

NEWSLETTER No. 29, June 2003

http://www.mpi-stuttgart.mpg.de/cpd/html/newsletter.html

IN THIS ISSUE

Watching The Action

(Andy Fitch, Editor)

ISSN 1591-9552

CPD Chairman's Message

This issue of our newsletter is a special one. From the very beginning powder diffraction was regarded a sensitive method to follow phase transitions in polycrystalline material driven by PTX. The main drawbacks of the method were always the offsets between the (fast) action and the recording and the readout. The situation has drastically changed within the last few years opening challenging new fields for the method of powder diffraction. This newsletter can be considered a state of the art reference of *in situ* powder diffraction. Special thanks to Andy and all the contributing authors who put a lot of effort into this project. This reminds me that as an incentive for prospective authors it should be noted that we have an ISSN number (see bottom of the front page) and all papers in the CPD newsletter are quotable papers.

Some of you might already have noticed that I finally moved the CPD website to my home institution (see page 3). It has been slimmed down a bit to allow for better maintenance. Finally, **all** issues of the CPD newsletter are now available for download as PDF files. We are still in the process of correcting some of the OCR scanned pages but this task will be completed soon.

I apologize for the delay in sending out the previous newsletter but we are in a learning process how to keep costs low and how to handle printing, mailing, and customs. Since the largest expenses are due to mailing costs, I ask you please to report address changes to me in good time.

Robert Dinnebier

CPD projects

RIETVELD REFINEMENT OF ORGANIC STRUCTURES

Increasing numbers of organic crystal structures are being solved and refined from powder diffraction data. The basic arrangement of the molecules in the structure can often be determined by direct methods, or by direct-space approaches. However, experience shows that problems can arise in the subsequent Rietveld refinement. For example, unless restrained by appropriate bond distances and angles molecules can distort unrealistically from a reasonable molecular structure. So how good are these Rietveld refinements? Is the problem a fundamental one of powder diffraction? eg. the ambiguities and correlations caused by peak overlap or defining the background etc. lead to inaccurate structures. Or can some of the blame be attributed to poor refinement practice? We plan to put onto the CPD web site a number of good quality powder diffraction patterns from organic compounds of known crystal structure and of different complexity. These can be downloaded, and powder crystallographers can try out their own prowess at Rietveld refinement, by comparing their refined structures with the accepted single-crystal structures. This should be a learning exercise for us all. Any suggestions as to compounds that would appear particularly appropriate for this project are very welcome. Please contact the CPD chairman.

SIZE-STRAIN ROUND ROBIN

Results have been presented at international conferences (e.g. at IUCr in Geneva) and a paper has been submitted to Acta Cryst. A summary was given in CPD newsletter No. 28. A report is also on line at http://www.boulder.nist.gov/div853/balzar/.

From the Editor of Newsletter 29

Powder diffraction as a technique is particularly well suited to studying the behaviour of materials with changes in temperature, pressure, composition, or to follow the evolution of a system with time. For example, the method is often used to look at the structural phase transitions of a compound on heating or cooling, or to identify intermediate steps in the synthesis, dehydration or calcination of a material, maybe under conditions similar to those used in a large-scale industrial process. Such work has been carried out routinely using standard laboratory X-ray tubes and detectors. With the availability of intense synchrotron X-ray and neutron sources at central facilities, the time to measure a good quality diffraction pattern can be significantly reduced to even a few tens of milliseconds when exploiting multi-channel detectors with appropriate readout electronics. This means that fast physical or chemical processes can now be monitored in-situ. Neutrons and hard X-rays are highly penetrating, so can be used to look at bulk systems in complex sample environments. When following the structural changes that occur with temperature in a material, measurements can now be made at many temperatures, possibly at hundreds of temperatures, in a realistic period of time. Such experiments are revealing a wealth of new information about the detailed evolution of crystalline systems. This newsletter contains a number of articles describing some of the experimental approaches used, and giving clear ideas of the increased understanding that results. So why not join in the action as well?

Andy Fitch

WWW sites related to powder diffraction

The Commission on Powder Diffraction (CPD): http://www.mpi-stuttgart.mpg.de/cpd/index.html
The International Union of Crystallography (IUCr): http://www.iucr.org/
The International Centre for Diffraction Data (ICDD): http://www.icdd.com/
The International X-ray Analysis Society (IXAS): http://www.ixas.org/
CCP 14: http://www.ccp14.ac.uk/

Submitting a proposal for neutron diffraction or synchrotron radiation X-ray diffraction is possible at many (publicly funded) large scale facilities in the world. It represents an important and frequently unique opportunity for powder diffraction experiments. A useful guide and information can be accessed through the following web-site, maintained by R. Dinnebier at http://www.pulverdiffraktometrie.de/

This list is far from being complete and needs input from users and readers of the CPD Newsletter. Please send comments to *R. Dinnebier* (r.dinnebier@fkf.mpg.de)

THE IUCR COMMISSION ON POWDER DIFFRACTION - TRIENNIUM 2002-2005

Chairman: Dr R. E. Dinnebier (Robert)
Max-Planck-Institut für Festkörperforschung,
Heisenbergstrasse 1, D-70569 Stuttgart, Germany
Telephone: +49-711-689-1503 | Fax: +49-711-689-1502
e-mail: r.dinnebier@fkf.mpg.de

Secretary: Prof. A. N. Fitch (Andy)
ESRF, BP220, F-38043 Grenoble Cedex, France
Telephone : +33 476 88 25 32 | Fax: +33 476 88 25 42
e-mail: fitch@esrf.fr

Dr R. Delhez (Rob)
Laboratory of Materials Science, Delft University of Technology, Rotterdamseweg 137 2628 AL Delft, The Netherlands
Telephone: +31 15 2782261 | Fax: +31 (15) 278 6730
e-mail: R.Delhez@tnw.tudelft.nl

Prof. N. Masciocchi (Norberto)
Dipartimento di Scienze Chimiche, Fisiche e Matematiche,
Università dell'Insubria,
via Valleggio 11, 22100 Como (Italy)
Telephone: +39-031-326227 | Fax: +39-031-2386119
e-mail: norberto.masciocchi@mail.co.uninsubria.it

Dr C. R. Hubbard (Cam)
Diffraction and Thermophysical Properties Group, MS 6064, Bldg 4515, High Temperature Materials Laboratory, Metals & Ceramics Division, Oak Ridge National Laboratory, Oak Ridge, TN 37831-6064
Telephone: 865-574-4472 | Fax: 865-574-3940
e-mail: hubbardcr@ornl.gov

Dr D. Balzar (Davor)
Department of Physics & Astronomy
University of Denver
2112 E Wesley Ave, Denver, CO 80208-0202
Telephone: 303-871-2137 | Fax: 303-871-4405
e-mail: balzar@du.edu

Prof. G. J. Kruger (Gert)
Department of Chemistry & Biochemistry, Rand Afrikaans University, P O Box 524, Aucklandpark, South Africa
Telephone: +27 11 489 2368 | Fax: +27 11 489 2360
e-mail: gjk@na.rau.ac.za

Dr. I. Madsen (Ian)
CSIRO Minerals
Box 312, Clayton South 3169
Victoria, Australia
Telephone: +61 3 9545 8785 | Fax: +61 3 9562 8919
e-mail; Ian.Madsen@csiro.au

Prof. W. I. F. David (Bill)
Rutherford Appleton Laboratory (CCLRC), Chilton, Oxon. OX11 OQX, United Kingdom
Telephone: +44 1235 445179 | Fax: +44 1235 445383
e-mail: bill.david@rl.ac.uk

Prof. M. Delgado (Miguel)
Laboratorio de Cristalografía, Departamento de Química, Núcleo Universitario Dr. Pedro Rincón Gutiérrez, Sector La Hechicera. Edif. "A". Nivel Patio. Universidad de Los Andes, Mérida, Venezuela
Telephone: +58 274240-1372
e-mail: migueld@ula.ve

ICDD Representative
Prof. R. L. Snyder (Bob)
Department of Materials Science & Engineering, Georgia Institute of Technology, Columbus, 771 Ferst Dr. N.W., Atlanta, GA 30332-0245, USA;
Telephone: +1 (404) 894-2888 | Fax: +1 (404) 894-2888
e-mail: bob.snyder@mse.gatech.edu

Consultants
Prof. P. Scardi (Paolo)
Dipartimento di Ingegneria dei Materiali e Tecnologie Industriali, Università di Trento, 38050 Mesiano (TN), Italy;
Telephone: +39 0461 882417/67 | Fax: +39 (461) 881977
e-mail: Paolo.Scardi@ing.unitn.it

Dr F. Izumi (Fujio)
National Institute for Research in Inorganic Materials
1-1 Namiki, Tsukuba, Ibaraki 305-0044, Japan
Telephone: +81-298-51-3354 (ext. 511); FAX: +81-298-52-7449
e-mail: izumi@nirim.go.jp


XRD
Counts (x10000)
Quantitative Results
Rietveld Quantification Results
Done

YOUR PARTNER IN X-RAY DIFFRACTION

STOE

STOE STADI P

Powder diffractometer

STOE & Cie GmbH   P.O.Box 101302   D-64213 Darmstadt
Phone: (+49) 6151 / 98870 Fax: (+49) 6151 / 988788
E-mail: stoe@stoe.com Homepage: http://www.stoe.com

- Pure Kα_1 radiation using Fe, Co, Cu or Mo radiation
- High resolution yielding well-defined peak profiles
- Transmission / Debye-Scherrer or Bragg-Brentano mode
- Analysis of air-, moisture-sensitive and micro samples
- Enclosing control and evaluation software package WinX^{POW}
- Various high- and low-temperature systems and sample changers
- Scintillation counter, position sensitive and imaging plate detectors
- High throughput and combinatorial analysis

Crystal Structure Visualization

Diamond is an application for the exploration and drawing of crystal structures. With its high data capacity, its wide range of functions beginning with the generation of molecules reaching up to the construction of rather complicated inorganic structural frameworks, *Diamond* is the tool for molecular and solid state chemists as well as for surface and material scientists.

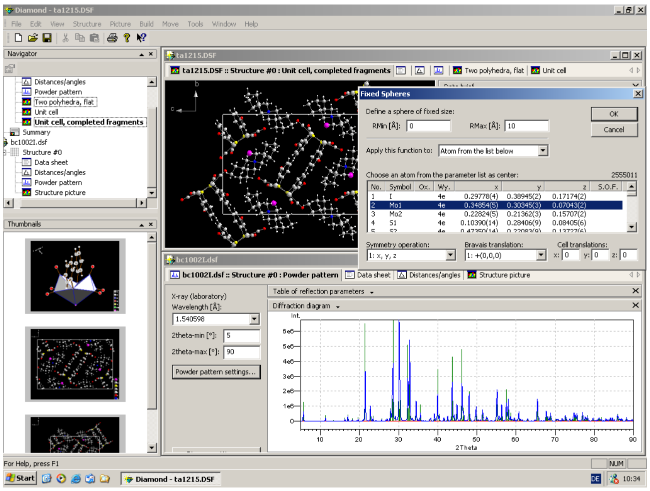

Define a sphere of fixed size:
RMin [Å]: 0   RMax [Å]: 10
Apply this function to: Atom from the list below
Choose an atom from the parameter list as center: 2555011

No.	Symbol	Ox.	Wy.	x	y	z	S.O.F.
1	I		4e	0.29778(4)	0.38945(2)	0.17174(2)	
2	Mo1		4e	0.34854(5)	0.30345(3)	0.07043(2)	
3	Mo2		4e	0.22824(5)	0.21362(3)	0.15707(2)	
4	S1		4e	0.10390(14)	0.28406(9)	0.08405(6)	

Symmetry operation: 1: x, y, z
Bravais translation: 1: +(0,0,0)
Cell translations: x: 0 y: 0 z: 0

X-ray (laboratory)
Wavelength [Å]: 1.540598
2theta-min [°]: 5
2theta-max [°]: 90

CRYSTAL IMPACT GbR
Postfach 1251
D-53002 Bonn
Germany

Tel.: +49 (228) 981 36 43
Fax: +49 (228) 981 36 44
E-mail: info@crystalimpact.com
http://www.crystalimpact.com

Phase Identification from Powder

Match! is an easy-to-use software for phase identification from X-ray powder diffraction data. Using an elaborate algorithm, it compares the user's diffraction pattern to the patterns stored in the ICDD PDF database in order to identify the phases which are present in the user's sample. Single as well as multiple phases can be identified based on both peak data and raw (profile) data (if present).
***Match!* will become available in 3rd quarter 2003.**

Structure Solution from Powder

Endeavour uses an innovative concept: a combined global optimization of the difference between the calculated and measured diffraction pattern and of the potential energy of the system.
Since *Endeavour* is based upon the experienced Diamond visualization technology, the user can watch the crystal structure evolving from a completely random arrangement of atoms to the final model during the structure solution process.

Free-of-charge demonstration versions are available for download from our webpage.

CRYSTAL IMPACT

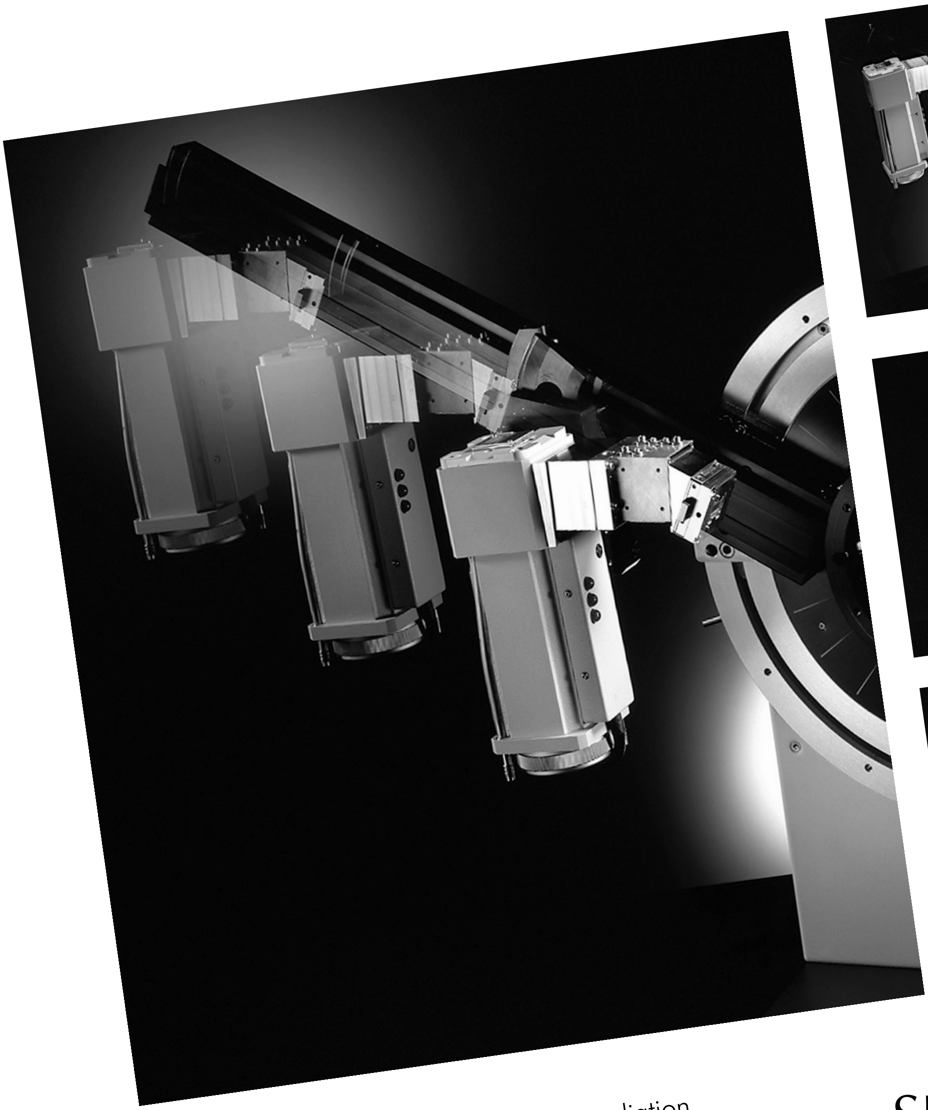

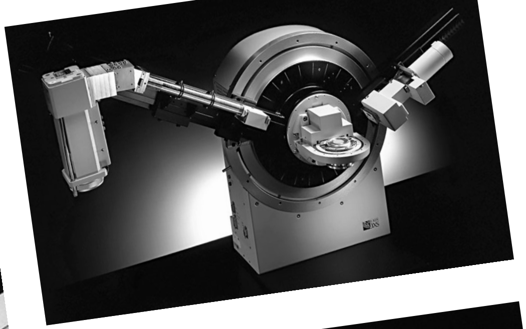

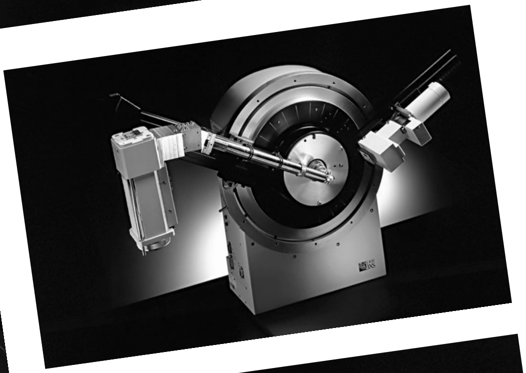

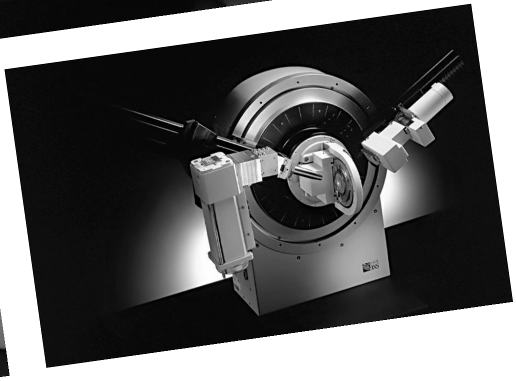

Rietveld Refinement Using Time Resolved Synchrotron X-ray Powder Diffraction Data to Study Transformations in Zeolites

John B. Parise[1,2] ***, Yongjae Lee***[3]***, Jonathan C. Hanson***[4]***, Thomas Vogt***[3] ***and Joseph A. Hriljac***[5]
[1]Geosciences, [2]Chemistry, State University of New York, Stony Brook NY 11794-2100, USA; Department of [3]Physics, [4]Chemistry, Brookhaven National Laboratory, Upton NY 11973, USA; [5]Department of Chemistry, University of Birmingham, Birmingham, B15 2TT, UK.
John.Parise@sunysb.edu, *yollee@bnl.gov*

Introduction

Phases stable under particular conditions of pressure-temperature-composition-time (PTXt), and their physical properties under these conditions, are often best studied using time resolved diffraction. Often these transformations either destroy single crystals or occur in technologically important materials that crystallize as sub-micron "single" crystals. Although quench experiments provide samples more easily studied at ambient conditions, data collected *in situ* are required when structural states such as cation ordering are not quenchable from the PTX conditions of interest. This is particularly the case for zeolitic materials. These open networks, exemplified by the 4- connected aluminosilicate frameworks, transform readily upon changing pressure, temperature, hydration-state and the type of ion-exchangeable cation occupying cavities of molecular dimension within the crystal structure. Indeed most processes, including the synthesis of the native material, hydration-dehydration and ion-exchange, involve induction periods and/or are kinetically hindered. Time resolved studies reveal much about the mechanism of transformation.

The quality of data required depends on the information being sought. The optimization of synthetic conditions only requires identification of the phases, the PTX conditions over which they are stable [1,2] and many of these can be carried out in the laboratory setting, particularly since the more widespread availability of area detectors. Powder diffraction data suitable for Rietveld refinement require 1) access to brighter X-ray beams at 2nd.- and 3rd.-generation synchrotron storage rings and 2) versatile high pressure [3,4] and hydrothermal cells [5,6].

Structural models of zeolites in their various cation-exchanged forms, in their dehydrated and hydrated states, and with and without sorbents, are important to rationalizing their mode of operation. Monitoring these structural changes *in situ* and as a function of time allows the mechanism of transformation to be followed.

Experimental techniques

This short article will concentrate on studies close to ambient pressure. Devices suitable for studies at high pressure and high temperatures are described elsewhere [7-9] and have been used for some important time resolved studies of martensitic and pseudo-martensitic transformations [8]. For studies at ambient temperature and high pressures, the DAC (diamond anvil cell) is most commonly used.

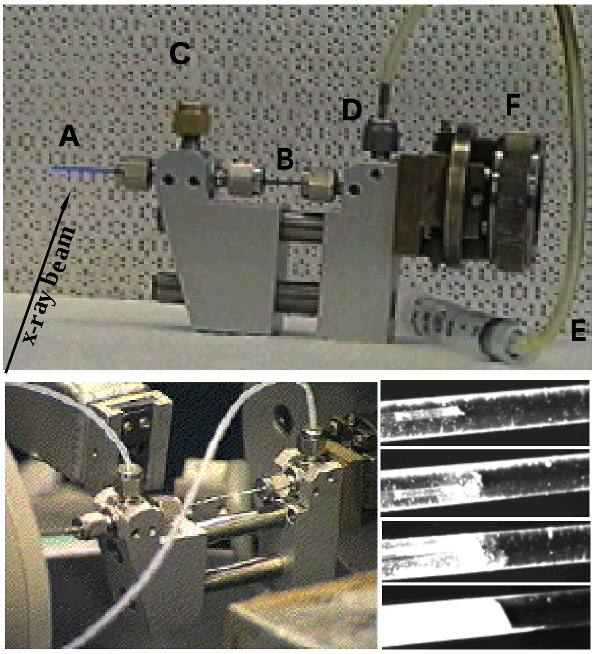

Figure 1. *Photographs (top) of a Small Environmental Cell for Real Time Studies (SECReTS) [10] and (left) installed at beamline X7A, NSLS. Positions at A and B allow X-ray access, and fluids (or vacuum for dehydration studies) are introduced through injection and exhaust ports C and D. The fitting F allows attachment to diffractometers and an air- or resistive heater directed at A or B allow studies to 250°C or 1000°C, respectively. The scenario (right) details injection capabilities. A saturated solution of* Na_2SO_4 *heated to 60°C and a saturated solution of* $BaCl_2$ *injected through a second capillary,* $\Phi = 0.2$ *mm to precipitate* $BaSO_4$ *while scattering is simultaneously recorded [10].*

For powder diffraction studies of materials transforming under hydrothermal conditions a number of cells are described in the literature [2,5,10-17] and one example is shown in Figure 1. Safety issues limit operating conditions to below the critical point of water (22 MPa, 374°C) or below that for the solvent being used in solvothermal reaction. They are used in time resolved studies employing achromatic or monochromatic sources, the choice predicated upon the goal of the experiment.

If time resolution is a priority, energy dispersive studies using a solid-state detector at a fixed angle offer a number of advantages, including simplicity of experimental design and excellent collimation. This scheme was used in conjunction with the ability to inject into hydrothermal systems [2,10] to study the precipitation and transformation of FeS to FeS_2 (pyrite). Several phases crystallize over a 1 – 60 minute period and the contention that, in the absence of oxygen, the transformation does not take place was tested. Previous quench studies were ambiguous on this point, chiefly because sampling of the reaction potentially contaminated the sample with oxygen. Introduction of even small amounts of oxygen causes the transformation to pyrite to begin. In situ studies with both ED and monochromatic diffraction from reacting samples demonstrate conclusively pyrite forms only in the presence of oxygen [2].

For the study of structure at atomic resolution, bright, energetic monochromatic beams (E > 12 keV) and fast area detectors enable high quality diffraction patterns to be acquired in a short period of time. Integration of the two-dimensional diffraction pattern provides data with reasonable signal-to-noise discrimination at data rates rivaling those attainable using energy dispersive techniques. These data are also suitable for Rietveld structural refinement.

Applications to ion exchange

The ion exchange properties of zeolites were amongst the first recognized and utilized [18]. They are the basis of detergent industry and are important for the clean-up of radioactive waste as well as a number of other agricultural and industrial applications. While quench studies are useful for determining the composition of sites occupied/replaced during ion exchange, *in situ* time-resolved work can provide information on the pathway taken. Many zeolites exchange ions at multiple sites and at different rates. Depending on the steric constraints of a particular site, exchange might be inhibited until a phase changes allows access. The pathway and the changes in framework geometry accompanying these are best addressed by following the process at the atomistic level. Ion exchange into faujasite and gismondine are excellent examples of structural exchange induced by ion exchange. The Faujasite (FAU) framework (Figure 2) contains a number of sites, some readily accessed through the large cage (eg II) and others accessible only after the exchanging cation negotiates the small entrance of the 6-ring window of the sodalite unit (I and I').

One example of these site-specific replacements and related phase transitions is the structural investigations of potassium-exchange mechanism in sodium-form of low-silica X (LSX) [19,20]. Compared to X and Y analogues (Figure 2), LSX exhibits enhanced ion exchange capacity due to the maximum Al content in the framework. Prior to time resolved studies *ex situ* synchrotron X-ray powder diffraction of Na- and K-end members of LSX as well as for the samples exchanged at the 20%, 42% and 80% K^+ levels were undertaken [21] These provided reasonable constraints on framework and extraframework cation positions in the subsequent refinements using the lower resolution time-resolved data. *In situ* synchrotron X-ray powder diffraction data (Figure 3) were collected using the SECReTS cell (Figure 1) at the beamline X7B of the NSLS. The detailed pathway of the site-specific ion exchange in LSX (Figure 4) was determined from these data [19] which were collected using a combination of IP and CCD, the later providing enhanced time-resolution.

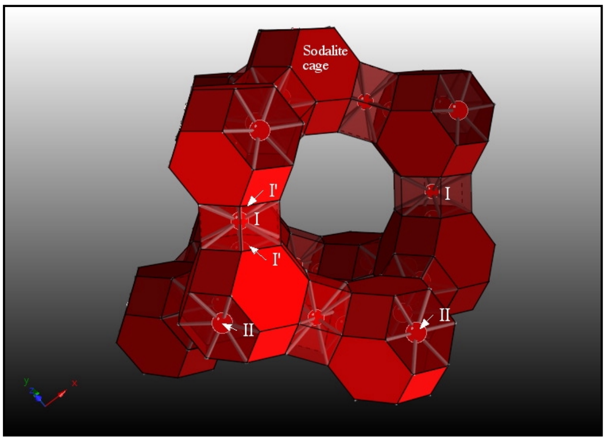

Figure 2. *Polyhedral representation of the Faujasite (FAU) framework Nodes represent T-sites (Al,Si) tetrahedrally coordinated to oxygen, which lies at the approximate mid-point of the straight lines. A pure silica framework would have unit cell contents* $Si_{192}O_{384}$. *Charge imbalance introduced when* Al^{3+} *substitutes for* Si^{4+} *implies cations are accommodated at sites extra to the framework close to 4-rings (III') and 6-rings (II) facing the large (super) cage, and at 6-rings within the smaller sodalite cage. These latter sites can only be accessed from the super cage through site II and lie close to the single 6-ring (I') or close to the center of a double 6-ring (I) column. Variations in the framework chemistry include low and high silica forms X and Y, respectively.*

The mechanism revealed by these early studies has since been confirmed in the Sr-K exchange in LSX and for various ion exchange couples in the GIS system [22]. The initial stage of the exchange in K-Na-LSX involves replacement at the most easily accessible wall sites [19]. Exchange at the various sites (Figure 2) can be monitored from Rietveld refinement along with geometric changes in the framework. These reveal (Figure 3) that replacement at the least accessible site I proceeds only after significant replacement at all other sites, and after the 6-ring access to the site has undergone considerable distortion as K-replaces Na at site I' (Figure 2). Na → K exchange also proceeds through a two-phase region in agreement with the result of the K → Na study. Strontium exchanges sodium via a narrow miscibility gap whereas a single phase is maintained throughout the course of Sr → K exchange. Changes in occupancy at each site suggest that ion exchange in LSX is cation-dependent as well as site-specific, a result that would have been difficult to obtain with static measurements alone [20].

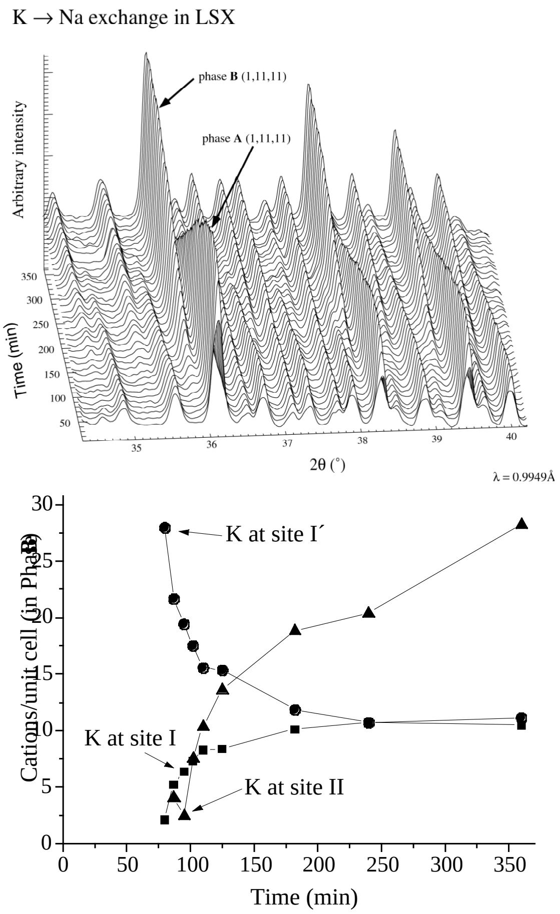

Figure 3. *(top) Synchrotron X-ray powder diffraction profiles as a function of time during the 6h of K-exchange into Na-LSX showing the cell collapse accompanying occupation of site I by potassium. (bottom) Variations of cation distribution during K-exchange into Na-LSX derived from Rietveld analyses using the in situ data and starting models from the ex situ study.*

In situ dehydration and re-hydration

Zeolite RHO, $(Cs, Na)_{12}Al_{12}Si_{36}O_{96}.nH_2O$; n ~ 48) is an exceptionally flexibible framework. Depending on composition (hydration state, type of exchangeable cation) T and P it adopts the centric (Im-3m) or acentric (I-43m) cubic structure above and below ~ 14.9 Å, respectively (Figure 4) [23]. For example in Cd-rho Cd^{2+} cations relocate from a D8R-site, blocking access to the α-cages, to the S6R-site, allowing access to the pores of RHO upon heating in a "trap door" mechanism [24]. The relocation was attributed to temperature-driven phase transitions but time-resolved *in situ* synchrotron X-ray powder diffraction experiments, performed using Pb-rho and Cd-rho, suggest that the phenomena result from chemical changes occurring during dehydration and re-hydration [24].

In situ synchrotron X-ray powder diffraction data indicate that water plays an important role in the greater than 5 Å "trap door" motion of Cd^{2+} in Cd-rho [25] and a number of other ion-excahnged forms of this zeolite. Upon heating in either air (Figures 5 and 6a) or in vacuum (Figure 6b), there is an initial decrease in cell parameter from 25°C to 75°C due to the loss of unbound water. A more gradual change in cell parameter is observed between 75°C and 450°C. A large increase in the cell parameter, which Rietveld refinement reveals is accompanied by a change from

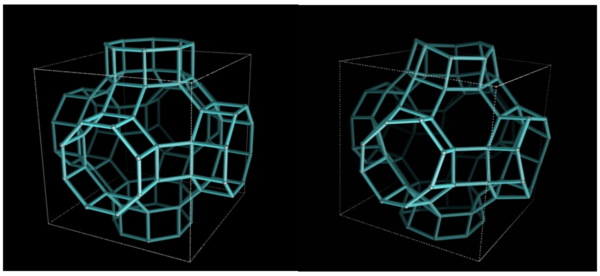

Figure 4. *RHO topology (see Figure 1) with α-cages linked via double 8-rings (D8R) which accommodate charge balancing, extra-framework cations along with sites at the single 8-ring (S8R) and single 6-ring (S6R). The framework can adopt a centric (C-form, Im-3m and acentric A-form, I-43m) forms shown at left and right, respectively.*

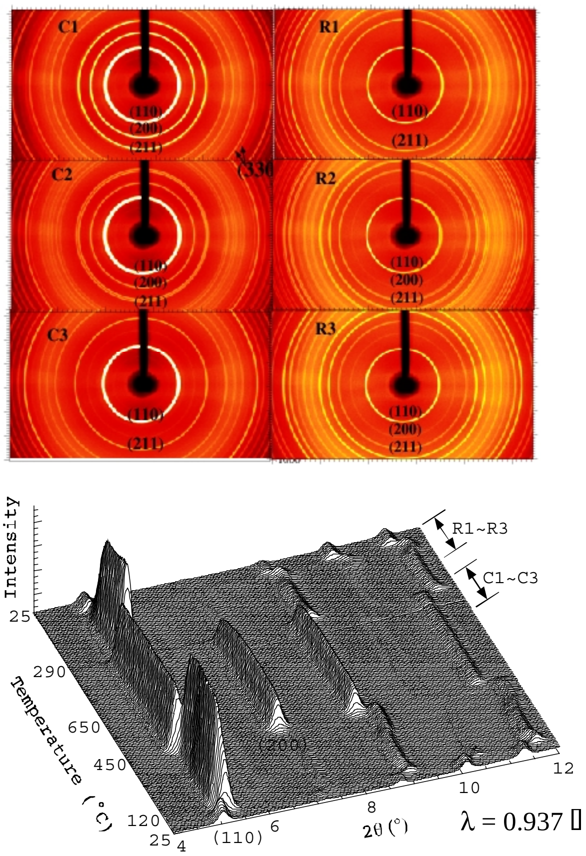

Figure 5 *Time-resolved XPD patterns typical of those collected on an IP detector (top) for Cd-rho, heated and cooled under atmosphere. See Figure 6 for cell parameter variations and derived extraframework cation positions as a function of temperature. The 1-D patterns (bottom) integrated using the Fit2D software of Hammersley [26,27], clearly show a number of phase transitions.*

the acentric to centric structure and a relocation of Cd^{2+} from the S8R site to the S6R site, takes place at higher temperatures. There is a marked difference in the behavior of Cd-rho between cooling in air and vacuum (Figure 6). With the exception of a small temperature hysteresis, the reaction pathway is directly reversed upon cooling in air, while these changes do *not* occur upon cooling under vacuum. These observations suggest that water may play a significant role in the relocation of cations from the S6R back to the S8R. Experiments in which rho is cooled over other gases such as N_2 and Kr did not cause the Cd to relocate from the S6R-site in the high temperature form. It is likely that water acts as a transport agent in the original cation relocation from the S8R to the S6R site [24]

(a) Cd-rho under atmosphere

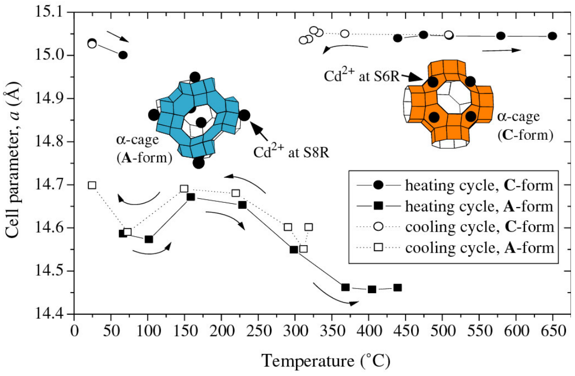

(b) Cd-rho under vacuum

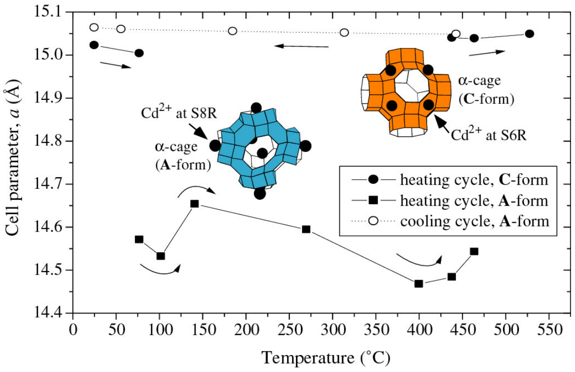

Figure 6. *Changes in cubic cell constant (Å) for (a) Cd-rho, heated under atmosphere, and (b) Cd-rho, heated under vacuum analyzed using in-situ synchrotron X-ray powder diffraction data. Polyhedral representations illustrate the cation distribution in the α-cage of RHO determined from Rietveld refinement.*

Conclusions

Phase transitions driven by PTX can now be studied routinely as a function of t using synchrotron sources. In the future combinations of variables, high pressure and low temperature for example, will allow new phenomena to be explored in microporous (zeolites) and in solid-state materials in general. We have not been exhaustive but rather attempted to offer a flavor of what is possible with one class of materials. Other problems worthy of study were excluded, for example the range of earth and planetary materials occupying the pressure regimes from vacuum to TPa. For zeolites *in situ* studies concentrating on the atomic scale mechanisms, derived from Rietveld refinement, are helping to address some larger questions. These include the incipient stages of crystallization, the response of the framework to environmental variables and how these affect selectivity and reactivity.

Acknowledgements

This work was supported by the National Science Foundation through grant NSF-DMR 0095633. This work made use of beamlines X7A and X7B at the NSLS; these facilities are supported by the U.S. Department of Energy, office of Energy Sciences, Division of Materials Sciences (X7A) and Division of Chemical Sciences (X7B) under contract DE-Ac02-98CH10886.

References

[1] Cahill, C. L.; Parise, J. B. (2000) On the formation of framework indium sulfides, Dalton Trans. **9**, 1475-1482.

[2] Cahill, C. L.; Benning, L. G.; Barnes, H. L.; Parise, J. B. (2000) *In situ*, time-resolved X-ray diffraction of iron sulfides during hydrothermal pyrite growth, Chem. Geol. **167**, 53-63.

[3] Chen, J. H.; Kikegawa, T.; Shimomura, O.; Iwasaki, H. (1997) Application of an imaging plate to the large-volume press MAX80 at the photon factory, J. Synchrot. Radiat. **4**, 21-27.

[4] Shimomura, O.; Yamaoka, S.; Yagi, T.; Wakatsuki, M.; Tsuji, K.; Kawamura, H.; Hamaya, N.; Aoki, K.; Akimoto, S. In *Solid State Physics Under Pressure: Recent Advances with Anvil Devices*; Minomura, S., Ed.; KTK Sci. Pub.: Tokyo, 1985, pp 351-356.

[5] Parise, J. B.; Tan, K.; Norby, P.; Ko, Y.; Cahill, C. In *MRS Proceedings "Solid state chemistry of inorganic materials"*; Davies, P., Jackobson, A., Toradri, C. T., Vanderah, T., Eds.: Boston Fall meeting, 1997; Vol. 453, pp 103-114.

[6] Schoonen, M. A. A.; Barnes, H. L. (1991) Mechanisms of pyrite and marcasite formation from solution:I. Nucleation of FeS_2 below 100^{o}C, Geochimica Cosmochimica Acta **55**, 1495-1504.

[7] Chen, J.; Weidner, D. J.; Vaughan, M. T.; Li, R.; Parise, J. B.; Koleda, C.; Baldwin, K. J. (1998) Time resolved diffraction measurements with an imaging plate at high pressure and temperature, Rev. High Press. Sci. Technol. **7**, 272-274.

[8] Chen, J. H.; Weidner, D. J.; Parise, J. B.; Vaughan, M. T.; Raterron, P. (2001) Observation of cation reordering during the olivine-spinel transition in fayalite by in situ synchrotron x-ray diffraction at high pressure and temperature, Phys. Rev. Lett. **86**, 4072-4075.

[9] Parise, J. B.; Chen, J. (1997) Studies of crystalline solids at high pressure and temperature using the DIA multi-anvil apparatus, Eur. J. Sol. St. Inorg. Chem **34**, 809-821.

[10] Norby, P.; Cahill, C.; Koleda, C.; Parise, J. B. (1998) A reaction cell for in situ studies of hydrothermal titration, J. Appl. Crystallogr. **31**, 481-483.

[11] Evans, J. S. O.; Francis, R. J.; O'Hare, D.; Price, S. J.; Clark, S. M.; Gordon, J.; Neild, A.; Tang, C. C. (1994) An apparatus for the study of the Kinetics and Mechanism of Hydrothermal Reactons by in situ Energy dispersive X-ray diffraction, Rev. Sci. Inst **66**, 2442-2445.

[12] Francis, R. J.; O'Brien, S.; Fogg, A. M.; Halasyamani, P. S.; O'Hare, D.; Loiseau, T.; Ferey, G. (1999) Time-resolved in-situ energy and angular dispersive X-ray diffraction studies of the formation of the microporous gallophosphate ULM-5 under hydrothermal conditions, J. Am. Chem. Soc. **121**, 1002-1015.

[13] Jensen, T. R.; Norby, P.; Hanson, J. C.; Simonsen, O.; Skou, E. M.; Stein, P. C.; Boye, H. A. (1998) Hydrothermal synthesis and crystal structure of alpha-$LiZnAsO_4$, J. Mater. Chem. **8**, 969-975.

[14] Norby, P.; Hanson, J. C.; Fitch, A. N.; Vaughan, G.; Flaks, L.; Gualtieri, A. (2000) Formation of alpha-eucryptite, $LiAlSiO_4$: An in-situ synchrotron X-ray powder diffraction study of a high temperature hydrothermal synthesis, Chem. Mat. **12**, 1473-1479.

[15] O'Hare, D.; Evans, J. S. O.; Francis, R. J.; Halasyamani, P. S.; Norby, P.; Hanson, J. (1998) Time-resolved, in situ X-ray diffraction studies of the hydrothermal syntheses of microporous materials, Microporous Mesoporous Mat. **21**, 253-262.

[16] O'Hare, D.; Evans, J. S. O.; Francis, R.; Price, S.; O'Brien, S. (1998) The use of in-situ powder diffraction in the study of intercalation and hydrothermal reaction kinetics, Materials Science Forum **278-2**, 367-378.

[17] Schoonen, M. A. A.; Barnes, H. L. (1991) Mechanisms of pyrite and marcasite formation from solution: III. Hydrothermal processes, Geochem. Cosmochem. Acta **55**, 3491-3504.

[18] Breck, D. W. (1984) *Zeolite Molecular Sieves*; Krieger: Malabar,FL

[19] Lee, Y.; Cahill, C. L.; Hanson, J. C.; Parise, J. B.; Carr, S. W.; Myrick, M. L.; Preckwinkel, U. W.; Phillips, J. C. In *Proceedings of the 12th International Zeolite Conference*; Treacy, M. M. J., Marcus, B. K., Bisher, M. E., Higgins, J. B., Eds.; Materials Research Society: Baltimore, Maryland, USA, 1998; Vol. 4, p 2401.

[20] Parise, J. B.; Cahill, C. L.; Lee, Y. J. (2000) Dynamic powder crystallography with synchrotron X-ray sources, Can. Mineral. **38**, 777-800.

[21] Lee, Y. J.; Carr, S. W.; Parise, J. B. (1998) Phase transition upon K^+ ion exchange into Na low silica X: Combined NMR and synchrotron X-ray powder diffraction study, Chem. Mat. **10**, 2561-2570.

[22] Tripathi, A.; Parise, J. B.; Kim, S.-J.; Lee, Y.; Johnson, G. M.; Uh, Y.-S. (2000) Structural changes and cation site ordering in Na- and K-form of aluminogermanates with the zeolite GIS topology, Chem. Mater. **12**, 3760-3769.

[23] Corbin, D. R.; Abrams, L.; Jones, G. A.; Eddy, M. M.; Harrison, W. T. A.; Stucky, G. D.; Cox, D. E. (1990) Flexibility of zeolite RHO framework. In-situ X-ray and neutron powder structural characterization of divalent cation-exchanged zeolite RHO, J. Am. Chem. Soc. **112**, 4821-4830.

[24] Reisner, B. A.; Lee, Y.; Hanson, J. C.; Jones, G. A.; Parise, J. B.; Corbin, D. R.; Toby, B. H.; Freitag, A.; Larese, J. Z.; Kahlenberg, V. (2000) Understanding negative thermal expansion and 'trap door' cation relocations in zeolite rho, Chem. Commun., 2221-2222.

[25] Parise, J. B.; Corbin, D. R.; Abrams, L. (1995) Structural changes upon sorption and desorption of Xe from Cd-exchanged zeolite rho: a real-time synchrotron x-ray powder diffraction study, Microporous Mater. **4**, 99-110.

[26] Hammersley, A. P. "FIT2D: V9.129 Reference Manual V3.1," 1998.

[27] Hammersley, A. P.; Svensson, S. O.; Hanfland, M.; Fitch, A. N.; Hausermann, D. (1996) Two-dimensional detector software: From real detector to idealised image or two-theta scan, High Pressure Res. **14**, 235-248.

Beyond Rietveld Refinement – Non Crystallographic Information from Powder Diffraction

J.S.O. Evans and S. Allen
Department of Chemistry, University of Durham,
South Road, Durham, DH1 3LE, UK.
john.evans@durham.ac.uk

Over recent decades powder diffraction has evolved from a technique used to gain relatively crude analytical information into one of the most powerful tools available to solid state chemists, condensed matter physicists and materials scientists. Quantitative phase analysis, microstructural information, detailed structural studies from Rietveld refinement and ab-initio structure solution procedures are now routinely performed in many laboratories around the world and provide key insight into the properties of materials. With increases in X-ray and neutron fluxes at central facilities and huge improvements in detector technologies, data quality in terms of signal to noise, q-range and resolution from such experiments has improved dramatically, allowing increasingly complex problems to be tackled.

In addition to tackling increasing complexity, these instrument improvements can be exploited in an alternative way: by accepting data of slightly lower quality one can obtain individual diffraction data sets extremely quickly. This allows one to perform not just single diffraction experiments but experiments as a function of time, temperature, pressure, magnetic field, composition, or a variety of other external perturbations to a system. By following the evolution of diffraction data as a function of such perturbations, considerable extra information on a material's properties can often be obtained. In this short article we will highlight examples from our work in which variable temperature diffraction data have been used to give not only "crystallographic" information about the evolution of structural coordinates as a function of temperature, but "non-crystallographic" additional information such as the energy and magnitude of atomic vibrations in the solid state, information on order-disorder phase transitions, and information on activation energies for ionic migration. The examples selected are naturally biased by our own interests, but will hopefully be illustrative of the general methodology of "parametric diffraction" in which multiple data sets are collected and treated as an ensemble of evolving information. There are, of course, many other examples of diffraction=f(x) in the literature from other workers, as well as elegant examples of chemical reactions being followed in real time. We will not attempt to cover these in this article.

Why perform parametric diffraction studies? Consider the common scenario facing a researcher: one has been allocated a day at a central facility to study a powdered material as a function of temperature – what temperature points should be selected and how long should one collect at each temperature? Such a question is extremely hard to answer until the experiment has been performed!

We were faced with this dilemma when studying ZrW_2O_8, a material that displays isotropic negative thermal expansion (NTE), using the High Resolution Powder Diffractometer (HRPD) at the ISIS facility of the Rutherford Appleton Laboratory.[1,2] On this instrument a "normal" data collection time for Rietveld-quality data might be 3-4 hours. We decided to take an extreme approach in our experiment and collect diffraction data in 5 minute time slices. This allowed us to collect variable temperature data sets in 2 K intervals at 260 experimental temperatures in a little over 24 hours of measurement time. The data from this experiment proved to contain a wealth of crystallographic and non-crystallographic information.

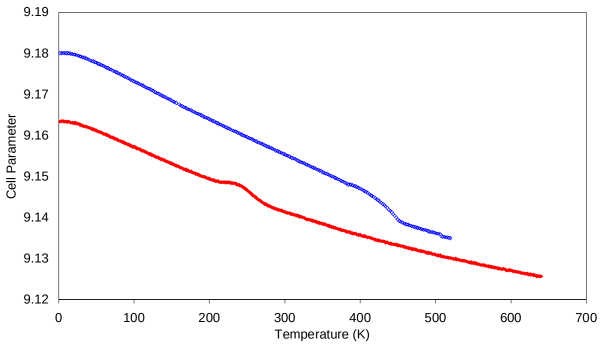

Figure 1. *Unit cell parameters of ZrW_2O_8 (upper curve) and $ZrWMoO_8$ (lower curve) from 5 min. neutron powder diffraction experiments recorded in 2 K steps. Error bars are smaller than the plotted points.*

From an initial round of Rietveld refinements it was clear that many of the parameters refined evolved smoothly with temperature (a background coefficient, for example, at T K being closely related to its value at T ± 2 K). This means that many parameters in the refinements could be modelled as smoothly-evolving functions, thus reducing the effective number of parameters refined at each temperature. Figure 1 shows perhaps the most important result of the study – the unit cell parameter as a function of temperature. The material shows continual contraction from 2 K to 520 K. Thanks to the extremely high precision of the cell parameter determination (a = 9.18000(3) Å at 2 K), if one assumes a simple model for the heat capacity one can use cell parameter data to extract information on the Einstein or Debye temperature of the material, useful information about the energy scale of the vibrational modes responsible for NTE. From the contributions required to describe a(T) fully, a crude picture of the vibrational density of states emerges.

There is, however, no need to make the a priori assumptions regarding the phonon density of states which are implicit in these simple models for the heat capacity of a material. Since it is the population of phonons of different energies, each of which has an intrinsic tendency to expand or contract the lattice (expressed via a mode Gruneisen parameter), that cause thermal expansion, it follows that the expansion data themselves must contain direct information about these modes. Figure 2 follows this line of thinking and shows a maximum entropy reconstruction of the Gruneisen-parameter-weighted phonon density of states derived directly from the unit cell parameter of Figure 1. From this curve one can see that the modes responsible for NTE have an energy of ~5 meV (40 cm^{-1}). There are higher energy modes (~73 meV, 590 cm^{-1}) which tend to expand the lattice. This unusual information on the energy scale of vibrational modes is obtained directly from powder diffraction data.

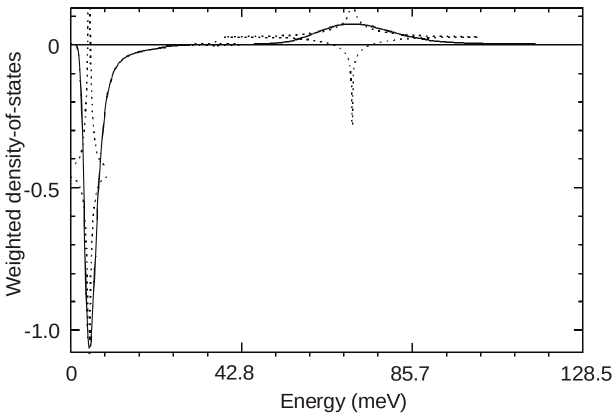

Figure 2. *Gruneisen-parameter-weighted phonon density of states derived from cell parameter data of Figure 1.*

Since a full Rietveld refinement was performed for each of the 260 data sets in Figure 1, the temperature evolution of structural parameters can also be followed. In fact, by treating the evolving data sets as an ensemble, fractional coordinates at any temperature can be determined to similar precision to performing traditional "long" data collections at that temperature. Detailed information about bond distances and angles is therefore retained during this data collection method. Figure 3a shows one set of derived parameters - anisotropic displacement parameters of one oxygen atom as a function of temperature. These give insight into the magnitude of the atomic vibrations responsible for contraction. Again, despite the rapid data collection times, useful information about structural parameters can clearly be obtained.

Figure 3b shows the fractional occupancy of a second oxygen site in the material as a function of temperature. As the material is warmed to around 450 K an order-disorder transition occurs and the atom becomes dynamically disordered over two possible lattice sites. This disordering can again be followed by parametric Rietveld refinement and the order parameter can be related to simple models. By using rapid data collection times, there is a wealth of different information available from a 24 hour experiment!

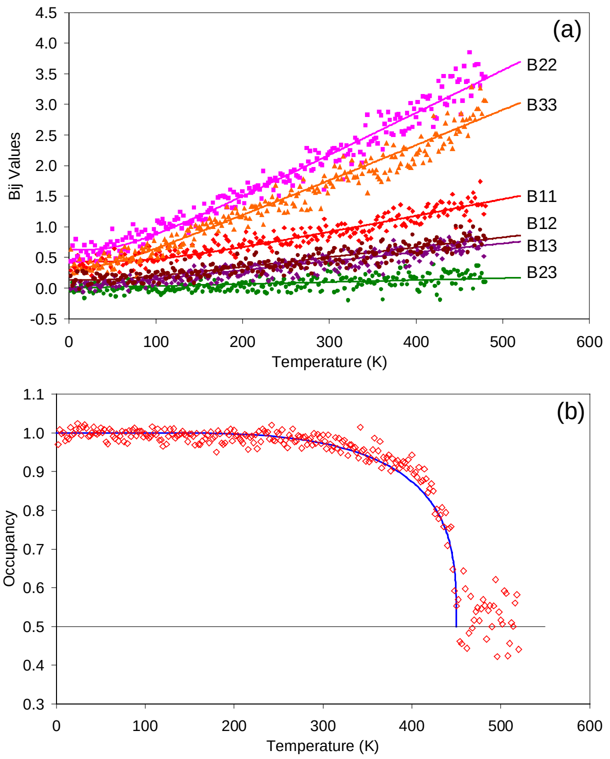

Figure 3. *ADP's of one O site and fractional occupancy of another as a function of temperature from 5 minute data collections on ZrW_2O_8. The solid lines in (a) are a fit to a simple Einstein model and in (b) to a 3D Ising model for the order-disorder transition.*

Figure 1 also shows the temperature evolution of the unit cell parameter of a related material, $ZrWMoO_8$, as a function of temperature.[3] A similar experiment was performed to that described above in which a sample of $ZrWMoO_8$ was cooled rapidly to 2 K and data collected in 6 minute time slices as the sample was warmed. Again NTE is seen from very low temperatures, as had been anticipated for the material. However, in this case an unusual "hump" was observed in the cell parameter from around 200 K; by ~300 K evidence of this hump had disappeared. It's worth noting that in a "traditional" data collection strategy, where one collected data in 30-50 K intervals, this hump could be missed entirely, or might be ignored as "one rogue point". Using parametric methods its presence cannot be missed.

Subsequent experiments showed that the origin of this hump was again the oxygen order-disorder process described above for ZrW_2O_8. In $ZrWMoO_8$, one oxygen is dynamically disordered over two sites at room temperature and only orders below ~270 K. In the experiment of Figure 1 we had inadvertently quenched the high temperature disordered form on rapidly cooling the sample. During the data collections, which were performed on warming, the material gained sufficient thermal energy for the oxygen ions to start to order. However the rapid rate of data collection meant that the material had insufficient time to order fully at any given temperature before it had been warmed further, leading to the "hump" in the cell parameter. In this type of experiment one is essentially collecting diffraction data as a function of both time and temperature and performing a kinetic study. By making various approximations about the processes involved it is actually possible to extract an estimate of the activation energy for the oxygen ion migration directly from the temperature/time dependence of the cell parameter. It is also important to note that parametric studies give conclusive evidence for oxygen migration in these materials at around 200 K – an extremely low temperature for ionic migration in the solid state.

Rapid data collections, and the wealth of information obtainable from them, are not restricted to experiments at central facilities. In the case of $ZrWMoO_8$ we have performed variable temperature/time X-ray diffraction experiments at our home laboratory to further characterise the oxygen migration. Using a Bruker d8 diffractometer equipped with a Ge(111) incident beam monochromator, an mBraun linear psd and an Anton-Paar TTK450 cryofurnace we have been able to further study the kinetics of this process in a number of ways. In one set of experiments (quench/hold experiments) we have quenched the material from 473 K (where it is fully disordered) to a series of temperatures between 200 and 250 K and monitored the evolution of diffraction peaks as a function of time (Figure 4a). From the temperature dependence of the extracted rate constants one can estimate an activation energy for the migration process.

Kinetic information can also be extracted from temperature/time experiments similar to those producing the "hump" in Figure 1 (quench/warm experiments). In a single series of experiments we have quenched the sample to low temperature and collected diffraction data as the material is warmed at a steady rate to high temperature and then slow-cooled back to low temperature. Figure 4b shows the Rietveld-refined

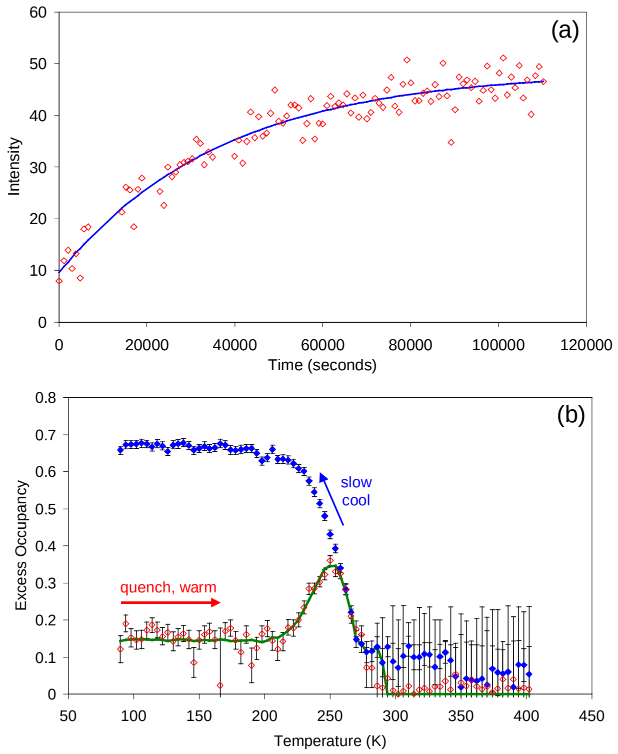

Figure 4. *(a) summed intensity of (111), (221), (301) and (401) reflections as a function of time extracted from 13 minute scans of a quenched sample of $ZrWMoO_8$. (b) excess occupancy of a lattice site derived from Rietveld refinement of a quenched sample of $ZrWMoO_8$ heated at 15 K/hr to 400 K then cooled at 19 K/hr. The solid line in (b) is a fit of excess occupancy to a simple cumulative kinetic model. Both plots are derived from laboratory X-ray diffraction data.*

excess occupancy for one site from these measurements. As the material is warmed the quenched-in disordered oxygen arrangement begins to order, leading to a hump in the excess occupancy with temperature; on slow cooling an equilibrium ordered state can be achieved. Again, by using a cumulative rate expression, (the total degree of ordering at any temperature, T, being dependent on the rate of ordering at that temperature and the rates at all previous temperatures the material has been exposed to), one can extract kinetic information directly from these data, the solid line in Figure 4b yielding an activation energy of around 39 kJ mol^{-1}. Gratifyingly, the quench/hold methods of Figure 4a and the quench/warm methods of Figure 4b give rise to similar estimates of the activation energy.

In summary, we hope this short article has shown some of the exciting extra information that can be obtained by parametric diffraction studies. Such methods are not universally applicable, and there will always be cases in which a full understanding of a material can only be obtained by long data collections yielding the highest possible quality data. For many systems, however, this mode of data collection should at least be considered. To finish with a deliberately biased viewpoint, in the approximately 5 years we have been collecting data in this mode, we have rarely regretted adopting a parametric approach!

We would like to thank a number of people whose insight/expertise/technical assistance has been invaluable in these studies including W.I.F. David, R.M. Ibberson, K.S. Knight and J. Bones at the Rutherford Laboratory; co-workers on the publications listed below; and the EPRSC for access to central facilities and the provision of laboratory diffraction facilities via JREI GR/M35222/01.

References

[1] W. I. F. David; J. S. O. Evans; A. W. Sleight, *Europhys. Lett.*, 1999, 46, 661.

[2] J. S. O. Evans; W. I. F. David; A. W. Sleight, *Acta Cryst. B*, 1999, 55, 333.

[3] J. S. O. Evans; P. A. Hanson; R. M. Ibberson; U. Kameswari; N. Duan; A. W. Sleight, *Journal of the American Chemical Society*, 2000, 122, 8694.

Structural Information from In-Situ Powder Diffraction Experiments

Poul Norby
Department of Chemistry, University of Oslo,
N-0315 Oslo, Norway
p.a.norby@kjemi.uio.no

In-situ experiments play an increasingly important role in studies of materials of technological interest as well as in fundamental studies of materials. The field has developed tremendously, and emphasis is shifting from method development to studies of materials and systems of scientific or technological interest. When the materials involved are crystalline, diffraction methods are often used in order to obtain in-situ structural information. The access to synchrotron X-ray sources has had a major impact on the development of in-situ powder diffraction. The very high intensity of the synchrotron X-ray beam allows fast data collection. The tunability of the X-ray energy makes it possible to use hard radiation, so that container materials can be penetrated. Finally, it is possible to collect high resolution powder diffraction data, allowing even subtle structural changes to be determined in-situ.

In-situ studies may be performed as time resolved experiments, where a chemical reaction or physical process is followed. One examples of this type of experiments is in-situ synchrotron X-ray powder diffraction studies of hydrothermal crystallisation of zeolites and microporous materials. In-situ experiments may also be performed under static or equilibrium conditions, where the objective is to investigate structural properties of materials, for instance catalysts, under actual working conditions.

Numerous studies have demonstrated the versatility and strength of using in-situ powder diffraction in studies of materials synthesis and chemical reactions, and an increasing number of research groups are developing and using in-situ powder diffraction. Angle dispersive as well as energy dispersive synchrotron X-ray powder diffraction has been used, in addition to conventional X-ray diffraction and neutron diffraction.

It is important to stress that combining different and complementary characterization methods, both in-situ and ex-situ, will often give far more information than using one method alone. One may use information about local order from e.g. EXAFS/XANES or MAS NMR in combination with information about long range order from diffraction. Another example is in-situ studies of synthesis where e.g. Dynamic Light Scattering or Small Angle Scattering is used to follow the nucleation process, while the development and growth of larger, crystalline species are followed by diffraction methods.

Starting at the Chemistry beamline X7B at the National Synchrotron Light Source, NSLS, at Brookhaven National Laboratory, BNL and continuing at the European Synchrotron Radiation Facility, ESRF, in Grenoble, we have developed equipment and techniques for time resolved in-situ powder diffraction using synchrotron X-ray radiation. A capillary-based micro reaction cell was designed, allowing control over the environment of the sample. The cell is very versatile, and has been used to study for instance hydrothermal synthesis, ion exchange, intercalation, adsorption, solid state reactions and solid-gas reactions. In order to be able to collect time resolved powder diffraction data suitable for Rietveld analysis with a time resolution of a few seconds, a Translating Imaging Plate system was developed [e.g. 1-3]. By translating an imaging plate behind a screen with a vertical slit (Figure 1), a continuous series of powder diffraction patterns is collected. The time resolution is dependent on the size of the slit and the translation speed. Later, a modified version of the Translating Imaging Plate System was built at the Italian beam line, GILDA, at ESRF [4], and a Rotating Slit device for a MAR-345 imaging plate system, allowing a time resolution below 100ms, was developed for the Swiss-Norwegian beam line, SNBL, at ESRF [5].

The following examples demonstrate how in-situ studies may reveal surprising and important information about structural rearrangement under non-ambient conditions. It illustrates how Rietveld refinement of time resolved synchrotron X-ray powder diffraction data may be used to obtain real time structural information and how this information may be used together with in-situ and ex-situ MAS NMR spectroscopy to understand cation migration and cation distribution in zeolites.

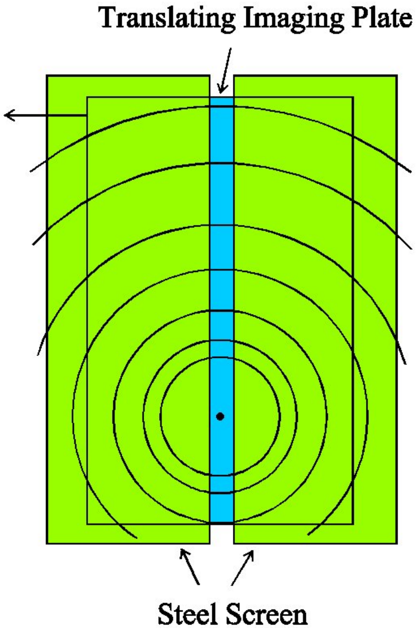

Figure 1. *Principle sketch of the Translating Imaging Plate system. An imaging plate is translated behind a steel screen with a vertical opening. As only a small strip of the imaging plate is exposed to the diffracted beam, a time resolved series of powder diffraction patterns is recorded.*

Zeolites and other microporous materials are used extensively as e.g. adsorbents and catalysts, as they have crystallographically ordered channels and cages of molecular dimensions. From crystal structure determinations, the size and shape of channels and cages, as well as the positions of the extra-framework cations, may be determined. It is well known from studies of hydrated and dehydrated zeolites that the presence or absence of water molecules may dramatically alter the position and coordination of extra-framework cations. The coordination requirements of the cations and the strong interaction between water molecules and cations mean that when water is removed, the cations may move in order to obtain more energetically favourable coordination. In a number of studies the dehydration of zeolites has been followed using in-situ powder diffraction and Rietveld refinement. This allows real-time observation of the dehydration process, where disappearance of individual water molecules is observed together with cation migration and framework relaxation [e.g. 6,7].

It is surprising, however, that adsorption of organic molecules may also lead to significant cation migration and redistribution. We have performed a number of studies, where synchrotron X-ray powder diffraction was used in combination with ^{23}Na MAS-NMR spectroscopy to follow the adsorption of hydrofluorocarbons (e.g. HFC-134, CHF_2CHF_2) in zeolites with faujasite type structure. A three-dimensional representation of the powder diffraction patterns during adsorption of HFC-134 in zeolite Y is shown in Figure 2. The most visible feature is the sudden decrease in intensity of the first reflection (111) when exposing the dehydrated zeolite to HFC-134. However, significant changes in the higher angle reflections are observed as well. Structure refinements of zeolite Y with adsorbed HFC-134 revealed that the interaction between the HFC molecules and the cations were sufficiently strong to cause migration of the cations [8]. This demonstrates clearly that it is crucial not to rely on structural studies performed on e.g. dehydrated zeolites at ambient conditions when predicting adsorption sites. It is necessary to take into account that adsorption may cause redistribution of the cation sites as well as relaxation of the framework.

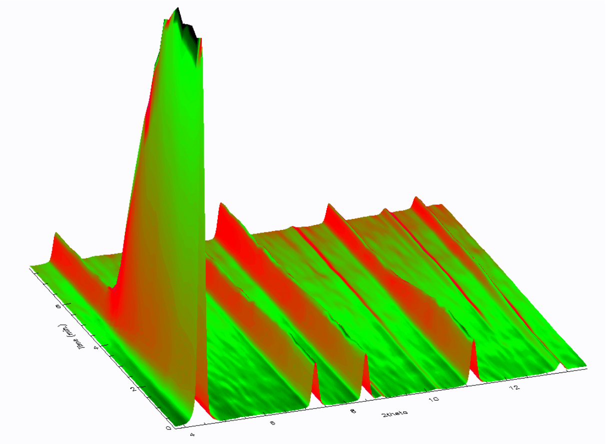

Figure 2. *Three-dimensional representation of time resolved powder diffraction patterns collected during adsorption of HFC-134 on zeolite Na-Y. The very dramatic and fast decrease in intensity of the first reflection corresponds to the time when the sample is exposed to HFC-134.*

In a related study, cation migration and cation distribution in zeolite Cs(Na)-Y were investigated as a function of temperature and hydration state using ^{133}Cs and ^{23}Na MAS-NMR and in-situ synchrotron X-ray powder diffraction [9]. A sample of partially Cs-ion-exchanged zeolite Y (aqueous solution, 0.1 M, 80ºC) was heated under vacuum in a capillary-based micro reaction cell. Powder diffraction data were collected during heating and subsequent cooling under vacuum using the Translating Imaging Plate system at X7B, NSLS. Figure 3 shows the results of a Rietveld refinement of a series of powder diffraction patterns collected during dehydration. The observed patterns are shown together with the difference between observed and calculated patterns in a 3-dimensional representation.

An interesting observation when ion exchanging zeolite Na-Y with cesium cations in aqueous solution, is that repeated ion-exchange/calcination cycles increase the cesium content of the zeolite. The reason for this was clearly seen when the crystal structure zeolite Cs(Na)-Y was followed in-situ during heating under vacuum to 500ºC.

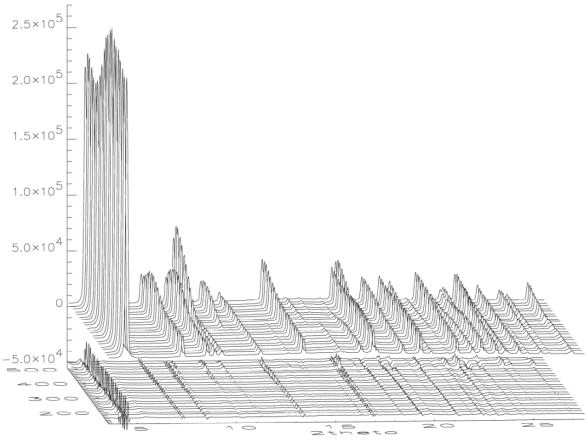

Figure 3. *Observed and difference powder diffraction pattern after Rietveld refinement of a series of in-situ powder diffraction patterns collected during dehydration of zeolite Cs(Na)-Y in vacuum.*

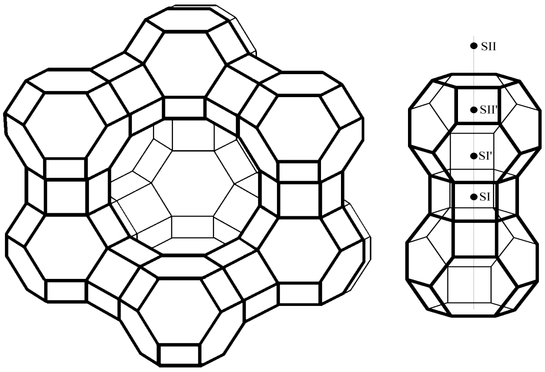

Figure 4. *The framework structure of zeolite Y (faujasite, FAU) shown as connection of the tetrahedral framework atoms. To the right, some cation positions are shown:* ***SII*** *in the supercage, just outside the six-ring opening to the sodalite cage.* ***SII'*** *on the opposite side of the six-ring inside the sodalite cage.* ***SI*** *in the hexagonal prism and* ***SI'*** *in the sodalite cage, facing the double six-ring.*

Figure 4 shows the framework structure of zeolite Y (Faujasite structure) and some of the extra framework cation positions. Only the tetrahedral atoms are shown in the Figure. The structure may be seen as sodalite cages interconnected by hexagonal prisms forming larger super-cages. Figure 5 shows refined populations of the various cation positions for cesium and sodium during heating [9]. Initially, after the first ion exchange, all cesium cations are situated in the large super-cage while the sodium cations are situated in the small sodalite cage. This may be understood when looking at the size of the rings giving access to the cages (The number of atoms in the rings in zeolite type materials is conventionally given counting only the tetrahedral atoms, i.e. a six-ring consists of six tetrahedral atoms and six oxygen atoms). The smaller sodalite cages are interconnected with double six-rings and have six-rings openings to the large super-cage. The super-cages are also interconnected in a three-dimensional arrangement, but the openings between the cages are 12-rings. The cesium cation is too large to pass through a six-ring at ambient conditions. Aqueous ion exchange will therefore result in only the sodium cations in the large super-cages being exchanged, which explains why only partial ion exchange is accomplished.

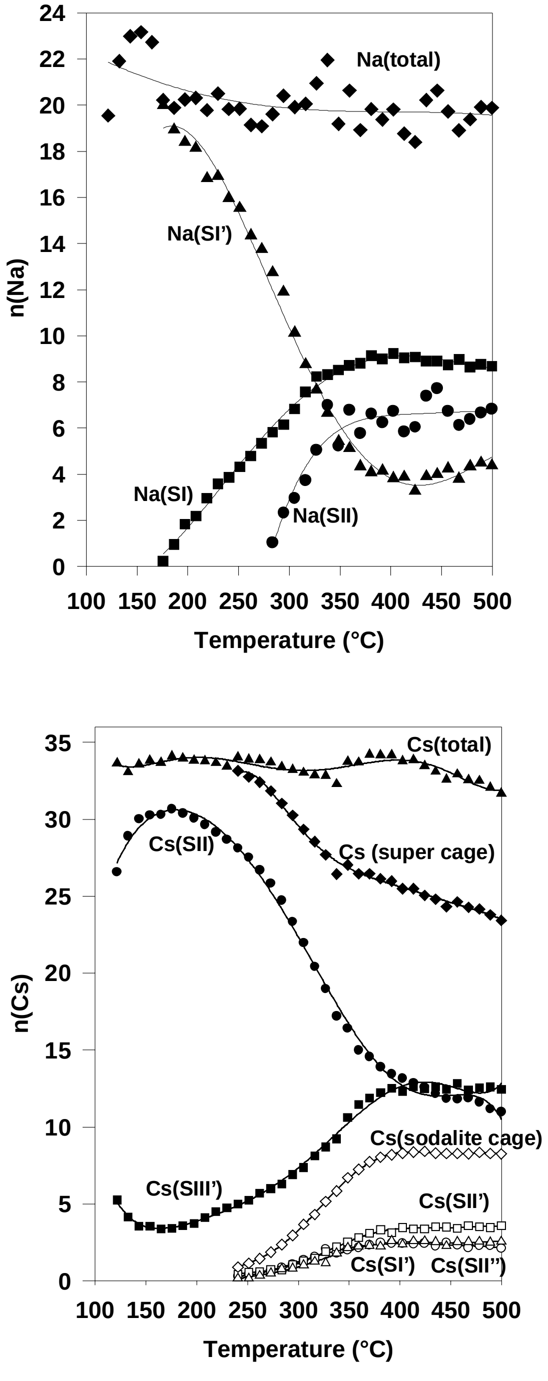

Figure 5. *Refined population of sodium (top) and cesium (bottom) in the various cation sites during dehydration to 500ºC under vacuum.*

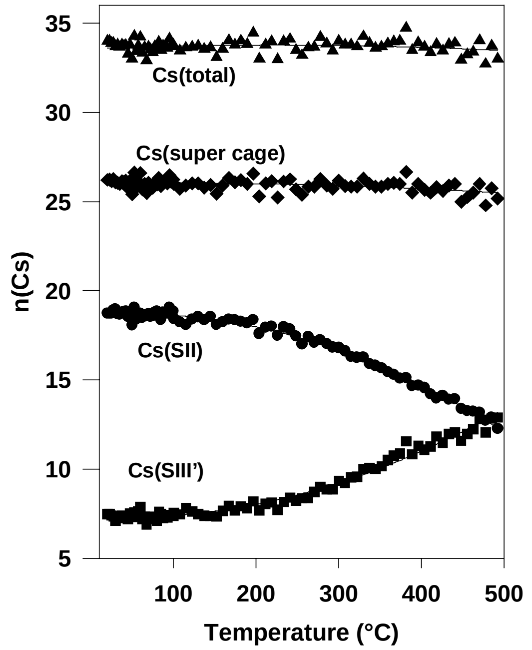

Figure 6. *Refined populations of the cesium cations in sites SII and SIII' (in the supercage) during cooling from 500ºC to room temperature under vacuum.*

However, when heating the sample a migration of cations is observed. The redistribution of cesium cations below 250ºC occurs exclusively between sites in the super-cage. However, above 250ºC migration of cesium cations between the super-cage and the sodalite cage is observed. At the same time sodium cations migrate into the super-cage. This explains why the calcination steps are necessary when increasing the cesium exchange by repeated ion exchange cycles.

After dehydration under vacuum to 500ºC, the sample was cooled (still under vacuum) while collecting powder diffraction data. Figure 6 shows the cesium cation populations for the anhydrous zeolite during cooling. A significant redistribution of cesium cations in the super-cage is observed between site SII (in front of the 6-ring entrance to the sodalite cage) and SIII (in front of a 4-ring in the super-cage). At high temperatures the number of cesium cations per unit cell in the two sites is approximately equal. As the temperature is lowered, site SII becomes increasingly populated, and this is the predominant site at low temperatures.

Redistribution of the cesium cations in the sodalite cage is also observed during cooling. The redistribution of cesium cations in the sodalite cage and in the super-cage is, of course, related. For instance, when the SII sites is occupied by a cesium cation, site SII' (in the sodalite cage on the other side of the six-ring) is less likely to be occupied because of the proximity of the two cation sites. Steric and electrostatic considerations may be used, together with knowledge about the temperature dependent occupancy of the various sites, to build up a model of possible local arrangements of the cations [9]. In addition to obtaining information about the population of the various cation sites, structural details, such as unit cell variations and changes in individual bond distances and angles, may be followed in-situ [9].

An important observation in this study is that the distribution and preferred site occupancy of cations in zeolites is very dependent on temperature and e.g. adsorbed molecules. One implication of this in relation to catalysis and adsorption is that using structural information obtained at ambient conditions to predict adsorption sites or catalytic reaction mechanisms may well lead to incorrect conclusions. It is necessary to perform in-situ experiments, and to determine the structure at operating conditions in order to understand the interactions fully. In addition, the use of complementary characterization tools (in this case X-ray diffraction and MAS-NMR) is in many cases critical in order to obtain reliable structural information from in-situ experiments.

References

[1] P. Norby "Synchrotron powder diffraction using Imaging Plates; Crystal structure determination and Rietveld refinement" *J. Appl. Cryst.* **30** (1997) 21-30.

[2] P. Norby “Hydrothermal Conversion of Zeolites: An In-situ Synchrotron X-ray Powder Diffraction Study” *J. Amer. Chem. Soc.* **119** (1997) 5215-5221.

[3] P. Norby and J. C. Hanson, "In-situ Synchrotron Powder Diffraction Studies of Hydrothermal Synthesis of Zeolites and Zeolite-like Materials: Formation of CoAPO-5." *Catalysis Today* **39** (1998) 301-309.

[4] C. Meneghini, G. Artioli, P. Norby, A. Balerna, A. Gualtieri and S. Mobilio “A Translating Imaging Plate System for In-situ Experiments at the GILDA Beamline.” *J. Synchr. Rad.* **8** (2001) 1162-1166.

[5] P. Norby, H. Fjellvåg and H. Emerich “Fast time resolved in-situ powder diffraction studies of high-temperature oxidation/reduction reactions” ESRF Highlights 2001 (2002) 88-89.

[6] K. Ståhl and J.C. Hanson ”Multiple cation sites in dehydrated brewsterite. An in-situ X-ray synchrotron powder diffraction study” *Microporous Mesoporous Mater.* **32** (1999) 147-158.

[7] G. Artioli, K. Ståhl, G. Cruciani, A. Gualtieri and J.C. Hanson “In situ dehydration of yugawaralite” *Amer. Mineral.* **86** (2001) 185-192.

[8] C.P. Grey, F.I. Poshni, A.F. Gualtieri, P. Norby, J.C. Hanson and D.R. Corbin. "Combined MAS NMR and X-ray Powder Diffraction Structural Characterization of Hydrofluorocarbon-134 Adsorbed on Zeolite NaY: Observation of Cation Migration and Strong Sorbate-Cation Interactions" *J. Amer. Chem. Soc.* **119** (1997) 1981-1989.

[9] P. Norby, F.I. Poshni, C.P. Grey, A.F. Gualtieri and J.C. Hanson "Cation migration in zeolites; a combined in-situ synchrotron X-ray powder diffraction and MAS NMR investigation of dehydration of zeolite Cs(Na)-Y." *J. Phys. Chem. B.* **102** (1998) 839-856.

Neutron Diffraction Studies of Self-Propagating High-Temperature Synthesis

Erich H. Kisi and Daniel P. Riley
School of Engineering
The University of Newcastle,
Callaghan NSW 23087, Australia
meehk@cc.newcastle.edu.au

Introduction

Self-propagating High-temperature Synthesis (SHS), uses the heat of reaction as the primary energy source in the production of a material. Once ignited by an ignition source (laser, electron beam, furnace or electric arc) the reaction becomes self-sustaining and converts reactants to products very rapidly (0.1-100 s). The extreme rapidity and violently exothermic nature of the reactions makes it difficult to determine the precise kinetic sequence using standard laboratory techniques (eg. it is extremely difficult to halt the process to examine intermediate products using XRD or microscopy, without influencing the microstructure). *In-situ* diffraction experiments offer the ideal solution giving access to phase identification, phase quantification, crystal structure data and occasionally microstructural data in a real-time sequence.

Rapid powder diffraction data collection has until recently been the preserve of synchrotron X-ray instruments. However, some relatively recent developments in instrumentation have allowed SHS to be studied using neutrons [1]. Neutron diffraction has some useful characteristics for the study of SHS reactions:

i) the low absorption coefficient for most materials allows large samples to be used (SHS is difficult to sustain in small samples),
ii) large samples also overcome problems associated with volatilisation which causes the surface of the sample to be different from the bulk,
iii) large ancillaries such as furnaces are readily used,
iv) neutron diffractometers generally cover a large range of d-spacing.

In addition, neutron scattering lengths for the elements bear different relationships to each other than do the X-ray form factors, making the techniques complementary in solving multi-site occupancy problems.

The particular material chosen as an example here is Ti_3SiC_2 and related ternary carbides [2]. The material has an unusual combination of properties that is neither ceramic nor metallic. It has the refractory and high temperature properties normally associated with ceramics, combined with the electrical and thermal conductivity of a metal [2]. The material exhibits sufficient ductility to enable it to be readily machined with ordinary machine tools and has a range of other attractive properties [2].

The heat of formation for Ti_3SiC_2 is quite large making it an excellent candidate for production by SHS. Here we summarise the results of *in-situ* neutron powder diffraction studies of Ti_3SiC_2 at 380 ms and 900 ms time resolution.

The Experiments

The experiments were conducted on the instrument D20 at the Institut Laue-Langevin, Grenoble, France [1]. D20 is equipped with a 1500 element microstrip detector spanning 0-160^o 2θ and can record an entire diffraction pattern (diffracted intensity permitting) at arbitrarily short times down to a lower limit of 30 μs. Cold-pressed pellets of the reactants were heated in the D20 furnace at ~100^{o}C/min through the critical range 800-1000^{o}C to initiate the reaction whilst diffraction patterns were simultaneously recorded. In one series of experiments, 0.5 s patterns were followed by 0.4 s for data download and in later work 0.3 s patterns were able to be downloaded in 0.08 s. The systems studied have included Ti_3SiC_2 formation from 3Ti-SiC-C, and 3Ti-Si-2C mixtures and Ti_3AlC_2 formation from 12Ti-Al4C3-C5 mixtures. The results shown here are for the system 3Ti-SiC-C. However the behaviour of the other systems is very similar.

Results

An overview of part of the diffraction patterns for the SHS reaction 3Ti+SiC+C → Ti3SiC2 is shown in Figure 1 and a three dimensional rendering of a similar region is shown in Figure 2 [3]. The data are rich in structural, microstructural and kinetic detail that can be used in a number of ways.

1. Reaction Mechanisms

From close inspection of the data it was clear that the SHS reactions proceed in five stages. *Pre-heating of the reactants* assists in the ignition by reducing the overall heat requirement. The diffraction patterns show only the expected thermal expansion below 880^{o}C. *The $\alpha \rightarrow \beta$ phase transformation in Ti* forms the next stage. This phase transition is readily seen at the left-hand end of Figure 2 and was found to be a necessary precursor to the SHS reaction in all cases studied. *The pre-ignition reaction stage* consists of local reaction of Ti with C. As this reaction is exothermic, it provides local temperature increases that are the real ignition sources. The fourth stage is the formation of a *single solid intermediate phase* in <0.5 s and is the true SHS or combustion reaction in this system. It produces a pronounced discontinuity in the diffraction data of Figures 1 and 2. The intermediate phase has a simple NaCl structure (like TiC) and it persists for six seconds as the only phase present. We believe that the intermediate phase is a solid solution of Si in TiC that is relatively stable at the combustion temperature but becomes unstable as the temperature decreases. The final stage is *the rapid nucleation and growth of the product phase* Ti_3SiC_2 as shown by Figures 1 and particularly 2.

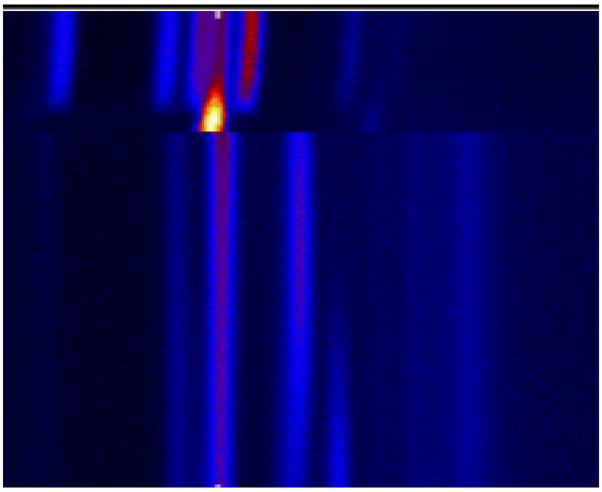

Figure 1. *Plot of ~300 diffraction patterns recorded during SHS of Ti_3SiC_2. The horizontal axis is 2θ (~24 - 42^o), the vertical axis is time and the diffracted intensity is indicated by brightness/colour changes.*

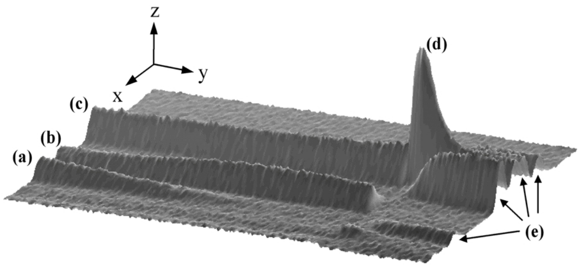

Figure 2. *3-D plot of a portion of the diffraction patterns during SHS of Ti_3SiC_2. The reaction progression is from left to right on the y-axis. The x-axis represents 2θ and the z-axis is the diffracted intensity. The marked peaks are: a) α-Ti, b) α-Ti, β-Ti, c) SiC, d) the TiC-like intermediate phase, and e) Ti_3SiC_2.*

2. Reaction Kinetics

Although they were recorded in only 300 or 500 ms, the diffraction patterns have sufficient intensity for Rietveld analysis. The refined scale factors may then be used for quantitative analysis [4] to examine the reaction kinetics. An example is shown in Figure 3 for the experiment shown in Figures 1 and 2. The data shown depict the fraction of the intermediate phase, *f*, converted into the product phase. A fit to a simple Avrami type kinetic equation:

$$f = 1 - e^{-Ct^{n}} \qquad (1)$$

is also shown. To extract meaningful values for the Avrami exponent, n and the constant C, the sample temperature as a function of time also needs to be known (see section 3 below). Similar data are available for all of the phases within the samples.

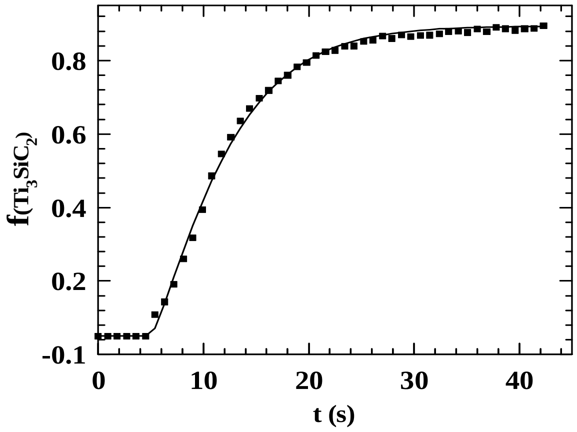

Figure 3. *Fraction of the sample converted to Ti_3SiC_2 during the post-combustion period (t has been zeroed at combustion).*

3. DiffractionThermometry and DTA

Additional data on the state of the sample is available from the lattice parameters obtained during Rietveld analyses. Using known thermal expansion coefficients, the mean sample temperature can be estimated. Typical data are shown in Figure 4 which shows the SHS combustion temperature (2596 K) followed by post-SHS cooling of the sample. A pronounced lattice parameter anomaly that occurs during the precipitation of Ti_3SiC_2 is thought to be due to the release of latent heat and has been used to propose a diffraction based thermal analysis technique [5]. By solving the differential equation:

$$\frac{dT_R}{dt} = nC\frac{-M\Delta H_R}{mC_p}t^{n-1}e^{-Ct^{n}} \qquad (2)$$

an estimate for the enthalpy of formation can be obtained. Here M is the sample mass, m the mass of Ti_3SiC_2 formed, C_p is the heat capacity of the phase assembly present, ΔH_R is the formation enthalpy, T_R is the difference between the sample temperature and the interpolated baseline cooling curve (shown in Figure 4), and n and C are the Avrami constants above. It is anticipated that other kinetic studies may benefit from this type of analysis.

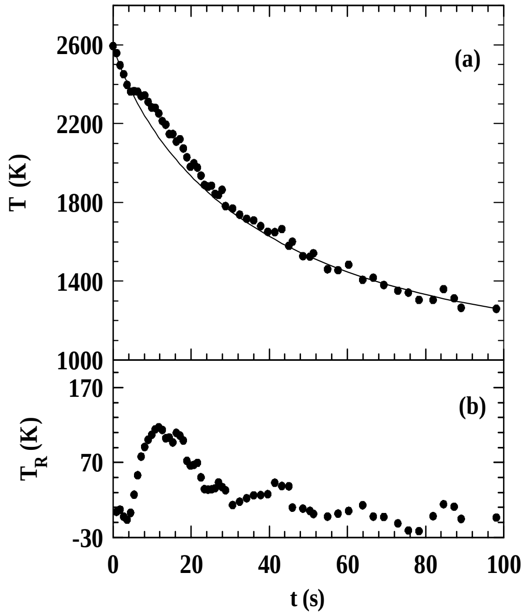

Figure 4. *(a) Post-combustion sample temperature (estimated from lattice parameters) superimposed on an interpolated cooling curve. (b) The difference between the sample temperature and the baseline cooling curve, a diffraction DTA curve.*

Conclusions

Rapid *in-situ* diffraction studies can reveal all of the complexities of a combustion synthesis reaction in a single snap-shot. Further analysis is used to extract phase quantities, transformation kinetics and the sample temperature. Crystal structure data as a function of time and temperature is also available. In some cases, the transition enthalpy may be estimated from diffraction DTA.

References

[1] http://whisky.ill.fr/YellowBook/D20/

[2] T. El-Raghy and M.W. Barsoum, “Processing and Mechanical Properties of Ti_3SiC_2: I, Reaction Path and Microstructure Evolution”, *J. Am. Ceram. Soc.*, **82**, 2849-2854, 1999.

[3] D.P. Riley, E.H. Kisi, T.C. Hansen and A.W. Hewat “Ultra-high speed neutron diffraction study of self-propagating high-temperature synthesis of Ti_3SiC_2: I Reaction Mechanism. *J. Am. Ceram.* **85**, 2417-2424, 2002.

[4] R.J. Hill and C.J. Howard, “Quantitative Phase Analysis from Neutron Powder Diffraction Data Using the Rietveld Method” *J. Appl. Crystallogr.* **20**, 467-474, 1987.

[5] E.H. Kisi and D.P. Riley “Diffraction Thermometry and Differential Thermal Analysis”, *J. Appl. Crystallogr.* **35**, 664-668, 2002.

Time-Resolved, In-Situ Energy Dispersive X-Ray Diffraction Studies of the Structural Transformations of Templated Zinc Phosphates under Hydrothermal Conditions

Alexander J. Norquist and Dermot O'Hare
Inorganic Chemistry Laboratory, University of Oxford, Oxford OX1 3QR UK.

dermot.ohare@chem.ox.ac.uk

Introduction

A great deal of effort is focussed upon understanding crystallisation mechanisms and kinetics of microporous solid formation. These materials have attracted this attention owing to their desirable optical, catalytic or sorption properties [1]. It is hoped that an understanding of the mechanisms leading to the formation of these zeolite-like structures will lead to the rational synthesis of new functional materials [2]. Such open-framework materials are usually synthesised under hydrothermal condition, often in the presence of aggressive mineralizers, such as HF_{aq} or H_3PO_4, requiring the use of thick-walled reaction vessels. In recent years we have been developing reaction cells that allow us non-invasively to probe these experimentally challenging reaction conditions by *in situ* diffraction methods [3].

Synchrotron generated X-rays are produced with high intensity over a wide energy range (typically 5 to 120 keV). This allows researchers to perform powder diffraction experiments in the energy dispersive mode, which utilises the full spectrum of the incident X-ray flux simultaneously. An energy dispersive X-ray diffraction (EDXRD) experiment involves the measurement of the intensity spectrum of scattered X-rays by a fixed angle solid-state photon counting and energy dispersive detector, with which each Bragg reflection is characterised by an energy that is dependent upon the angle of the detector [4]. Minimal collimation of the incident beam is required owing to the lack of monochromation. The flux incident on the sample is high (~10^{10} photon s^{-1}) and sufficiently intense to penetrate large volume samples in thick-walled reaction vessels. The use of fixed angle detectors negates the need for large windows required for the passage of X-rays through the apparatus, and devices with bulky heaters and pressure containment vessels can be constructed [5]. The EDXRD method is widely used for the study of pressure-induced phase transitions of inorganic solids using confined cells [6]. However, 'laboratory-sized' reaction vessels can be employed, which are identical in design to apparatus used in preparative chemistry. This limits the number of additional reaction variables introduced by variations in vessel design. We have constructed a large-volume hydrothermal reaction cell from which EDXRD data may be collected at temperatures up to 250 ºC and 20 bar autogeneous pressure [7]. This reaction vessel is virtually identical in design and construction to the 23 mL Parr hydrothermal autoclaves widely used in research laboratories. A schematic of the experimental apparatus is shown in Figure 1. This cell was designed to operate on the energy dispersive beam line 16.4 at the SRS, Daresbury Laboratory, UK. The beam line is equipped with three energy discriminating detector which allow us to measure a wide range of d-spacing simultaneously, for our experiments it is typically 1 – 14 Å, although this 'window' can be adjusted by moving the fixed angle of the detectors. A small area of the autoclave walls has been thinned to approximately 0.4 mm which gives us acceptable attenuation of the incident and diffracted X-ray beam. We still have sufficient X-ray beam intensity to collect individual EDXRD scans on the order to 30 seconds to 1 minute. Each reaction is contained in a Teflon sleeve, from which a characteristic Bragg reflection at 4.9 Å is observed. The cell has been used by us for a variety of studies, including the elucidation of crystallisation mechanisms and the determination of reaction kinetics under real laboratory conditions, without introducing additional reaction variables through quenching studies [8].

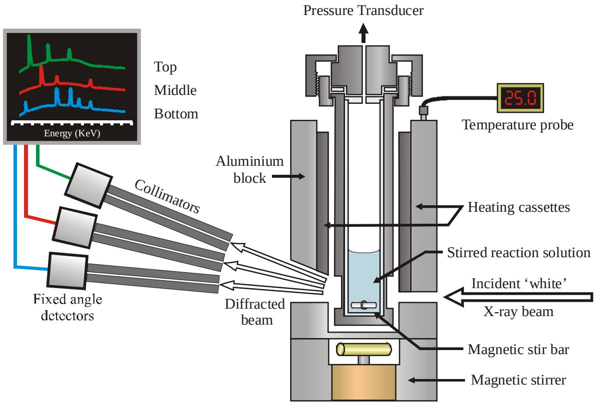

Figure 1. *Schematic showing the experimental apparatus used for recording in situ EDXRD data on hydrothermal reactions.*

In situ study of a hydrothermal reaction

The incorporation of transition metal centres into microporous solids has enabled researchers to introduce chemically reactive sites into these porous structures. They exhibit a range of interesting and useful reactions including free-radical chemistry, photochemical reactions or redox chemistry. A host of transition metal centres have been synthesised, including Ti [9], V [10] and Zn [11] to name only three. The extended structures containing such metal centres can often be described in terms of oligomeric groups of coordination polyhedra, denoted secondary-building units or SBUs [12]. Férey demonstrated that a few types of SBU (M_2P_2 tetramers, M_3P_3 hexamers and M_4P_4 octamers) could be used to describe the complex and varied structures in organically templated gallium phosphates, and Taulelle *et al.* have identified oligomeric 'building blocks' using NMR spectroscopy

[13]. C. N. R. Rao *et al.* recently began exploring the use of amine phosphates as precursors for the formation of organically templated zinc phosphates [14]. This investigation led to the isolation of two M_2P_2 tetrameric SBUs that can transform to structures of higher dimensionality [15].

These studies were conducted *ex situ*. The tetrameric starting material ($[C_6N_2H_{18}][Zn(HPO_4)(H_2PO_4)_2]$ or ZPM-I) was placed in an autoclave with another amine template and deionised water. The reactants were heated for several hours, typically between 24 and 48 h. The solid products were recovered, isolated by filtration and characterised. No kinetic or mechanistic data can be obtained from such investigations owing to the robust containers required to contain the autogenous pressures generated in hydrothermal reactions.

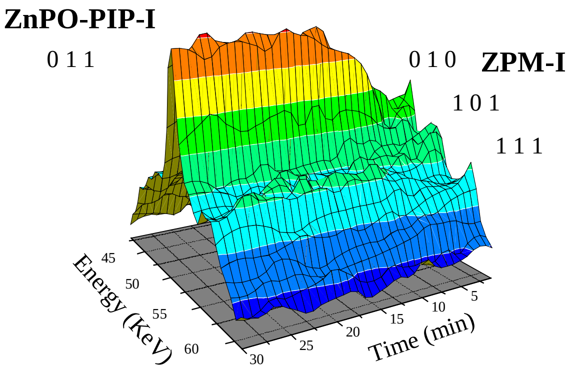

Figure 2. *A stack plot of the EDXRD data measured during the hydrothermal transformation of a molecular zinc phosphate monomer (ZPM-I) to an extended zinc phosphate network structure (ZnPO-PIP-I) at 60 ºC.*

The first reaction we studied involved the transformation of SBU-1 to $[C_4N_2H_{12}][Zn(HPO_4)_2(H_2O)]$ (ZnPO-PIP-I). ZPM-I was reacted with piperazine in deionised water. An autoclave containing the reaction gel of composition ZPM-I : piperazine : 250 H_2O was placed in a heating block at 60 ºC. A stack plot of the time-resolved EDXRD data for this transformation is shown in Figure 2. Characteristic Bragg reflections of ZPM-I, the 010, 101 and 111, are observed in the first pattern. The intensity of these reflections decreased dramatically over the next 5 minutes; at which point no reflections from the starting materials are observed. At this point one new Bragg reflection is observed, which corresponds to the 011 reflection of transformation product, ZnPO-PIP-I. The intensity of this Bragg reflection increases over the next 10-15 minutes, at which point the intensity remains constant. The Bragg reflections are integrated for each scan. The area of each reflection from a given phase is proportional to the amount of that phase present in the reaction at that time. The integrated peak intensities for the transformation of ZPM-I to ZnPO-PIP-I are shown in Figure 3. The decay of the starting material and growth of the final product do not mirror one another. In fact, the ZPM-I starting material is almost completely consumed before any ZnPO-PIP-I, the final product, is observed, suggesting a dissolution reprecipitation process, not a solid state transformation.

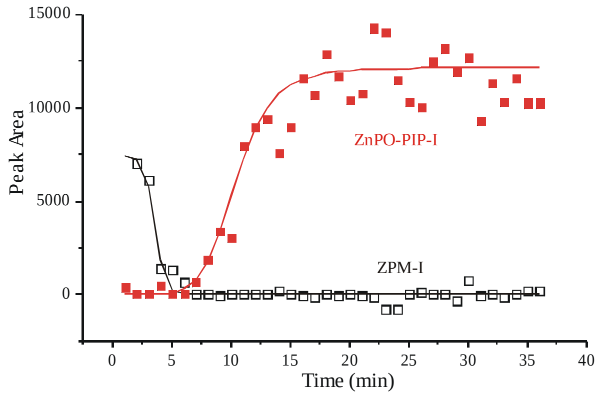

Figure 3. *Integrated peak areas of the ZPM-I (111) and ZnPO-PIP-I (011) Bragg reflections. The unfilled squares represent ZPM-I and the filled red squares represent ZnPO-PIP-I.*

A number of expressions have been proposed for the determination of mechanistic and kinetic parameters in solid-state reactions. The most common is the Avrami-Erofe'ev expression [16]. The mechanism of nuclei growth and rate of nucleation [17] can be obtained using a Sharp Hancock plot [18]. The analysis of the transformation of ZPM-I to ZnPO-PIP-I indicates that the reaction is phase boundary controlled, meaning that the rate limiting step is reaction at each crystallite, not diffusion of reactants or nucleation itself.

The second transformation studied involved heating ZPM-I in water, without adding an additional templating species. A reaction gel of composition ZPM-I : 100 water was placed in an autoclave, which in turn was placed in a heating block preset to 100 ºC.

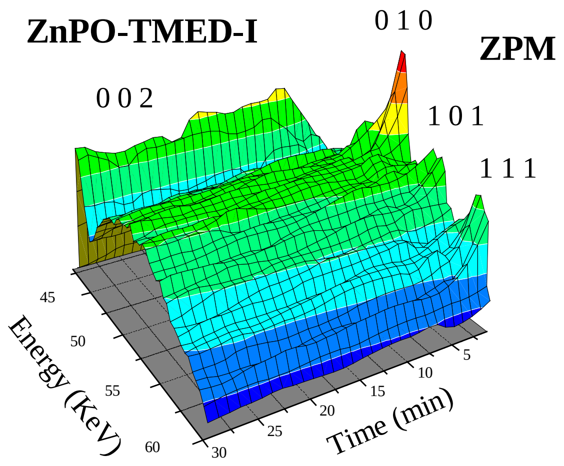

Figure 4. *A stack plot of the EDXRD data measured during the transformation of ZPM-I to ZnPO-TMED-I at 100 ºC.*

A stack plot of the EDXRD data is shown in Figure 4. Just as in the previous reaction, Bragg reflections from ZPM-I are observed in the first scan. The intensity of the 010 101 and 111 reflections declines quickly, their intensities fall to zero after approximately 5 or 6 minutes. A single Bragg reflection from $[C_6N_2H_{18}][Zn_3(H_2O)_4(HPO_4)_4]$ (ZnPO-TMED-I) [15a] is observed after only 2 or 3 minutes. The intensity of this reflection increases for approximately 10 minutes, at which time it remains constant for the duration of the experiment. A plot showing the integrated peak areas of both the ZPM-I starting material and ZnPO-TMED-I product as a function of time is shown in Figure 5. This data can be used to suggest that the transformation of ZPM-I to ZnPO-TMED-I is a dissolution reprecipitation mechanism, owing to the differences between the decline and growth curves.

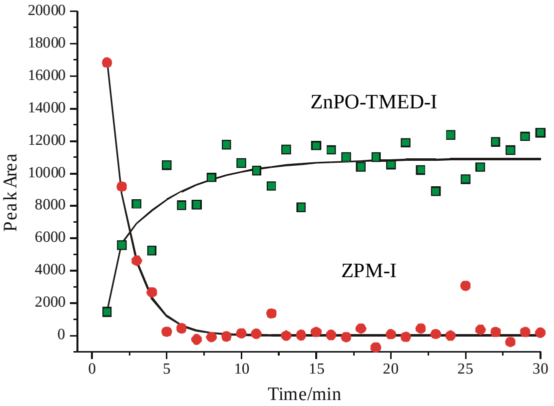

Figure 5. *Integrated peak areas of ZPM-I (111) and ZnPO-TMED-I (002) Bragg reflections. The red circles represent ZPM-I and the green squares represent ZnPO-TMED-I.*

The reaction mechanism was analysed using Sharp-Hancock plots in conjunction with the Avarmi-Erofe'ev equation. The transformation of ZPM-I to ZnPO-TMED-I is a diffusion-controlled process, where the rate limiting step is the transport of reactants through solution.

The use of EDXRD in conjunction with the *in situ* hydrothermal cell described above has enabled us to monitor crystallisations and transformations in an important family of compounds, organically templated zinc phosphates. This technique has allowed us to gain crucial understanding into the reaction kinetics and dynamics. The transformation of ZPM-I to both ZnPO-PIP-I and ZnPO-TMED-I under hydrothermal conditions occurs via a dissolution reprecipitation mechanism. The transformation to ZnPO-PIP-I is phase boundary controlled while the transformation to ZnPO-TMED-I is diffusion controlled. The accessibility of this information is crucial if any rational design of open framework metal phosphate structures is to occur.

Conclusions

The measurement of powder diffraction data during the synthesis of many inorganic materials requires the design and construction of specialised apparatus, but in the last five years much progress has been made by us and others. Analysis of the diffraction data and detailed quantitative kinetic measurements are first steps required in proposing reaction mechanisms, but clearly much more work is required in this new field before the rational design of new materials is possible.

References

[1] Cheetham, A. K.; *Science* **1994,** *264*, 794; Bierlein, J. D.; Arweiler, C. B.; *Appl. Phys. Lett.* **1987,** *49*, 917; Schollhorm, R.; *Chem. Mater.* **1996,** *8*, 1747.

[2] Davis, M. E.; *Stud. Surf. Sci. Catal.* **1995,** *97*, 35; Francis, R. J.; O'Hare, D.; *J. Chem. Soc. Dalton Trans.* **1998,** 3133.

[3] Walton, R. I.; O'Hare, D.; *Chem. Comunm.* **2000,** 2283.

[4] Giessen, B. C.; Gordon, G. E. *Science* **1968,** *159*, 973.

[5] Clark, S. M.; Nield, A.; Rathbone, T.; Flaherty, J., Tang, C. C.; Evans, J. S. O.; Francis, R. J.; O'Hare, D. *Nucl. Instrum. Methods B* **1995,** *97*, 98.

[6] Parise, J. B.; Weidner, D. J.; Chen, J.; Liebermann, R. C. *Ann. Rev. Mater. Sci.* **1998,** *28*, 349.

[7] Evans, J. S. O.; Francis, R. J.; O'Hare, D.; Price, S. J.; Clarke, S. M.; Flaherty, J.; Gordon, J.; Nield, A.; Tang, C. C. *Rev. Sci. Instrum.* **1995,** *66*, 2442.

[8] Francis, R. J.; O'Brien, S.; Fogg, A. M.; Halasyamani, P. S.; O'Hare, D.; Loiseau, T.; Férey, G.; *J. Am. Chem. Soc.* **1999,** *121*, 1002; Walton, R. I.; Loiseau, T.; O'Hare, D.; Férey, G.; *Chem. Mater.* **1999,** *11*, 3201.

[9] Ekambaram, S.; Serre, C.; Férey, G.; Sevov, S. C.; *Chem. Mater.* **2000,** *12*, 444.

[10] Khan, M. I.; Meyer, L. M.; Haushalter, R. C.; Schweitzer, A. L.; Zubieta, J.; Dye, J. L.; *Chem. Mater.* **1996**, *8*, 43; Do, J.; Bontchev, R. P.; Jacobson, A. J.; *J. Solid State Chem.***2000,** *154*, 514.

[11] Rao, C. N. R.; Natarajan, S.; Neeraj, S.; *J. Am. Chem. Soc.* **2000,** *122*, 2810.

[12] Férey, G; *J. Fluorine Chem.* **1995,** *72*, 187; Oliver, S.; Kuperman, A.; Ozin, G. A.; *Angew. Chem. Int. Ed.* **1998,** *37*, 46; Férey, G; *Chem. Mater.* **2001,** *13*, 3084.

[13] Taulelle, R.; Haouas, M.; Gerardin, C.; Estournes, C.; Louiseau, T.; Férey, G.; *Colloids Surf. A* **1999,** *158*, 299.

[14] Neeraj, S.; Natarajan, S.; Rao, C. N. R.; *Angew. Chem. Int. Ed.* **1999,** *38*, 3480; Rao, C. N. R.; Natarajan, S.; Neeraj, S.; *J. Solid State Chem.* **2000,** *152*, 302; Natarajan, S.; Neeraj, S.; Rao, C. N. R.; *Solid State Sci.* **2000,** *2*, 87.

[15] Neeraj, S.; Natarajan, S.; Rao, C. N. R.; *J. Solid State Chem.* **2000,** *150*, 417; Ayi, A. A.; Choudhury, A.; Natarajan, S.; Neeraj. S.; Rao, C. N. R.; *J. Mater. Chem.* **2001,** *11*, 1181.

[16] Avrami, M. *J. Phys. Chem.* **1940,** *8*, 212; Avrami, M. *J. Phys. Chem.* **1941,** *9*, 177; Erofe'ev, B. V.; Dokl, C. R.; *Acad. Sci. URSS* **1946,** *52*, 511.

[17] Hulbert, S. F.; *J. Br. Ceram. Soc.* **1969,** *6*, 11.

[18] Hancock, J. D.; Sharp, J. H.; *J. Am. Ceram. Soc.* **1972,** *55*, 74.

In-Situ Time Resolved Powder Diffaction Studies in Heterogenous Catalysis; Coupling the Study of Long Range and Local Structural Changes

***Peter J. Chupas*[1]*, Clare P. Grey*[1]*, Jonathan C. Hanson*[2]*, Jae-Yong Kim*[2]*, Jose Rodriguez*[2]*, Xiangyun Qiu*[3]*, Simon J.L. Billinge*[3] *and Peter L. Lee*[4]**
[1] Chemistry Department, State University of New York at Stony Brook; [2] Chemistry Department, Brookhaven National Laboratory; [3] Department of Physics and Astronomy, Michigan State University; [4] Advanced Photon Source, Argonne National Laboratory, USA.
pchupas@ic.sunysb.edu

Introduction

The application of in-situ time resolved powder diffraction to study structural changes that occur during chemical reactions has become a standard method at synchrotron sources. With respect to heterogeneous catalysis, the understanding of the structural changes, both on the local and long range length scales, that are the consequence of reaction conditions, is paramount to understanding fully the functioning of many catalysts. Time resolved diffraction experiments which *combine* high-energy X-rays (>80 keV) with area detectors open the possibility of coupling both reciprocal and real space methods to probe both long range and local structural changes simultaneously [1]. This is particularly advantageous in the study of chemically induced structural changes, commonly encountered in heterogeneous catalysis. Here we illustrate the application of the approach to monitor the reduction of CuO, a material that is ubiquitous in compositions of methanol synthesis and water-gas shift catalysts [2]. Activation of the catalysts requires reduction of the CuO, producing small metallic Cu particles which are the active centers for catalysis. We have therefore been studying the reduction of CuO under controlled conditions using H_2 to examine the formation of centers active for catalysis (3).

Experimental

All diffraction experiments were performed at the 1-ID beamline at the Advanced Photon Source (APS) located at Argonne National Laboratory, Argonne, IL (USA). High energy X-rays were selected using a double bent Laue monochrometer capable of providing a flux of 10^{12} photons/second and operating with X-rays in the energy range of 50-200 keV.

In-situ diffraction experiments were performed with a specially designed “flow cell” (Figure 1), which allows the flow of reactant gas over the sample during acquisition of powder diffraction data. The temperature was controlled in steps as follows; 2 hour ramp from room temperature to 350ºC. During the experiment 4%H_2 in He was passed over the sample at a rate of 8 cm^3 per minute.

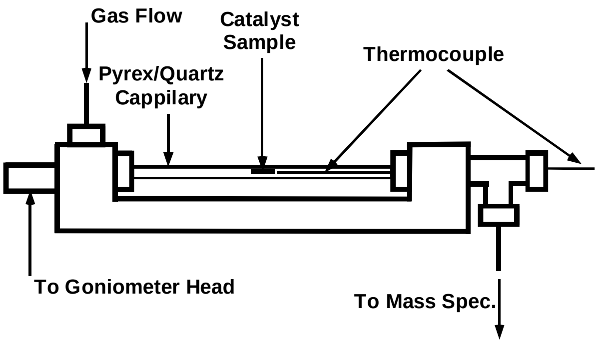

Figure 1. *Diagram of flow cell for in-situ experiments.*

A MAR345 image plate camera was mounted orthogonal to the beam path, with the beam centered on the IP. When using the 99 keV X-rays, a LaB_6 standard was used to calibrate the sample to detector distance and tilt of the IP relative to the beam path, using the software Fit2D [4]. All raw two-dimensional image data were integrated using the software Fit2D and files output as intensity versus 2θ. Ten second exposures yielded data that provided very good statistics for the refinement techniques described below.

Results

The in-situ reduction of CuO was followed using high energy X-rays coupled with a two dimensional image plate (IP) detector. The results are shown in Figure 2.

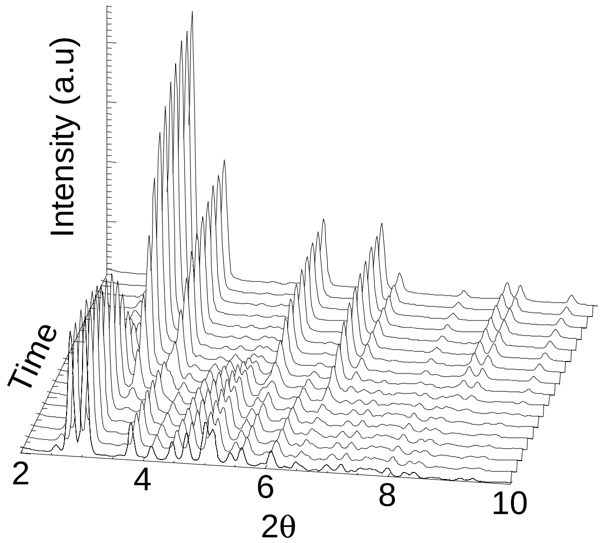

Figure 2. *Time resolved in-situ powder diffraction of the reduction of CuO.*

The reduction of CuO to Cu metal takes place at approximately 280ºC. The reduction to Cu is quite fast and occurs on the order of minutes. During this period both CuO and Cu are evident, and we are currently investigating the structural **changes** that occur.

High energy X-rays provide several experimental advantages in the structural analysis of time resolved data. Utilization of high-energy X-rays allow for larger values of momentum transfer to be probed (> 18 $Å^{-1}$), opening up the possibility for the application of real space methods (pair distribution function, PDF, analysis) to probe changes to local structure during reaction conditions. The G(r)s obtained from the diffraction patterns (IP data) at the beginning of the in-situ experiment and at the end of the in-situ experiment are shown in Figure 3. For example, the first Cu-O peak drops dramatically and a new peak at 2.6 Å (Cu-Cu) is observed. Traditional Bragg refinement of the same diffraction data used for PDF analysis provides for an improved parameter to data ratio. Exceptional Bragg profile refinements of beginning and final phases can be obtained, but disorder in mixed phase results in poorer fits and significant features in the difference electron density maps, which we are attempting to interpret. Following the reduction using real space methods may open up the further understanding of the reduction process, as the changes to the Cu-O coordination during the final stages of reduction may not be evident in the Bragg profile refinements.

Conclusions

High energy X-rays open up the possibility for qualitatively new time-resolved experiments which couple both reciprocal and real space approaches to structural analysis. The application of X-rays with energies between 80-120 keV allows for collection of powder diffraction data to high momentum transfer (>18 $Å^{-1}$) using commercial image plate cameras at sampling rates which will allow monitoring relevant structure changes under process conditions. This allows for both Rietveld and PDF analysis to be carried out on the same data sets probing both long range and local structural changes simultaneously.

Acknowledgements

Financial support from the Basic Energy Sciences program of the Department of Energy (D.O.E.) is gratefully acknowledged (DE-FG0296ER14681, DE-AC02-98CH10086 and DE-FG02-97ER45651). Use of the Advanced Photon Source was supported by the U.S. D.O.E., Office of Basic Energy Sciences, under contract No. W-31-109-Eng-38.

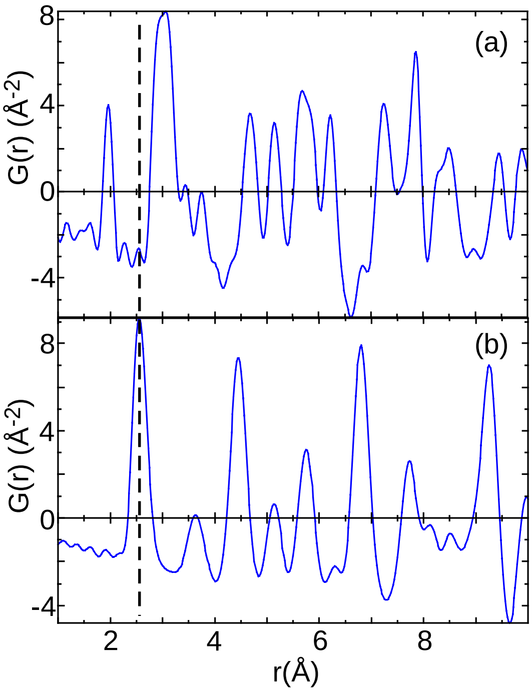

Figure 3. *G(r) for (a) CuO at the beginning of the time resolved experiment and G(r) for (b) Cu formed at the end of the time resolved experiment. The guideline shows the Cu-Cu first shell distance.*

References

[1] P.J. Chupas, X. Qiu, P.L. Lee, J.C. Hanson, C.P. Grey, S.J.L. Billinge, in preparation.

[2] J.M. Thomas and W.J. Thomas, *Principles and Practice of Heterogeneous Catalysis*, VCH, 1997.

[3] J.A. Rodriguez, J.-Y. Kim, J.C. Hanson, M. Perez and A.I. Frenkel, *Catalysis Letters*, (2003) 85, 247-254. (and references therein).

[4] A.P. Hammersley, *ESRF Internal Report*, ESRF98HA01T, "FIT2D V9.129 Reference Manual V3.1", 1998. A.P. Hammersley, S.O. Svenson, M. Hanfland, A.N. Fitch and D. Hausermann, *High Presssure Research*. 1996, 14, 235-248.

[5] I.-K. Jeong, J. Thompson, Th. Proffen, A. Perex and S.J.L. Billinge, "PDFgetX, a program for obtaining the atomic Pair Distribution Function from X-ray powder diffraction data."

Phase Mapping and Transformation Dynamics in Fusion Welds

Joe Wong
Lawrence Livermore National Laboratory,
University of California, P.O. Box 808, Livermore,
CA 94551 USA.
wong10@LLNL.gov

Introduction

Site-specific and time-resolved diffraction techniques utilizing intense synchrotron radiation have recently been employed to map the phases and their solid-state transformation in the heat-affected zone in a number of fusion welds *in-situ* during the welding process. These in-situ probes yield kinetics and microstructural evolution data not previously obtained with conventional ex-situ, post-mortem methods. Thus far, the synchrotron data provide not only some of the crucial experimental information for understanding the phase dynamics and microstructural development in fusion welds, but also realistic inputs for simulations as well as validating various kinetic models of phase transformation in welding metallurgy. The experimental progress to date in these synchrotron diffraction studies will be reviewed in this paper.

Synchrotron Radiation

Synchrotron radiation is emitted as the major loss mechanism from charged particles such as electrons and positrons, in circular motion at relativistic energies. The properties of synchrotron light emitted from electrons with velocities near that of light are drastically different from the classical dipole radiation [1] and demonstrate its importance as a novel and powerful light source [2]. Synchrotron radiation was experimentally discovered by Elder et al. [3] using the General Electric 70 MeV betatron and studied theoretically by Schwinger [1]. The properties of synchrotron radiation may be summarized [4] as follows: i) broad spectral distribution tunable from IR to the x-ray region; ii) higher intensity, > 10^6 times that of an x-ray tube; iii) plane polarized, with the electric vector in the orbital plane of the circulating particles; iv) high natural collimation, which is important for small specimens and v) sharply pulsed time structure. A detailed historical account of the discovery has been given by Pollock [5].

The spectral distribution of synchrotron radiation from the Stanford Positron-Electron Accumulation Ring (SPEAR) [4] is shown in Figure 1 with the electron beam energy E_e from 1.5 to 4.5 GeV as the parameter. As can be seen, the radiation is an intense continuous distribution extending from the infrared into the hard X-ray regime of the electromagnetic spectrum. Compared with the Bremsstrahlung output of a 12 kW standard X-ray tube, synchrotron radiation is higher in intensity by a factor of 10^6 or more. This reduces the measurement time for a typical diffraction measurement from hours to seconds or less.

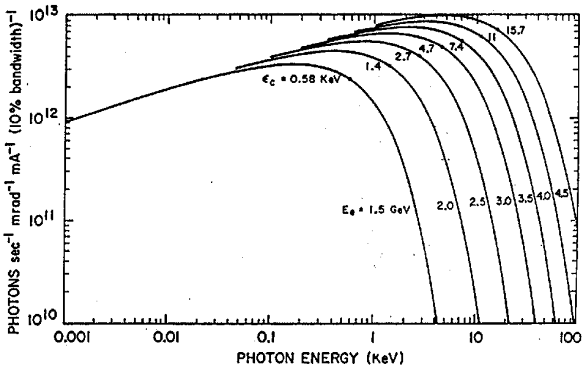

Figure 1. *Spectral distribution of synchrotron radiation from SPEAR having a radius of curvature of 12.7 m. After Doniach et al. [4].*

Fusion Welds

During fusion welding, rapid thermal cycling induces solid state phase transformations both on heating and on cooling, and causes melting and solidification in those parts of the weld where the liquidus temperature has been exceeded. From a practical standpoint, solid state phase transformations play an important role in welding related problems such as sub-solidus cracking, cold cracking and distortion caused by residual stresses [6-8]. Solution and understanding of these problems will greatly be facilitated by the development of experimental methods capable of determining phase transformation behavior in the steep thermal gradients and at the high cooling rates that occur *during* welding. Until a few years ago [9] no direct method existed for investigating solid state phase transformations that *are* taking place in fusion welds.

In this paper, we briefly describe a couple of novel synchrotron-based diffraction techniques that have been developed and applied successfully to investigate the phase distribution, transformation kinetics and chemical dynamics in the fusion welds of a number of metallurgical systems. These include a commercially pure titanium, and *AISI* 1005 carbon-manganese steel.

Synchrotron Diffraction Methods

Space-resolved X-ray diffraction (SRXRD).

The high intensity provided by synchrotron radiation emitted from a multi-pole wiggler insertion device was used to advantage to produce a sub-millimeter probe to record diffraction patterns as a function of position in the weld during welding to follow the phases and map their location in the heat affected zone (HAZ) or the fusion zone (FZ). The measurements were first performed on the 31-pole wiggler beam line, BL 10-2 [10] at Stanford Synchrotron Radiation Laboratory (SSRL) with SPEAR operating at an electron energy of 3.0 GeV and an injection current of

~100 mA. The synchrotron white beam was first focused by a toroidal mirror to the source size of ~1mm vertical x 2mm horizontal, and monochromatized downstream with a double Si(111) crystal. The focused monochromatic beam was then passed through a tungsten pinhole to render a sub-millimeter beam on the sample at an incident angle of ~25°. A photon energy of 12.0 keV (λ = 0.1033 nm) was chosen to maximize the number of Bragg peaks in a selected 2θ window to facilitate phase identification, and to be far enough in energy above the Ti and Fe-edges to minimize the background contribution due to Ti or Fe K-fluorescence from the sample (K-edge: Ti = 4.966 keV, Fe = 7.112 keV) [11].

SRXRD patterns were measured during welding by positioning the beam at a pre-determined location with respect to the welding electrode. A 50 mm, 2048-element position sensitive silicon photodiode array detector was used to record the diffraction patterns. The detector together with the associated ST121 data acquisition system were manufactured by Princeton Instruments (now Roper Scientific) [12], and was used to store and display the X-ray diffraction data in real time. By incrementally jogging the weld to new locations in 200 μm intervals, a series of space-resolved X-ray diffraction patterns was collected along a lineal scan direction perpendicular to and away from the centerline of the weld. A schematic of the SRXRD setup is shown in Figure 2. Details of the apparatus has been given elsewhere [13].

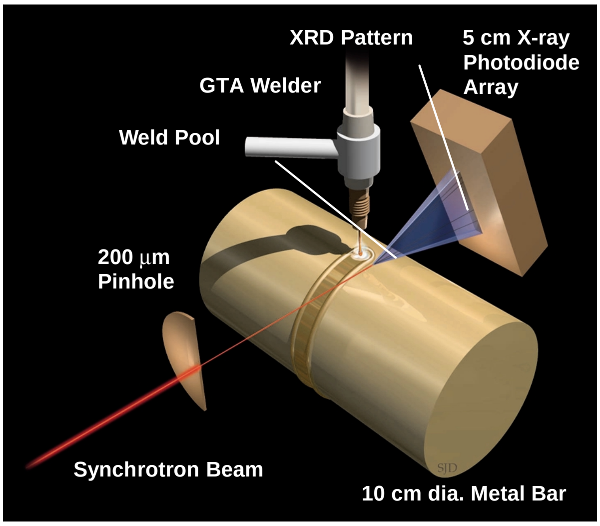

Figure 2. *Schematics of the SRXRD setup for in-situ phase mapping and real time observation of phase transformation in fusion welds [13].*

Figure 3 is a plot of an experimental SRXRD run of a carbon-manganese fusion weld at 1.9 kW. The starting position was 2.0 mm from the center of the weld. The data were collected using a 10 keV photon beam, a pinhole of 180 μm, jog size 200 μm/step and an integration time of 20 s/scan. It can be seen that in the first 8 jogs, no Bragg peaks were recorded indicative of the liquid state. The δ(110) reflection appeared at jog #9. This was followed by 11 frames of pure γ(fcc), beyond which, γ and α coexisted for another 9 frames. At frame 29 and beyond, only α persisted as the X-rays now probed the base metal.

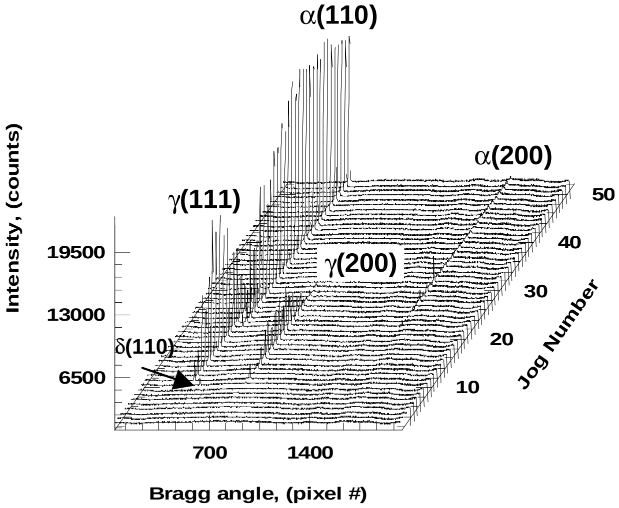

Figure 3. *An experimental SRXRD scan recording the sequence of phase transformation from the liquid → δ□(bcc) → γ□(fcc) → α□(bcc) as a function of position in a carbon-manganese fusion weld at 1.9 kW.*

Time-resolved x-ray diffraction (TRXRD).

The TRXRD procedure consists of first positioning the X-ray beam at a pre-determined location in the FZ or HAZ using the electrode position as center of the liquid pool. Experimentally, a time resolution of 100 ms in conjunction with a 260 μm pinhole was adequate to capture the $\alpha \rightarrow \gamma$ phase transformation upon heating and the $\gamma \rightarrow \alpha$ transformation upon cooling in the HAZ of plain carbon steel welds. For phase transformations in the FZ, a 50 ms time resolution using a 730 μm pinhole was used to incorporate more grains into the diffraction beam [14]. The TRXRD technique was originally developed for chemical dynamics study of fast, high temperature solid combustion reactions [15,16].

Phase Mapping

Commercially Pure Titanium.

In commercially pure grade 2 titanium, the allotropic transformation from a hcp α-phase to a bcc β-phase occurs at ~915^{o}C. A transition from a β-Ti bcc pattern at high temperature inside the HAZ, to a α+β-mixed zone, and eventually to the α-Ti hcp pattern have been recorded in real time. In addition to phase transformations, the material undergoes annealing and re-crystallization in the cooler region and outside of the HAZ. SRXRD data obtained from different starting positions with respect to the weld center may be classified into five principal diffraction patterns. Examples for each of the principal patterns are displayed in Figure 4 together with one for the α+β-coexistence region.

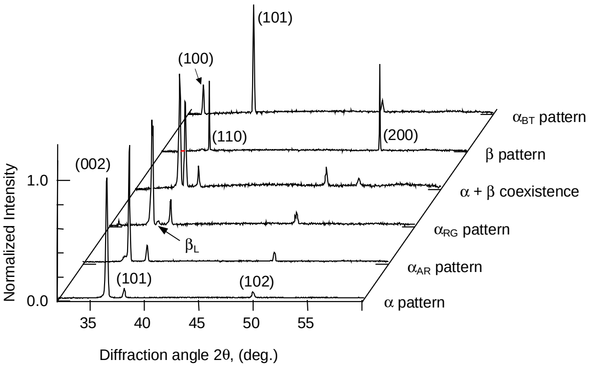

Figure 4. *Principal diffraction patterns observed in various locations in the HAZ of commercially pure Ti fusion weld. Intensity is normalized to unity for the highest peak in each pattern [18].*

In Figure 5 the completed phase map presenting the locations of four principal diffraction patterns plus β_L with respect to the HAZ of the weld is shown. Twenty one individual scans, each having 40 XSRXRD patterns, are displayed together with two calculated weld isotherms. For scans presented by two bars side-by-side, the left bar represents the presence of α-Ti and the right bar for β-Ti. Each bar again is subdivided into regions with different shadings to indicate the different types of diffraction patterns that were present: (α_{AR}) is the annealed and recrystallized α-Ti; (α_{RG}) denotes a recrystallized α-Ti phase which exhibits large diffraction domains; (α_{BT}) is the back transformed α-Ti that forms from the region of the HAZ that once contained β-Ti; (β) is the β-Ti phase; (β_L) is the β-Ti that coexists with α-Ti in low amounts predominantly together with α_{BT}. The α pattern is not shown in this phase map since the SRXRD data were not recorded far enough in to the cold region of the HAZ. The principal diffraction patterns and associated microstructure have been described in detail elsewhere [17,18].

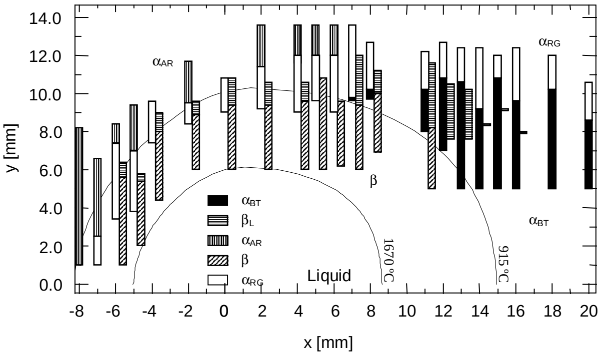

Figure 5. *Complete phase map of a 1.9 kW fusion weld of commercially pure titanium and calculated transformation isotherms [18].*

AISI 1005 Carbon-Manganese Steel.

In Figure 6 the completed phase map and the distribution of the α-Fe, γ-Fe, δ-Fe, and liquid phases in the HAZ are shown. The coexistence of γ-Fe with α-Fe, or γ-Fe with δ-Fe, was identified at numerous SRXRD locations as evidenced by simultaneous recording of the fcc and bcc diffraction patterns. These regions indicate either a phase is in the process of transforming or that two phases are coexisting in a two-phase region of the HAZ. Superimposed on Figure 6 are three major weld isothermal boundaries calculated using an analytical heat flow model described elsewhere [19]. The calculated isotherm at 1529°C represents the liquid weld pool boundary, which extends 4.4 mm from the weld centerline, and was made equal to the actual weld pool width by adjusting the heat source distribution parameter [19]. The γ/(γ+α) boundary is represented by the 882°C isotherm, and the $Fe_3C/(\alpha+\gamma)$ eutectoid is represented by the 720°C isotherm. These calculated boundaries represent the locations where phase transformations would occur under equilibrium conditions. However, since the kinetics of the phase transformations require a finite time to take place, the location where the phase transformation is finally completed is displaced behind the calculated isotherms. Thus, the calculated isotherms represent the point where the phase transformations *can* begin to occur; the locations where the transformations are complete can be determined by SRXRD measurements. The difference between the calculated isotherms (start locations) and the SRXRD completion locations is related to the kinetics of a given phase transformation.

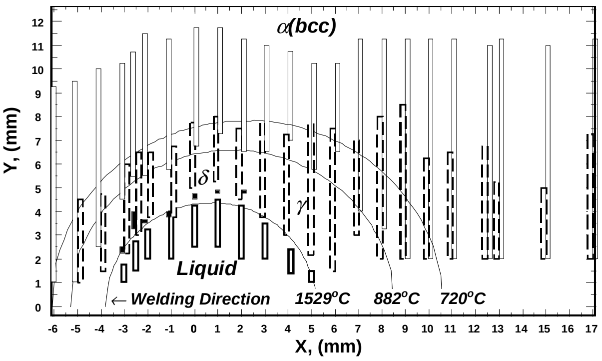

Figure 6. *SRXRD map showing the locations of the α-Fe, γ-Fe, δ-Fe and liquid phases present in the AISI 1005 steel fusion weld at 1.9 kW. The calculated weld isotherms are superimposed on to the critical phase transformation temperatures. Notations - α: thin line; γ: dotted line; δ: filled; liquid: thick line [19].*

Phase Dynamics

AISI 1005 carbon-manganese steel may be considered as a pseudo-binary Fe-C system containing 0.05 wt% of carbon. With increasing temperature, the system undergoes the following transformations: α(bcc) → γ(fcc) → δ(bcc) → liquid. The phase distribution and microstructural evolution in the vicinity of this fusion weld has been studied using SRXRD [19]. The nature of the solidification product from the liquid pool, and the chemical dynamics associated with the α→γ transformation in a positive thermal gradient (heating) and the γ→α transformation in a negative thermal gradient (cooling) have also been recently elucidated in detail with a time resolution down to 50 ms [14]. With an experimental weld pool width of 8.5 mm, and by positioning the X-ray beam at a position 5 mm and another at 3 mm from the electrode, one can now probe the dynamics of phase transformation in the HAZ and FZ of the steel weld respectively. The results are summarized as follows.

***Phase Transformation in the HAZ*.**

Figure 7 shows a series of TRXRD patterns recorded in the HAZ at a location 5 mm away from the center of the liquid pool. The data were recorded with a time resolution of 100 ms. For clarity of presentation, only every 15th of the 600 TRXRD patterns is shown in the pseudo 3D plot given in Figure 7a. As the arc was turned on and off, diffraction patterns were continuously recorded to follow the annealing and phase transformations in real time in both the heating and cooling cycles. Frame-by-frame qualitative analysis of the TRXRD data yielded a real time sequence of events in the HAZ, schematically given in Figure 7b. In this plot, t = 0 corresponds to the start of TRXRD measurement at room temperature. At t = 1.0 s, the arc was turned on and heating began. Annealing of the bcc α-phase took place in the next 7.1 s. At t = 8.1 s, the fcc γ-phase first appeared, marking the start of the α→γ transformation. This transformation was completed within 1.1 s, and at t = 9.2 s, only γ-Fe existed and persisted for the whole length of time the arc was on.

At t = 25.0 s, the arc was turned off. The γ-phase cooled and at t = 25.7 s, the first back-transformed α-Fe was observed, signifying the start of the reverse γ→α transformation. At t = 26.1 s, all γ-Fe disappeared, denoting completion of the γ→α. transformation. From then, only α-Fe existed and cooled with time. It is interesting to note that the α→γ transformation upon heating takes about twice as long as the γ→α transformation upon cooling.

Phase Transformation in the FZ.

In Figure 8a, the TRXRD patterns recorded in the FZ at a position 3 mm away from the center of the liquid pool are shown. The data were recorded using a time resolution of 50 ms [14]. Again, for graphic clarity, only every 15th of the 600 TRXRD patterns is shown. Frame-by-frame qualitative analysis of the TRXRD data yielded the following real time sequence of events in the FZ schematically show in Figure 8b.

Again, t =0 corresponds to the start of TRXRD measurement at room temperature. At t = 1.20 s, the arc was turned on and heating began. Annealing of the bcc α-phase took place in the next 1.30 s, which was much shorter than that (7.1 s) in the HAZ. At t = 2.50 s, the fcc γ-phase first appeared, marking the start of the α→γ transformation in the FZ on heating. Similar to that in the HAZ, this transformation was completed within 1.10 s, and at t = 3.60 s, only γ-Fe existed and persisted for an interval of 10.50 s. At t = 14.10 s, all γ disappeared and no diffraction peaks were observed signifying the system melted.

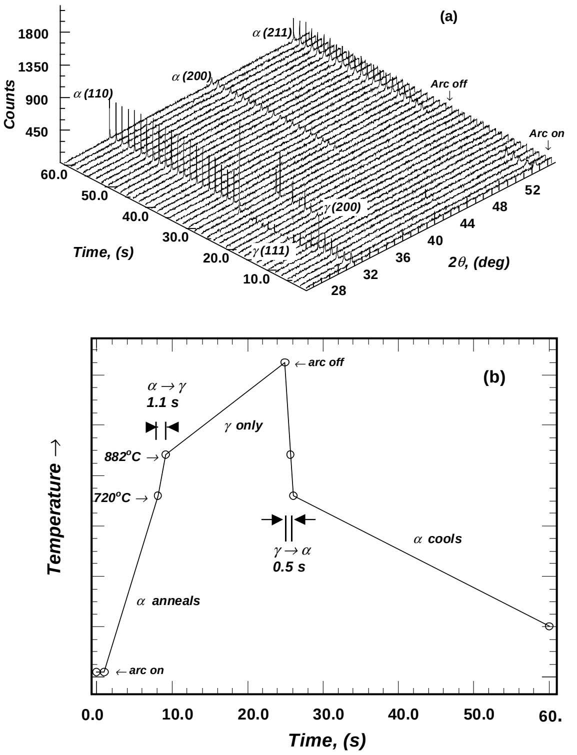

Figure 7. *(a) TRXRD patterns recorded in the HAZ of a 1.9 kW carbon-manganese steel spot weld at a position 5 mm from the weld center with 100 ms time resolution. For clarity, only every 15th of the 600 frames is plotted. (b) Temperature-time schematics depicting the recorded TRXRD events shown in (a). After [14].*

At 17.35 s, the arc was turned off. The γ-phase reappeared and cooled. At = 18.10 s, the first back transformed α-Fe was observed, signifying the start of the γ→α transformation. At t = 18.65 s, all γ-Fe disappeared, denoting completion of the γ→α transformation. From then, only α-Fe existed and cooled with time. It is interesting to note that, also in the FZ, the α→γ transformation upon heating takes about twice as long as the γ→α transformation upon cooling.

Profile analysis [14] of the major Bragg reflections recorded in these TRXRD patterns reveals similarities and differences in the microstructural evolution with time in the HAZ and in the FZ. The latter undergoes melting and solidification in addition to solid state transformations. With increasing temperature, the cell constant of the α-phase prior to and during the α→γ transformation and that of the γ-phase just after the same transformation exhibit a decrease. This unusual lattice contraction with temperature rise may be attributed to dynamical processes involving diffusion of impurities or alloying elements. In the FZ, the γ-Fe that forms has a preferential (200)-texture upon solidification of the liquid, whereas upon cooling in the

HAZ, the γ-Fe retains largely a (111)-texture induced in the α→γ transformation on heating. Upon cooling in the HAZ, the width of the γ(111) reflection increases initially, indicative of micro-strain developing in the fcc lattice, but decreases as expected with reduction of thermal disorder upon further cooling all the way to the completion of the γ→α transformation. In the FZ, however, the micro-strain in the γ-phase increases steadily upon solidification, and more rapidly in the entire duration of the γ→α transformation on further cooling. The final microstructure of the FZ is likely to consist of a single α-phase dispersed in two morphological entities, whereas in the HAZ, the α-phase persists in one morphological entity in the final microstructure [14].

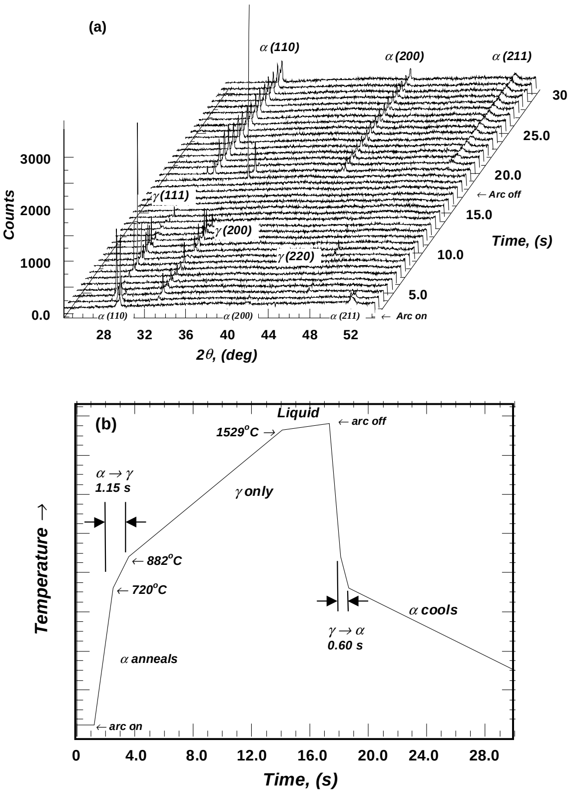

Figure 8. *(a) TRXRD patterns recorded in the FZ of a 1.9kW carbon-manganese steel weld at a position 3 mm from the weld center with a 50 ms time resolution. For clarity, only every 15th of the 600 frames is plotted. (b) Temperature-time schematic depicting the recorded TRXRD events shown in (a).*

Concluding Remarks

1. The synchrotron SRXRD and TRXRD methods have produced for the first time both real space and real time data on the phases, their location and transformation time in the HAZ and FZ of fusion welds.
2. Profile analysis of the Bragg reflections associated with various occurring phases yielded detailed information on their microstructure in terms of annealing, re-crystallization, grain growth, texturing as well as micro-strain with the grains.
3. These in-situ crystallographic and microstructural data must be taken into account for realistic and meaningful modeling of transformation kinetics in fusion welds [20] and serve as test beds for evaluating models for phase transformation in these technologically important systems.

Acknowledgements

This work was performed under the auspices of the US Department of Energy by the University of California, Lawrence Livermore National Laboratory under Contract No. W-7405-Eng-48. The author would like to thank J.W. Elmer, E.M. Larson, M. Froeba, T. Ressler, P.A. Waide and A. Teruya for their collaboration and technical support in the course of developing these synchrotron tools for welding metallurgy.

References

[1] J. Schwinger, Phys. Rev., **75**, 1912 (1949).

[2] H. Winick, in H. Winick and S. Doniach (eds), *Synchrotron Radiation Research*, Plenum Press, New York, (1980), p. 11.

[3] F. Elder, R. Langmuir and H.C. Pollock, Phys. Rev., **74**, 52 (1948).

[4] S. Doniach, I. Lindau, W.R. Spicer and H. Winick, J. Vac. Sci. Technol., **12**, 1123 (1975).

[5] H. C. Pollock, Am. J. Phys., **51**, 278 (1983).

[6] *International Conference on Trends in Welding Science and Technology*, ed. S.A David and J.M. Vitek, ASM Intern., **1993**

[7] B.K. Damkroger, G.R. Edwards and B.B. Rath, Welding Journal, **68**, 290, (1989).

[8] M.C. Mcquire, M.L. Santella and B.K Damkroger, in *The Science of Metal Joining*, ed. by M. H., Cieslak, J. Perepezko, S. Kang and M.E. Glicksman, TMS (1992), p.41.

[9] Joe Wong, J. W. Elmer, P. Waide and E.M. Larson, Adv. X-Ray Analysis, **37**, 479 (1994).

[10] V. Karpenko, J.H. Kinney, S. Kulkarni, K. Neufeld, C. Poppe, K.G. Tirsell, Joe Wong, J. Cerino, T. Troxel, J. Yang, E. Hoyer, M. Green, D. Humpries, S. Marks and D. Plate, *Rev. Sci. Instrum.*, 60, 1451 (1980).

[11] J. A. Bearden and A. F. Burr, Rev. Mod. Physics, **39**, 125 (1967).

[12] ST121 Detector and Controller Manual, Princeton Instruments Rev. B. (1996).

[13] Joe Wong, M. Fröba, J.W. Elmer, P.A. Waide, E. Larson, J. Mater. Sc., **32**, 1493 (1997).

[14] Joe Wong, T. Ressler and J.W. Elmer, J. Synchrotron Rad. **10**, 154 (2003).

[15] Joe Wong, E. M. Larson, J.Holt, P.Waide, B. Rupp and R. Frahm, Science, **249**, 1906 (1990).

[16] E.M. Larson, Joe Wong, J. Holt, P. Waide, B. Rupp and L. Terminello, J. Mater. Res. **8**, 1533 (1993).

[17] J. W. Elmer, Joe Wong and Thorsten Ressler, Met. Mat. Trans. **29A**, 2761 (1998).

[18] T. Ressler, Joe Wong and J.W. Elmer, J. Phys. Chem. B, **102**, 10724 (1998).

[19] J. W. Elmer, Joe Wong and T. Ressler, Metal. Mater. Trans. **32A**, 1175 (2001).

[20] Z. Yang, J.W. Elmer, Joe Wong, and T.DebRoy, *Welding Journal*, **79**, 97s (2000).

SDPD Round Robin 2002 Results

Armel Le Bail,(1) ***and Lachlan Cranswick*** (2)
(1) *Université du Maine, CNRS UMR 6010, Avenue O. Messiaen, 72085 Le Mans, France*
alb@cristal.org
(2) *CCP14 - School of Crystallography, Birkbeck College, Malet Street, Bloomsbury, WC1E 7HX, London, UK*
l.m.d.cranswick@dl.ac.uk

Introduction

The total number of structure determinations by powder diffractometry (SDPD) is now more than 600. It has almost doubled during the last 4 years, since the first 1998 SDPD round robin (RR) [1-2]. Four years ago, the routine solution of 15-30 non-hydrogen-atom structures from powder data was not demonstrated at the SDPDRR-1. Although more than 70 potential participants downloaded the data, only two solutions were provided (by using the *DASH* program and the *CSD* package - software descriptions and Internet hyperlinks can be found at the CCP14 [4]) for the pharmaceutical sample (≈30 non-H atoms), and none for the inorganic one (15 non-H atoms). Four years later, we observe that the number of structures solved by SDPD remains below 100 per annum, in spite of an explosion of the number of different software packages available for powder structure solution, commercial as well as in the public domain or even open source, suggesting that a user could be lost in the maze and might not know which button to press. By the end of the XIXth IUCr congress (Geneva, August 2002), it was thus considered timely to verify if SDPD on demand had really become routine, meaning that software in hands other than those of their developers would produce solutions with some regularity and ease.

Samples and schedule

The first SDPD round robin was made knowing the cell and space group parameters. Thus, the indexing bottleneck was avoided. A number of attendees at the IUCr 2002 Geneva congress were interested in an indexing round robin, The SDPDRR-2 was thus organized in two steps [3] :

1- Indexing - September 9 to October 13, 2002 - 8 powder patterns
2- Structure solution and refinement - September 9 to November 17, 2002 - 3 powder patterns

The results of the indexing step were disclosed on October 14, 2002, because the experts in indexing could be different from the experts in structure solution. Owing to the presupposed larger difficulty at step 2, only the first three of the eight powder patterns to be indexed at step 1 were considered for the structure solution step 2. The description of the samples was the following :

Sample 1 - probable formula $Al_2F_{10}[C_6N_4H_{20}]$ - probable impurity : pyrochlore structure, cubic, *Fd*3*m*, a ≈ 9.8 , with possible formula $Al(F,OH)_3.xH_2O$ - Cartesian coordinates provided for the $C_6N_4H_{20}$ molecule, as found in $C_6N_4H_{20}.Cl_4$ - crystal chemistry : the usual behaviour of Al in F environment is to form AlF_6 octahedra - reflection laboratory X-ray data from a Bruker D8 Advance diffractometer, CuKalpha, recorded from a micro sample (40 mg).
Sample 2 - probable formula $Sr_5V_3(F/O/OH/H_2O)_{22}$ - capillary synchrotron data, $\lambda = 0.79764$ Å.
Sample 3 - probable formula $C_{61}Br_2$ - Cartesian coordinates provided for the C_{60} molecule - capillary synchrotron data, $\lambda = 0.79764$ Å.
Sample 4 - probable formula $C_{20}H_{12}O_6$ - capillary synchrotron data, $\lambda = 0.79776$ Å.
Sample 5 - probable formula $C_{16}H_{26}O_6$ - capillary synchrotron data, $\lambda = 0.79776$ Å.
Sample 6 - probable formula $C_{21}H_{15}Bi_2O_9$ - capillary synchrotron data, $\lambda = 0.79764$ Å.
Sample 7 - probable formula $C_7H_5BiO_4$ - capillary synchrotron data, $\lambda = 0.79764$ Å.
Sample 8 - probable formula $Rb_7Cr_6F_{25}$ - reflection laboratory X-ray data from a Bruker D8 Advance diffractometer, CuKalpha.

The hunt for accurate peak positions is software- and user-dependent. The round robin participants were encouraged to use the software of their choice, though a list of peak positions was provided for each sample, obtained by using *PowderX* in default peak-finding mode. At step 1, we expected only one cell proposal from every participant, for each sample (or at least for samples 1-3 from people making SDPDs routinely), together with the list of indexed peaks, and figures of merit, the name of the software (for indexing and peak position hunting), a statement telling if the cell was ascertained by applying *CHEKCELL* or/and a whole pattern fitting decomposition program (if yes, the software name and the method name - Pawley or Le Bail fit, etc), and finally a space group proposal (telling if estimated manually or with the help of software, giving the software name, if any), plus explanations judged necessary (use of databases like CSD, ICSD, ICDD, etc). However, giving a list of possible unchecked cells ordered by decreasing value of figures of merit was accepted too. Robin Shirley passed on CDT files (converted from the *PowderX* peak list) ready for using the *CRYSFIRE* suite (which links to over eight indexing programs). One can note that a new Monte Carlo indexing software (*McMaille*) was born during the round robin and that improvements of *Index*, by Joerg Bergmann, were proposed. For step 2, all details of the structure solution and refinement were expected to be provided by the participants on a form available at the SDPDRR-2 Web site [3]. Slightly more than 100 participants downloaded the data.

Results and discussion

A citation is appropriate, from a chapter of the recent book "Structure Determination from Powder

Diffraction Data" [5] : "*Sadly, despite the excellent quality of synchrotron data and the ingenuity of the scientists who collect it, not all structures can be solved. Every laboratory has a supply of powder data sets which stubbornly refuse to yield to structure solution. It is the existence of these sets that will act as a continual challenge to both instrumental and algorithmic developments*." We completely subscribe to that statement. It suggests that the more than 600 structures determined *ab initio* from powder diffraction during the last 20 years are the tip of the iceberg. SDPD is known to be quite difficult, but scientists are secret about their failures, so that SDPD could even be much more difficult than usually admitted. It was thus decided to include in this second SDPD round robin some of those (splendid) "*data sets which stubbornly refuse to yield to structure solution*." These are samples 4-8 for which we had no structure solution, so that the cell proposals themselves cannot be confirmed. Of course, some samples having known (unpublished) solutions were also incorporated (samples 1 to 3).

Step 1 : The indexing bottleneck - Six participants sent results in due time for step 1, giving generally cell parameters for samples 1 to 3. Only one participant suggested cell parameters for samples 5, 7 and 8 of the supplementary series (samples 4 to 8). These contributions appeared so scarce (6% return rate) that it was announced that post-deadline proposals would be accepted.

Table 1. Participant (Pn) cell proposals to samples 1-8 (Sn)

	S1	S2	S3	S4	S5	S6	S7	S8
P1	X	X	X					
P2	X	X	X					
P3	X	X	X					
P4		X						
P5	X	X	X		X		X	X
P6	X	X	X					

For samples 1-2, all the returned cell proposals were correct (sample 1, monoclinic : a = 10.323 Å, b = 7.395 Å, c = 8.535 Å, β = 91.29°; sample 2, monoclinic : a = 11.239 Å, b = 8.194 Å, c = 19.943 Å, β = 106.727°). Sample 3 is cubic (a = 18.88 Å), it was proposed by three of the five participants having sent a cell proposal, while the two remaining ones proposed a tetragonal subcell (possibly due to default volume restrictions in the software used - but an application of the LePage algorithm via *Chekcell* should have revealed the error). Software or program suites used were *CRYSFIRE* (P1, P3), *DICVOL* (P2), *ITO* (P4), *Index* (P5) and *X-Cell* (P6).

For samples 4 to 8, only one response was obtained in due time for three of the five data - using the *Index* software of Joerg Bergmann [6].

More post-deadline results were sent by participants 5 and 6 (the latter using *X-Cell* [7]). Without any crystal structure, we can neither confirm nor invalidate these cell proposals. These samples 4-8 are part of the great mass of iceberg under the surface.

Table 2. Post-deadline cell proposals to samples 1-8.

	S1	S2	S3	S4	S5	S6	S7	S8
P5	X	X	X	X	X		X	X
P6	X	X	X	X	X	X	X	X

It appears that powder indexing is not easy and not routine. It is known since three decades that bad data are the main cause of indexing failures. "Bad" data means both inaccurate and impure. Efforts are made in some indexing software in order to be more efficient with at least a two-phases mixture, since inaccuracy can be fought by more efforts at the recording step for well crystallized samples. However, the main problem is that an indexing software user may not have the information that the data are either inaccurate or impure or both.

Nowadays, indexing is not simply the application of an indexing software which may produce several different cells with neighbouring figures of merit. The whole suite of operations after recording a powder pattern and after failing to identify any known compound (search/match process [8]) is (in brackets are given the techniques/software selected by the participants) : peak search [*PowderX* - as provided with the round robin data; *WinPlotr*; *CMPR*], indexing *sensu stricto* [see list above], cell reduction [*LePage*], visual checking and more [*Chekcell*], whole pattern fit checking [*Fullprof*; *Rietica*; *Materials Studio*; Pawley/Le Bail methods], space group proposal [*Chekcell*, *Materials Studio*, manual]. The cell proposals have to be checked against the whole pattern, not only the 20-30 first peak positions, and this produces cell parameters refinement as well as more data for estimating systematic extinctions from which one or several possible space groups are deduced. The next step (structure solution) can be quite time-consuming, so that a powder diffractionist will not make any further effort if the probability to have found the true cell and space group is not high (this is a question of self-convincing, as indexing is still considered as an art).

Step 2 - Structure solution and refinement - Two participants sent successful results for samples 1 and 2 (none for sample 3). This is no more than for the SDPDRR-1 in 1998. The software used are *FOX* (P2) [9] and *TOPAS* (P7) [10].

Table 3 - Participant (Pn) structure proposals to samples 1-3.

	S1	S2	S3
P2	X	X	
P7	X	X	

Participant 2 solved the sample 1 structure by using *FOX* according to the following strategy : location of structural units in direct space by simulated annealing in the parallel-tempering mode. Three independent entities (two AlF_6 octahedra and the $C_6N_4H_{20}$ molecule) were allowed to rotate and move in the *P*2/*c* space group, corresponding to 18 degrees of freedom. The final Rietveld refinement was made by using the *FULLPROF* software. Much more details are given by the participants at the SDPDRR-2 Web site [3].

Participant 7 solved the sample 1 structure by using *TOPAS* according to the following strategy : molecule location in direct space, simulated annealing, structure determination using step intensity data, starting with 3 "rigid" bodies (including 2 for AlF_6 octahedra). For the $C_6N_4H_{20}$ molecule, 3 rotational and 3 translational degrees of freedom and 4 torsion angles were used.

Participant 2 solved the sample 2 structure with *FOX* in a similar way as for sample 1 : either 3 tetrahedra VO_4 and 5 cubes SrO_8 or 3 octahedra VO_6 and 5 cubes SrO_8 were rotated and translated (48 degrees of freedom in both cases). Both models have yielded the same correct positions for the cations. The positions of anions were determined by third modeling using free atoms.

Participant 7 solve the sample 2 structure with *TOPAS* by putting into the cell 30 independent atoms (no constraint/restraint) at random positions, locating them by simulated annealing.

Computer programs used by the organizers for the step 1 (indexing) were *TREOR*, *DICVOL*, *ITO*, *CRYSFIRE*, *McMaille*, and for step 2 (structure solution) *SHELXS* (sample 2) and *ESPOIR* (samples 1 and 3). Sample 1 was solved in the *Pc* space group by using 3 objects in the *ESPOIR* program (one AlF_6 octahedron, one AlF_4 square plane and the C_6N_4 molecule - fig. 1). *SHELXS* solved the sample 2 structure by direct methods, quite easily. *ESPOIR* could also solve the sample 2 structure in "scratch" mode (all atoms random at the beginning, going to their right place by Monte Carlo - fig. 2). Sample 3 could not be "solved" unless a global scattering factor for a sphere was used for modelling a disordered C_{60}. The Br atoms appeared located partially at 2 positions in the *I*-43*m* space group (fig. 3).

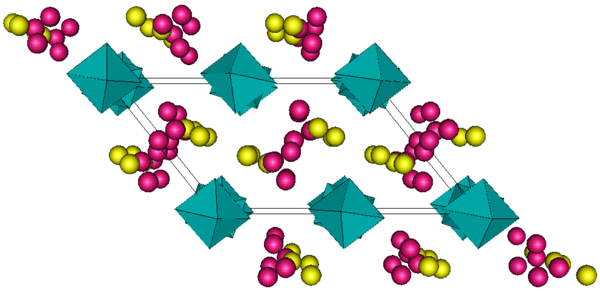

Figure 1. *Projection of the sample 1 structure along the b axis (H atoms not represented)*

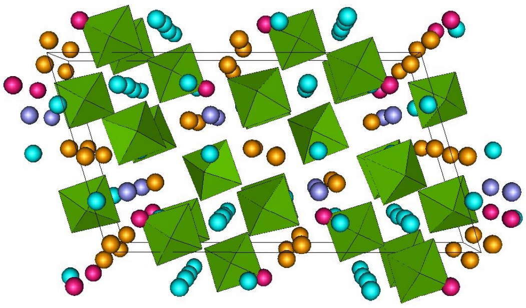

Figure 2. *Projection of the sample 2 structure along the b axis.*

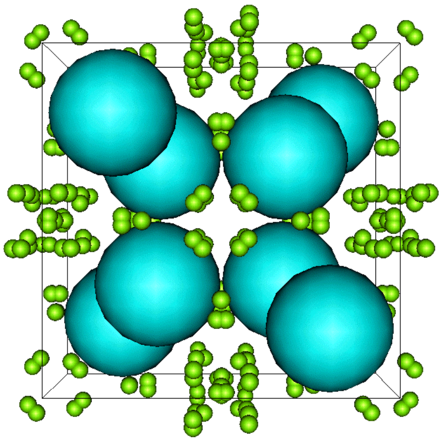

Figure 3. *The $C_{60}CBr_2$ mean structure model for sample 3. Big spheres represent the C_{60} molecules. Small spheres are the Br atoms.*

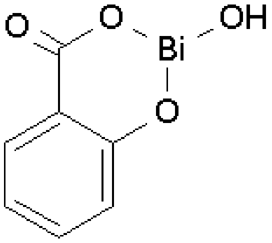

Figure 4. *Molecular formula for sample 7.*

The SDPDRR-2 is still open for post-deadline structure solution results for samples 4-8. More details can be found on these samples which could help. For instance, sample 7 is a commercial bismuth sub-salicylate [CAS: 14882-18-9] whose formula $C_7H_5BiO_4$ can also be found written as 2-(HO)$C_6H_4CO_2$BiO (pepto-bismol, a drug for traveler's diarrhea - can give you a black tongue). It was shown (together with sample 3) at the IUCR XVIII conference, (Glasgow, 1999), in a poster comparing the merits and advantages of synchrotron versus conventional X-ray [11]. Its molecular formula appears quite simple (fig. 4).

Conclusion

The two months allocated for solving at least one of 3 structures by SDPD methodology would have been quite enough if SDPD was routine (a rainy evening would have been sufficient). Only two final answers for samples 1 and 2 suggest that either SDPD experts are lazy or SDPD is still not routine. This will be the main SDPDRR-2 conclusion. Anyway, three computer programs certainly deserve special mention because they could provide exceptional results in due time : *Index* for indexing (participant 5) and *FOX* (participant 2) as well as *TOPAS* (participant 7) for structure solution. The SDPDRR-2 seems to establish the triumph of direct space methods (*FOX*, *TOPAS*). But statistics cannot seriously be deduced from two contributions (owing to the number of data downloads, the return is less than 2%). Considering that still fewer than 100 SDPDs are published per year, it was clearly utopian to expect that 3% of them could be solved in 2 months by people extremely busy at solving their own difficult problems. The final examination of the SDPD Internet Course [12] involves a complete SDPD, the subscribers having two weeks for the structure determination of a moderatly complex case. Some are able to finish the job in less time (4-5 days). Since subscribers at the end of the course become experts, this may define the mean time needed for a simple SDPD. That prohibiting time of several days may lead to a choice : either participants solve their own problems or they solve the round robin problems. Ordinary users could have preferred to solve their own problems. But software developers have other motivations which are to promote their product, in principle, so that wasting days to solve the round robin problems may appear worthwhile to them. Is the absence of software like *EXPO*, *DASH*, *POWDERSOLVE*, *PSSP*, *MRIA*, *FOCUS*, *SIMULATED ANNEALING*, *ENDEAVOUR*, *EAGER*, *OCTOPUS*, *SAFE* (etc) indicative of failure to solve or of lack of willing to solve ? We do not have answers.

For those wanting to continue to play with the SDPDRR-2 data sets, they will remain available [3], in the hope that they will not definitely stay in a category "*which stubbornly refuse to yield to structure solution*". Anyway, a doubling of the total number of SDPDs is expected again during the next four years, this will have to correspond to a new revolution that would allow 200 structures to be determined per year. A rendezvous is given for the SDPDRR-3 in 2006, expecting more successful participants than just two or three out of over a hundred participants.

References

[1] http://www.cristal.org/SDPDRR/

[2] http://www.iucr.org/iucr-top/comm/cpd/Newsletters/no25jul2001/cpd25.pdf

[3] http://www.cristal.org/sdpdrr2/

[4] CCP14: http://www.ccp14.ac.uk/

[5] P.W. Stephens, D.E. Cox & A.N. Fitch, in *Structure Determination from Powder Diffraction Data,* eds. W.I.F David, K. Shankland, L.B. McCusker & Ch. Baerlocher, Oxford Science Publications, Chapter 4 (2002) 49-87.

[6] http://www.bgmn.de/related.html

[7] M.A. Neumann, *J Appl. Cryst.* (2003). **36**, 356.

[DOI 10.1107/S0021889802023348]

[8] http://www.cristal.org/smrr/

[9] http://objcryst.sourceforge.net/

[10] http://www.bruker-axs.de/index.html?page=/products/gd/topas.php

[11] http://sdpd.univ-lemans.fr/glasgow/poster/glasgowposter.html

[12] http://sdpd.univ-lemans.fr/course/

The SDPD Internet Course in its Fourth Year - Overview

Armel Le Bail, Yvon Laligant and Alain Jouanneaux
Université du Maine, Avenue O. Messiaen, 72085
Le Mans, France
alb@cristal.org

The Structure Determination by Powder Diffractometry (SDPD) Internet Course [1-3] is a distance teaching/learning service which started in September 1999 at Le Mans University (France). A total number of 30 PhD-level participants have subscribed (12 in 2000, 6 in 2001 as well as in 2002 and 2003). They come from 18 countries: Algeria (1), Belgium (1), Canada (1), China (1), Cuba (1), UK (2), France (1), Germany (1), Greece (1), India (2), Israel (1), Italy (1), Japan (1), Korea (3), Portugal (1), Spain (2), Sweden (2) and USA (7), and five more have declared a recent interest, which could increase the participant number to 35, if confirmed. The English content of the course (in 10 sessions) mainly covers: phase identification, indexing, intensity extraction, structure solution using conventional (Patterson and direct methods) and direct-space techniques, structure completion and refinement by the Rietveld method. Participants are guided (instructions and documents sent by email) through lectures and solved exercises and are provided with a list of software to download. At the end of every session, they have to solve exercises by themselves.

The course is asynchronous (every participant going at his own speed), and registration is open all the year. The minimum duration for the course is 3 months (10 sessions of one week and a final examination of two weeks consisting of a complete SDPD), but there is no maximum limit. As can be seen in the figure giving the last session attained by participants, listed

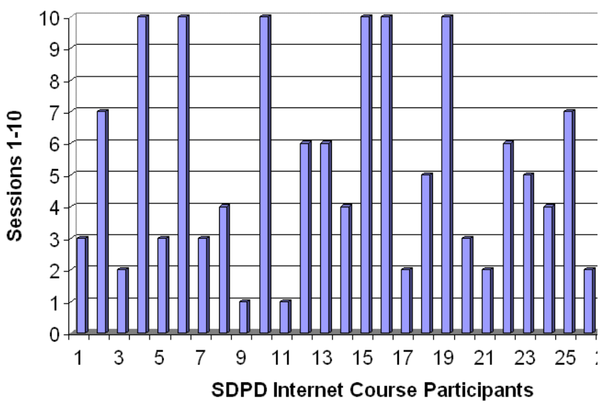

according to their registration order, only 3 among the 12 subscribers in 2000, 2 among 6 in 2001 and one among 6 in 2002 have completed the course. This does not mean that all the others have given up; only a few really have and for some of them very soon after session 1 or 2. This is slightly better than usual results for a distance-learning course, where 80% quit. However, a change was recently made in the registration arrangements: participants are now invited to pay the fees only if they decide to continue after the completion of the first two sessions. Another change is the new reduced fees for groups of subscribers coming from a single university or company.

A part of the course is also taught in the face to face mode to a few local first year PhD students, (6 students in 3 years), but the allocated time (15 hours) does not allow us to cover more than half of the Internet course content. Completing that course requires very high motivation and willingness, since SDPD is far from being yet a routine task, as shown by the recent round robin [4].

[1] SDPD Internet Course, http://sdpd.univ-lemans.fr/course/
[2] A. Le Bail, Y. Laligant and A. Jouanneaux, *Mat. Sci. Forum*, **378-381** (2001) 47-52.
[3] SDPD Internet Course, ECM-20 Krakow proceedings, http://sdpd.univ-lemans.fr/ecm20/sdpd.html
[4] SDPD Round Robin 2002, http://www.cristal.org/sdpdrr2/

A Guided Exercise of Quantitative Phase Analysis UsingEXPGUI Available on the CCP14 Web Site

A. F. Gualtieri
Dipartimento di Scienze dellla Terra, Università di Modena e R.E, Via S.Eufemia 19, 41100 Modena, Italy
alex@unimo.it

Introduction

In the last decade, quantitative phase analysis (QPA) using the Rietveld method [1-4] has been applied to systems of gradually increasing complexity (in the number of phases, their structural complexity and even their degree of structure order). In QPA using the Rietveld method, the weight fraction w_i of each i^{th} crystalline component in the mixture is calculated from the corresponding refined scale parameter S_i, according to the equation

$$w_i = \frac{S_i M_i V_i}{\sum_j S_j M_j V_j}$$

with M_i and V_i the unit cell mass and volume, respectively. This algorithm is based on the normalisation condition $\Sigma_i w_i = 1$. The scattering contribution of any amorphous component possibly existing in the sample is a part of the background and the above normalisation equation does not include it. The specific problem is usually solved using a suitably chosen internal standard, which is added in a known amount to the investigated mixture and treated as a mixture component itself. At the end of the Rietveld process, the refined phase fractions are converted into weight fractions and rescaled to the values of the original mixture by the ratio between the refined ($X_{s,c}$) and the known (X_s) amount of added standard. Whenever an amorphous phase exists in the system, the values of the weight fractions are overestimated to satisfy the normalisation condition. The percentage of the amorphous phase X_a in the original mixture can be calculated directly from the weight of the internal standard according to the equation

$$X_a = \frac{100}{(100 - X_s)}\left(1 - \frac{X_s}{X_{s,c}}\right)$$

One of the major challenges of QPA is to achieve accurate weights in complex systems containing crystalline and amorphous phases, as shown by the number of papers recently published, using an internal standard [e.g. 5-11] or using empirical functions to fit the contribution of the amorphous phase [12,13]. The interest in this area is predicted to increase if one considers that the appealing nano-science world describes crystal-size- dependent properties of systems that cover a broad range between the crystalline and the amorphous state. These analyses can be performed using the existing free software GSAS and EXPGUI.

This short summary introduces an extended version of a guided training exercise designed for the beginner who wants to make the first step into the world of quantitative phase analysis. The full guided training exercise of a ternary mixture containing an amorphous phase using EXPGUI is available online at CCP14, http://www.ccp14.ac.uk/solution/gsas/files/expgui_quant_gualtieri.pdf .

The GSAS and EXPGUI Packages

GSAS (General Structure Analysis System) is a comprehensive system for the refinement of structural models from X-ray and/or neutron diffraction data. GSAS has been written by Allen C. Larson and Robert B. Von Dreele [14]. Executable versions of GSAS are distributed freely, but the source code is not distributed. The CCP14 GSAS mirror site is ftp://ftp.ccp14.ac.uk/ccp14/ftp-mirror/gsas/public/gsas/ where the manual can also be found.

EXPGUI by Brian Toby, [15] is a graphical user interface (GUI) editor for GSAS experiment (.EXP) files and shell which allows all the other GSAS programs to be executed within a GUI. EXPGUI is not a replacement for the GSAS program EXPEDT. EXPGUI is written in the Tcl/Tk scripting language, so it is largely platform independent. Documentation is found at http://www.ncnr.nist.gov/xtal/software/expgui/expgui.html

If you are new to GSAS & EXPGUI, it is recommended to start with the user-friendly tutorial at http://www.ncnr.nist.gov/xtal/software/expgui/tutorial3 . There are also three tutorials in the GSAS manual as well as several on the CCP14 site. Two of the tutorials from the GSAS manual are repeated as examples for EXPGUI, http://www.ncnr.nist.gov/xtal/software/expgui/tutorial1 and http://www.ncnr.nist.gov/xtal/software/expgui/tutorial2

These tutorials are intended to be read in parallel with the GSAS manual. A web page covers problems related to GSAS & EXPGUI: NCNR GSAS FAQ page. Send your contributions (preferably in HTML) for for inclusion on this page to crystal@NIST.gov. Software bugs should be reported for GSAS to Bob Von Dreele (vondreele@anl.gov) and for EXPGUI to Brian Toby (brian.toby@NIST.gov).

A Real Case as a Training Exercise

The full guided training exercise avalable as a PDF file on the CCP14 web site is designed for the beginner of GSAS and EXPGUI. The ternary mixture contains corundum, hydroxyapatite and an amorphous phase. The refinement is described in detail step by step. The amorphous glass fraction must be determined indirectly with the aid of an internal standard [9]. The mixture is composed of 45 wt% glass, 10 wt% corundum NIST 676 (the internal standard) and 45 wt% hydroxyapatite NIST 2910. The glass has composition SiO_2 = 20.72%; BaO = 8.09%; PbO = 71.13%; Al_2O_3 = 0.02%; CaO = 0.02%; K_2O = 0.02%. The powder was obtained by carefully weighing the crystalline and the amorphous phases using an analytical balance and homogenized by hand grinding in an agate mortar. One of the problems in the quantification of the amorphous phase using the internal standard method is that the *standard* may not be fully crystalline. Corundum NIST 676 was annealed to increase the crystallinity essentially to 100%. Similarly, hydroxyapatite NIST 2910 was annealed for 1 day at 250°C to eliminate the certified amorphous fraction of 7.5(4.1)%.

Special attention is devoted to the refinement strategy which is of paramount importance to achieve a sound result. Practical advices and suggestions are also given together with literature citations. It is strongly encouraged to time some time to read the papers by McCusker et al. [16], Madsen et al. [17] and of course the GSAS manual before the refinement.

References

[1] Rietveld, H.M. (1969). *J. Appl. Cryst.*, **2**, 65-71.

[2] Bish, D.L. & Howard, S.A. (1988). *J. Appl. Cryst.*, **21**, 86-91.

[3] Bish, D.L. & Post, J.B. (1993). *Am. Min.*, **78**, 932-940.

[4] Hill, R.J. (1991). *Powder Diff.*, **6(2)**, 74-77.

[5] Artioli, G., Kern, A., Marchi, M. & Dapiaggi, M. (2002). Collected Abstracts, Proc. EPDIC-8, The 8th European Powder Diffraction Conference, Uppsala (SW) 23-26 May 2002, 202.

[6] De La Torre, A.G., Bruque, S. & Aranda, M.A.G. (2000). *J. Appl. Cryst.*, **34**, 196-202.

[7] De la Torre, A.G., Pajares, I., Martinez-Ramírez, S., Bruque, S. & Aranda, M.A.G. (2002). Collected Abstracts, Proc. EPDIC-8, The 8th European Powder Diffraction Conference, Uppsala (SW) 23-26 May 2002, 201.

[8] Feret, F.R. & Roy, D. (2002). *Spectrochimica Acta.,* **57**, 551-559.

[9] Gualtieri, A.F. (2000). *J. Appl. Cryst.*, **33**, 267-278.

[10] Guirado, F., Galí, S. & Chinchón, S. (2000). *Cement and Concrete Res.*, **30**, 1023-1029.

[11] Orlhac, X., Fillet, C., Deniard, P., Dulac, A.M. & Brec, R. (2000). *J. Appl. Cryst.*, **34**, 114-118.

[12] Riello, P., Canton, P. & Fagherazzi, G. (1998a). *J. Appl. Cryst.*, **31**, 78-82.

[13] Riello, P., Fagherazzi, G. & Canton, P. (1998b). *Acta Cryst.*, **A54**, 219-224.

[14] Larson, A.C,. & Von Dreele, R.B. (1994). Los Alamos National Laboratory Report LAUR 86-748.

[15] Toby, B.H. (2001). “EXPGUI, a graphical user interface for GSAS”, *J. Appl. Cryst.* **34**, 210-213.

[16] McCusker, L.B., Von Dreele, R.B., Cox, D.E., D Louër, & Scardi P. (1999). *J. Appl. Cryst.*, 32, 36-50.

[17] Madsen, I.C., Scarlett, N.V.Y. & Cranswick, L.M.D., Thaung Lwin (2001). *J. Appl. Cryst.*, **34**, 409-426.

Computer Corner

Updates on Freely Available Crystallographic and Powder Diffraction Software

(Suggestions, corrections, comments appreciated; especially if you know of new program features, program updates and announcements that should be mentioned here).

Lachlan M. D. Cranswick
Neutron Program for Materials Research (NPMR),
National Research Council (NRC),
Building 459, Station 18, Chalk River Laboratories,
Chalk River, Ontario, Canada, K0J 1J0
Tel: (613) 584-8811; Fax: (613) 584-4040
E-mail: l.m.d.cranswick@dl.ac.uk
WWW: http://neutron.nrc-cnrc.gc.ca/

Updated DrawXTL for Windows, Mac and UNIX by Larry Finger and Martin Kroeker

The latest feature updated and bugfix version of DrawXTL 3.2 is available on the web at via http://www.lwfinger.net/drawxtl and CCP14 mirrors. The program can read in crystal structure formats such as including CIF, SHELXTL, GSAS and CSD; then output Povray and VRML files of selected views with ball and stick and/or polyhedral rendering. While controlled using an ASCII file, there are also basic control interfaces for DrawXTL that run on Windows, Mac and UNIX. DrawXTL can be very effective for exact rendering of crystal structure diagrams, including those with complicated polyhedral connectivity.

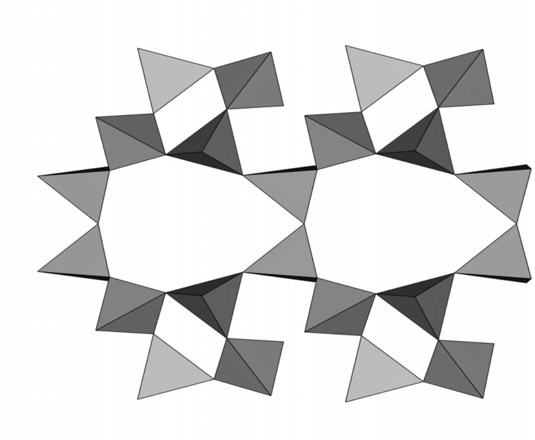

Fig 1: *An example of a publication quality structure drawing of heulandite (hydrated Calcium Sodium Aluminum Silicate) generated by DrawXTL and rendered in Povray. To appear in H.-R. Wenk and A. Bulakh (2003). Minerals, their Constitution and Origin. Cambridge University Press (in press)*

AXES for Windows by Hugo Mandar

An MS-Windows version of AXES by Hugo Mandar is now available via the web (as well as the older DOS version) at http://www.physic.ut.ee/~hugo/axes/ and CCP14 mirrors.

Functionality includes the ability to import powder diffraction data in a wide variety of file formats; then perform a wide variety of data analysis, including interlinking with other packages including powder indexing and structure refinement. A demonstration version of the Windows version of AXES is available and pricing varies depending on the type of institution: academic / government or commercial.

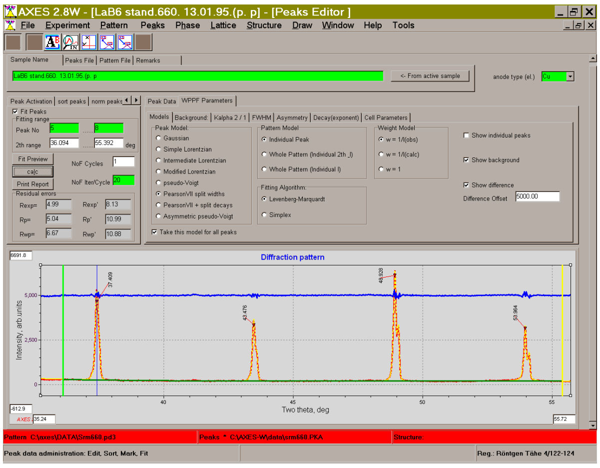

LaB6 stand.660. 13.01.95.(p. p
anode type (el.) Cu

☑ Fit Peaks
Fitting range
Peak No 5 8
2th range 36.094 ...... 55.392 deg
NoF Cycles 1
NoF Iter/Cycle 20
Residual errors
Rexp= 4.99 Rexp' 8.13
Rp= 5.04 Rp' 10.99
Rwp= 6.67 Rwp' 10.88

Peak Model:
○ Gaussian
○ Simple Lorentzian
○ Intermediate Lorentzian
○ Modified Lorentzian
○ pseudo-Voigt
● PearsonVII split widths
○ PearsonVII + split decays
○ Asymmetric pseudo-Voigt
☑ Take this model for all peaks

Pattern Model
● Individual Peak
○ Whole Pattern (Individual 2th _I)
○ Whole Pattern (Individual I)

Fitting Algorithm:
● Levenberg-Marquardt
○ Simplex

Weight Model
● w = 1/I(obs)
○ w = 1/I(calc)
○ w = 1

☐ Show individual peaks
☑ Show background
☑ Show difference
Difference Offset 5000.00

Pattern C:\axes\DATA\Srm660.pd3
Peaks * C:\AXES-W\data\srm660.PKA
Structure:
Peak data administration: Edit, Sort, Mark, Fit
Reg.: Röntgen Tähe 4/122-124

Fig 2: *Screen image of Pattern Fitting within AXES.*

Latest WinGX single crystal suite now interlinks with the Gnu Xtal System.

The lastest WinGX single crystal suite by Louis Farrugia at the University of Glasgow now interlinks with the Xtal single crystal suite, adding a variety of tools that are not only useful to single crystal types, but also powder diffraction people. The WinGX homepage is viewable via http://www.chem.gla.ac.uk/~louis/software/ and CCP14 mirrors while the Xtal suite homepage is now at http://xtal.sourceforge.net/

A tutorial on installing and spawning the Gnu Xtal System within WinGX is on the CCP14 website at: http://www.ccp14.ac.uk/tutorial/wingx/xtal_suite_within_wingx.html

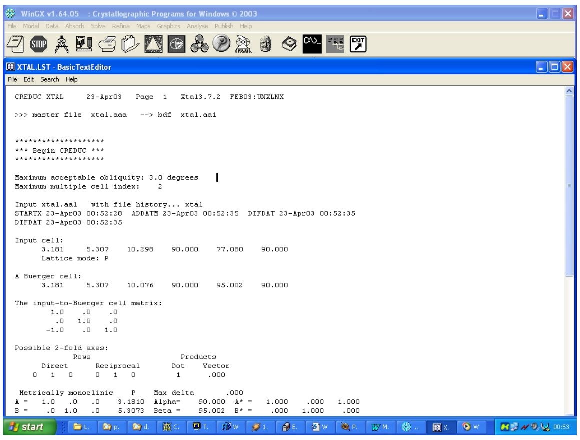

```
CREDUC XTAL     23-Apr03   Page  1   Xtal3.7.2  FEB03:UNXLNX

>>> master file  xtal.aaa   --> bdf  xtal.aa1


********************
*** Begin CREDUC ***
********************

Maximum acceptable obliquity: 3.0 degrees
Maximum multiple cell index:    2

Input xtal.aa1   with file history... xtal
STARTX 23-Apr03 00:52:28  ADDATM 23-Apr03 00:52:35  DIFDAT 23-Apr03 00:52:35
DIFDAT 23-Apr03 00:52:35

Input cell:
       3.181     5.307    10.298    90.000    77.080    90.000
       Lattice mode: P

A Buerger cell:
       3.181     5.307    10.076    90.000    95.002    90.000

The input-to-Buerger cell matrix:
         1.0    .0    .0
          .0   1.0    .0
        -1.0    .0   1.0

Possible 2-fold axes:
                Rows                    Products
       Direct       Reciprocal        Dot    Vector
    0   1   0      0   1   0           1      .000

 Metrically monoclinic    P    Max delta       .000
A =   1.0   .0   .0    3.1810  Alpha=    90.000  A* =   1.000    .000   1.000
B =    .0  1.0   .0    5.3073  Beta =    95.002  B* =    .000   1.000    .000
```

Fig 3: At the click of a button within WinGX: *running the Creduc cell reduction software (LePage and Flack) provided within the Gnu Xtal suite.*

Ad-aware "anti ad-ware" software for Windows

Most users of PCs would know the necessity of installing an anti-virus program. But another annoyance and threat from those browsing the web is that of spy-ware and ad-ware. These programs can be inadvertantly installed due to dubious webpages, or as part of other freeware programs (File sharing programs using the Gnutella protocol can be notorious for this). Effects of this include the screening of web adverts at random intervals, sending personal data to third party organisations and slowing down of the computer.

A good program that can be used for eliminating spyware and freely run for personal and ad-ware is that of is that of Ad-aware available at http://www.lavasoftusa.com/. In conjunction with an up to date anti-virus program, this can help minimize the effects of malicious programs.

File Name	Size	Creation Date	Objects Total
auto-quarantine- 06-0...	691 bytes	06-04-2003	1
auto-quarantine- 06-0...	2 kb	06/04/2003	25

2 items.

Ad-aware 6 Personal, Build 162

Fig 4: *Screen image of Ad-aware in action. In this case, allowing the view of "Quarantined Objects". On first running Ad-aware on "problem" PCs, 100s of problem files and Windows registry settings can often be found.*

Redhat Linux 9.0 released

The free Linux operating system (it is completely free if your time has zero value) is getting very slick and is becoming a match for Windows on desktop systems (it has been a superior general server system over MS-Windows for quite some time). An example of this is the recently released Redhat Linux 9, which includes the Open Office suite as discussed below. Installation seems to be getting easier, and the setup of printers is getting as intuitive as MS-Windows (in UNIX of old, the set up of printers could be a major and time consuming pain).

People interested in making it more difficult for Microsoft to pillage their research and computing may wish to check out Redhat and other Linux distributions such as SuSE, Mandrake, etc. Many of these operating systems seem to have a higher performance and standard of reliability than MS-Windows (my personal preference is to use the KDE "X" interface and not Gnome). Using programs such as FIPS to make a spare partition at the end of a large hard-disk with Windows installed on it; Linux can then be installed using the "Force LBA32" boot loading option.

Redhat Linux is available via http://www.redhat.com. At the time of writing, at least one mirror of the Redhat 9 ISO CD images was at ftp://mirror.phy.bnl.gov/pub/redhat/pub/redhat/linux/9/en/iso/i386/ . Other Redhat mirrors have been slow to update with the latest distribution. One caveate is that it is important to keep a Linux installation up to date and patched to restrict the ability of hackers to successfully attack the computer. Please note that some problems have been experienced with new update RPMs for Redhat 9. Also, removing un-needed Internet deamons such as "sendmail, portmap, etc" can be easily achieved by using the "setup" program within Redhat. Using "nmap –sS 127.0.0.1" can inform you if any errant internet deamons are still running.

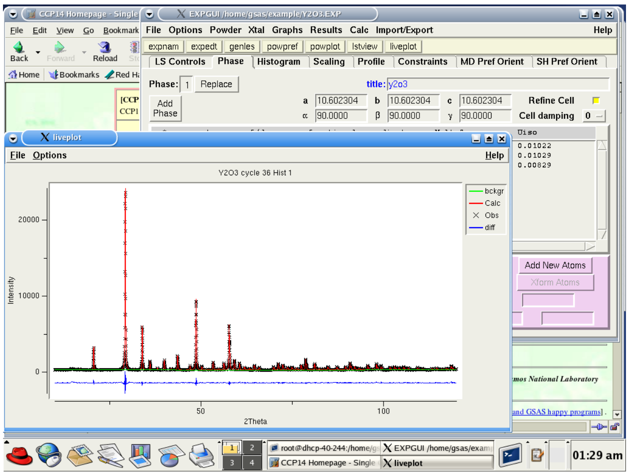

Fig 5: *Screen image of Redhat 9 with the KDE X-Windows interface running Bob von Dreele and Alan Larson's GSAS Rietveld via Brian Toby's EXPGUI interface (installed from Brian Toby's Linux RPM on his web/ftp site)*

Open Office (free open source office suite for Windows, Mac and UNIX)

For an office PC, one of the big computer costs after the hardware, is that of purchasing an office suite with word processor, spreadsheet program, drawing and presentation software. A suite worth watching and evaluating at various intervals is the Open Office suite at http://www.openoffice.org/ ; which is available for Windows, Linux, Mac OS X and Solaris.

While version 1.0 is the official release, the 1.1 Beta that is available for download seems to almost match MS-Office in functionality. An advantage of GPL software such as this is that it includes the source code. If bugs are found or new features are required, there is always the option of making your own code changes (or finding someone to make the code changes for you)

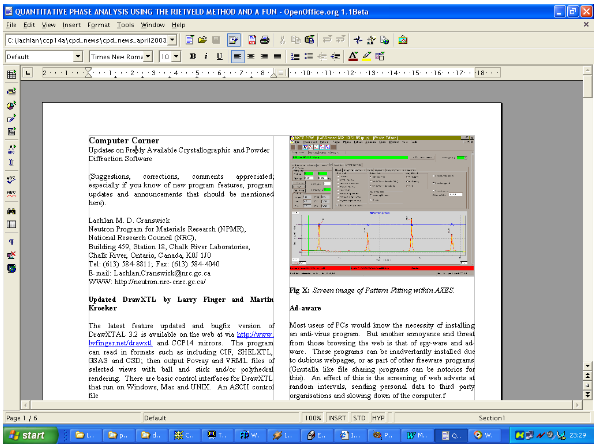

Fig 6: *Editing the Computer Corner article in Open Office 1.1Beta .(importing a file originally created in MS-Word).*

Rietveld Software Updates (as of late April 2003):

Hugo Rietveld website:
http://home.wxs.nl/~rietv025/
BGMN (21st March 2003)
http://www.bgmn.de/
DBWS (22nd February 2000)
http://www.physics.gatech.edu/downloads/young/download_dbws.html
Debvin (25th May 2001)
ftp://ftp.cc.uniud.it/DEBVIN/
GSAS (2nd January 2003)
ftp://ftp.lanl.gov/public/gsas/
EXPGUI (10th April 2003)
http://www.ncnr.nist.gov/programs/crystallography/
Jana (4th February 2003)
http://www-xray.fzu.cz/jana/jana.html
LHPM-Rietica (27th November 2001)
ftp://ftp.ansto.gov.au/pub/physics/neutron/rietveld/Rietica_LHPM95/
MAUD for Java (GPL'd) (15th March 2003)
http://www.ing.unitn.it/~luttero/maud/
Prodd (12th March 2002)
http://www.ccp14.ac.uk/ccp/web-mirrors/prodd/~jpw22/
Profil (24th May 2001)
ftp://img.cryst.bbk.ac.uk/pdpl/
Rietan 2000 (GPL'd) (29th January 2003)
http://homepage.mac.com/fujioizumi/rietan/angle_dispersive/angle_dispersive.html
Winplotr/Fullprof (23rd July 2002) (if Fullprof FTP site is unavailable, use the CCP14 Mirrors)
http://www-llb.cea.fr/winplotr/winplotr.htm
ftp://bali.saclay.cea.fr/pub/divers/fullprof.2k/
Winmprof (21st June 2001)
http://lpec.univ-lemans.fr/WinMProf/
XND (10th April 2003)
http://www-cristallo.polycnrs-gre.fr/xnd/xnd.html
ftp://ftp.polycnrs-gre.fr/pub/xnd/ (if XND FTP site is unavailable, use the CCP14 Mirrors)

All the above Rietveld programs are also available via the CCP14 based mirrors in UK, USA, Australia and Canada (http://www.ccp14.ac.uk/mirror/).

Summary lists of some software available via the EPSRC funded CCP14 website:

"What do you want to do?" (lists of software by single crystal and powder methods)
http://www.ccp14.ac.uk/mirror/want_to_do.html

Anharmonic Thermal Refinement Software
http://www.ccp14.ac.uk/solution/anharmonic/
Data Conversion for Powder Diffraction
http://www.ccp14.ac.uk/solution/powderdataconv/
Image Plate Software
http://www.ccp14.ac.uk/solution/image-plate/
Incommensurate Structure Software
http://www.ccp14.ac.uk/solution/incomm.htm
Indexing Software for Powders
http://www.ccp14.ac.uk/solution/indexing/
LeBail Method for Intensity Extraction
http://www.ccp14.ac.uk/solution/lebail/
Pawley Method for Intensity Extraction
http://www.ccp14.ac.uk/solution/pawley/
PDF, High Q Powder diffraction Analysis Software
http://www.ccp14.ac.uk/solution/high_q_pdf/
Peak Find/Profiling Software for Powder Diffraction
http://www.ccp14.ac.uk/solution/peakprofiling/
Pole Figure and Texture Analysis Software
http://www.ccp14.ac.uk/solution/pole_figure/
Powder Diffraction Data Visualisation
http://www.ccp14.ac.uk/solution/powder_data_visual/
Rietveld Software
http://www.ccp14.ac.uk/solution/rietveld_software/
Search-Match Phase Identification Software
http://www.ccp14.ac.uk/solution/search-match.htm
Single Crystal Structure Solution Software relevant to Chemical Crystallography
http://www.ccp14.ac.uk/solution/xtalsolution/
Single Crystal Structure Refinement Software relevant to Chemical Crystallography
http://www.ccp14.ac.uk/solution/xtalrefine/
Single Crystal Suites linking to multiple programs relevant to Chemical Crystallography
http://www.ccp14.ac.uk/solution/xtalsuites/
Spacegroup and Symmetry operator determination software and source code
http://www.ccp14.ac.uk/recomm/sym_operators_to_spacegroups.html
http://www.ccp14.ac.uk/recomm/spacegroups_to_sym_operators.html
Spacegroup and Structure Transformation Software
http://www.ccp14.ac.uk/solution/transform/
Structure Conversion and Transformation
http://www.ccp14.ac.uk/solution/structconv/
Structure Drawing and Visualisation
http://www.ccp14.ac.uk/solution/structuredrawing/
Unit Cell Refinement of Powder Diffraction Data
http://www.ccp14.ac.uk/solution/unitcellrefine/

COD (Crystallography Open Database)

Armel le Bail
Laboratoire des Fluorures, URA CNRS 449
Universite du Maine, Faculte des Sciences
72017 Le Mans Cedex, France; E-mail: alb@cristal.org

In the IUCr Newsletter 10-4 (2002), Bill Duax (Letter from the President) wrote : "Emerging nations can benefit from the use of the powerful techniques of X-ray crystallography in order to analyze, understand and use the unique natural resources within their countries whether mineralogical, chemical, or biological in nature."

This generous wish would more easily be achieved by a free access to a global crystallography open database (inorganic/metallic/organometallic/organic) which is the purpose of a new web server located at http://www.crystallography.net/ and offering atomic coordinates in the IUCr CIF files format, together with a search engine.

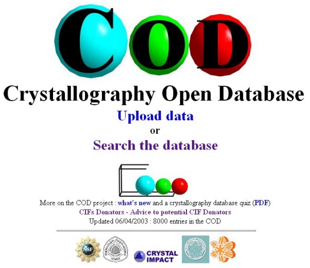
Crystallography Open Database
Upload data
or
Search the database
More on the COD project : what's new and a crystallography database quiz (PDF)
CIFs Donators - Advice to potential CIF Donators
Updated 06/04/2003 : 8000 entries in the COD

Fig. 1: *The* http://www.crystallography.net/ *Web page.*

An international advisory board supervises that good practices are respected (M. Berndt, D. Chateigner, X. Chen, M. Ciriotti, L.M.D. Cranswick, R.T. Downs, A. Le Bail, L. Lutterotti, H. Rajan, B.H. Toby, A.F.T. Yokochi). Rather than to systematically copy the atomic coordinates from the literature, individual authors and laboratories are requested to send their own CIFs prior to (or after) publication, which is possible if you have not sold your experimental results exclusively (facts and raw scientific data are in principle not copyrightable). Thanks to a few major donators (the American Mineralogist Crystal Structure Database for 3725 entries, the Institut de Physique de la Matière Condensée - Grenoble- for ~1200 entries, the CRISMAT -Caen- for ~850 entries and the Laboratoire des Fluorures -Le Mans- for ~450 entries), as well as to many individual contributors, the COD can already propose more than 8.000 CIFs. This is however only 2 % of an expected total number close to 400.000 entries.

The search in COD is realized by two powerful options :

1 - by combining in the way you choose : text (2 words or parts of words), elements (1 to 8, with formula numbers or not), volume (min and max), and strict number of elements.

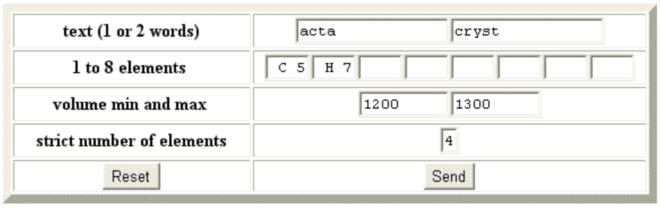

text (1 or 2 words)	acta cryst
1 to 8 elements	C 5 H 7
volume min and max	1200 1300
strict number of elements	4

Fig. 2: *Part of the COD simple but powerful search form.*

2 - By cell parameters ranges a_{min}-a_{max}, b_{min}-b_{max}, *etc.*

Given that the COD was built mainly for verifying if, knowing your sample cell, you are not redetermining an already known structure, these above search possibilities should fulfil basic needs (especially option 2 and using volume ranges in option 1, needing the cell knowledge). However, a real efficiency urgently requires completeness, so please upload your CIFs !

The whole COD system is based on open source software (Apache/MySQL/PHP) and can be downloaded by interested parties (contact cod@cristal.org). It is simple to install and would be quite useful to laboratories wanting to build their crystal database from their own crystal structure determinations, for either an intranet or an internet external access. Collecting all such laboratory fragments in the COD would serve invaluably the crystallographers community in the world and particularly in emerging nations. The CRYSTMET, ICSD and CSD commercial databases offer much more complete and powerful services than the COD which is limited to the minimum allowing a crystallographer to survive at low cost (though a not so cheap internet access is necessary).

Quantitative Mineral Analysis by XRD---RockJock

D.D. Eberl
U. S. Geological Survey, 3215 Marine St.
Boulder, CO 80303-1066, USA
E-mail: ddeberl@usgs.gov

Fig 1: From the *RockJock instruction manual. Photo by K. Mystkowski.*

RockJock, a free program for calculating mineral weight percents from powder X-ray diffraction data, now is available for downloading from the following USGS ftp site: ftp://brrcrftp.cr.usgs.gov/pub/ddeberl/ . The program is almost entirely automatic, requiring only that the X-ray intensities for a sample be entered into the program, that minerals likely to be present be chosen from a list, and that a button be clicked. RockJock is written in Microsoft Excel 2000 macro language, and requires a fast computer (>1 GHz), either a PC (Windows 98 of higher) or a Macintosh (System X). RockJock joins two other programs that also are available at the ftp site. MudMaster calculates crystallite size distributions and strain from the shapes of X-ray diffraction peaks using a modified version of the Bertaut-Warren-Averbach technique, and Galoper simulates the shapes of crystal size distributions from crystal growth mechanisms. Other associated programs also are available at the site.

RockJock (Eberl, 2003) offers a relatively simple and mostly automatic method for determining quantitatively the mineralogical composition of samples, including clay minerals, to within a few weight percent from powder X-ray diffraction data. The calculations are based on three previously published methods: (1) the matrix flushing technique of Chung (1974), in which integrated intensities of the unknown minerals are compared to that of an internal standard (in the case of RockJock, ZnO, zincite), thereby obviating the need for measuring the mass absorption coefficient for a sample; (2) the whole-pattern fitting routine of Smith and others (1987) for measuring integrated intensities by fitting the sum of pure mineral patterns to that of the measured XRD pattern, except that in RockJock key parts of the pattern which contain the 060 reflections for clay minerals also are fitted separately; and (3) the quantitative method of Srodon and others (2001) for sample preparation, and for the method of measuring clay mineral content from 060 reflections rather than from the more commonly used basal reflections.

The program operates as follows. After the measured pattern has been entered, the minerals present chosen from a list, and the Start button clicked, the measured pattern is justified in two-theta with respect to the peak positions of the internal standard. Then stored, standard patterns for the chosen minerals are called from a library. These patterns each are multiplied by a separate factor, and the resulting patterns are summed to match the measured pattern. The factors are adjusted by the Solver tool in Excel until the degree of fit parameter between the calculated and measured pattern is minimized. One also can include peak shifts in the Solver solution to account for changes in sample peak positions due to isomorphous substitutions, or these shifts can be made manually. Once the multiplication factors have been determined, then the integrated intensity for each standard pattern is known, and the weight percent of each mineral is calculated from previously determined mineral intensity factors (MIFs, which are the same as reference intensity rations, or RIRs, of earlier literature) that are stored in the program.

The Solver solution is made twice, once for the Full Pattern region (20 to 65 degrees two-theta using Cu K-alpha radiation) to measure non-clays, and again for the Clay region (58 to 65 degrees two-theta) to measure the clay content. Aluminous smectite + illite + mica are reported together, because their reflections are similar in the 060 (Clay) region. The more commonly used basal clay reflections are avoided during this analysis because their intensities often strongly depend on degree of crystal orientation, on mixed layering and on clay mineral chemistry.

One drawback to the RockJock approach is that the calculation is slow, taking up to half an hour or more for each sample. Calculation time is a function of the number of minerals present. However, the program can operate in an automatic mode, analyzing many XRD patterns in a single run, and therefore can be left to calculate overnight. A poem by Wallace Stevens in the instruction manual also helps pass the time.

The user eventually will want to develop their own set of standards for the program; but adequate results may be obtained using the standards currently present in the program, as is shown in the table below. Table 1 gives RockJock results for artificial mixtures prepared by D. McCarty for the Reynolds Cup competition, an international quantitative analysis contest first held in 2002 and now to be held every other year. The columns labelled zero contain the actual values used to make the three samples. The columns labelled 1 contain results for a Siemens D500 instrument, the same instrument on which the standards were run. The columns labeled 2 are for a Nicolet instrument, which has a different geometry from the Siemens, using the Siemens generated standards. Bias is defined as the sum of the absolute difference in weight percent between the actual values and the measured values.

Eberl, D.D., 2003, *User's guide to RockJock—a program for determining quantitative mineralogy from powder X-ray diffraction data.* U.S. Geological Survey Open File Report 03-78, 37 p.

Chung, F.H., 1974, *Quantitative interpretation of X-ray diffraction patterns of mixtures. I. Matrix flushing method for quantitative multicomponent analysis:* Journal of Applied Crystallography, v. 7, p. 519-525.

Smith, D.K., Johnson, G.G., Jr., Scheible, W., Wims, A.M., Johnson, J.L., and Ullmann, G., 1987, *Quantitative X-ray powder diffraction method using the full diffraction pattern:* Powder Diffraction, v. 2, p. 73-77.

Snyder, R.L. and Bish, D.L., 1989, *Quantitative analysis, in, Bish, D.L. and Post, J.E., eds., Modern powder diffraction:* Mineralogical Society of America Reviews in Mineralogy, v. 20, p. 101-144.

Srodon, J., Drits, V.A., McCarty, D.K., Hsieh, J.C.C., and Eberl, D.D., 2001, *Quantitative X-ray diffraction analysis of clay-bearing rocks from random preparations*: Clays and Clay Minerals, v. 49, p. 514-528.

Sample:	RC-AR1			RC-AR2			RC-AR3		
Diffractometer:	**0**	1	2	**0**	1	2	**0**	1	2
Microcline	**8.0**	8.5	7.7	**10.0**	12.3	11.7	**2.0**	1.8	1.9
Albite	**8.0**	9.5	10.1	**10.0**	10.7	11.9	**2.0**	2.8	3.9
Calcite	**5.0**	4.9	5.1	**3.0**	2.5	2.6	**17.0**	15.4	16.4
Dolomite	**3.0**	3.4	3.3	**2.0**	2.3	1.8	**5.0**	4.9	5.6
Halite	**3.0**	3.3	2.4	**2.0**	1.1	0.5	**5.0**	2.0	2.0
Pyrite	**2.0**	1.5	1.7	**3.0**	2.5	2.7	**2.0**	1.4	1.9
Siderite	**3.0**	2.6	2.0	**2.0**	1.8	1.7	**5.0**	4.1	3.6
Barite	**2.0**	1.8	2.4	**2.0**	2.0	2.2	**2.0**	2.8	2.3
Quartz	**20.0**	20.0	19.7	**40.0**	40.3	38.1	**15.0**	14.8	12.8
Gypsum	**0.0**	0.0	0.0	**0.0**	0.0	0.0	**5.0**	2.8	5.2
Kaolinite	**9.0**	8.1	9.7	**7.0**	6.2	8.3	**10.0**	7.3	9.4
Fe-smectite	**7.0**	6.7	7.2	**6.0**	6.5	5.6	**5.0**	5.7	4.4
Illite	**25.0**	23.6	25.2	**9.0**	6.5	10.5	**28.0**	25.7	31.2
Chlorite	**5.0**	5.3	3.7	**4.0**	4.2	4.0	**0.0**	0.7	0.0
Total	100.0	99.2	100.2	100.0	98.9	101.6	100.0	91.1	100.6
Bias	0.0	6.8	7.8	0.0	9.6	15.0	0.0	13.3	11.8

Table 1: *RockJock results for artificial mixtures prepared by D. McCarty for the Reynolds Cup competition.*

QUANTO, A USEFUL TOOL FOR PHASE QUANTIFICATION. FIRST APPLICATIONS TO PHARMACEUTICAL COMPOUNDS

Cinzia Giannini & Antonietta Guagliardi
Istituto di Cristallografia, CNR
Via Orabona 4, Campus Univ., 70125 Bari, ITALY
E-mail: antonella.guagliardi@ic.cnr.it
WWW: http://www.ic.cnr.it/

Emilio Tedesco
Novartis Pharma AG, Chemical & Analytical Dep.
Lichtstrasse 35, 4056 Basel, SWITZERLAND

In memory of our friend Emilio

INTRODUCTION

QUANTO [1] is a Rietveld [2] program specialized for quantitative phase analysis (QPA) of polycrystalline mixtures [3,4]. It has been designed for automatic runs and special care has been dedicated for making interactive runs as user-friendly as possible. Good performances of the automatic QUANTO approach were obtained for a large variety of mixtures, which allowed us to test a wide range of difficulties in terms of number of phases, low concentration detection, peak overlapping degree and quality of experimental pattern. Up to now the program has never been experimented on organic compounds. The collaboration with Novartis Pharma gave us this opportunity and the first applications of QUANTO to samples of pharmaceutical interest are here presented, together with a brief and general description of the program. Besides the standard Rietveld approach, a special method [5] is implemented in the program to adopt the Rietveld QPA even in case of unknown or imperfectly known crystal structure, provided that the experimental pattern of the pure phase is available. The method is able to combine intensities calculated from the structure of phases with a suitable model and “observed” intensities extracted from the pure pattern and read from an external file, for phases lacking of a suitable crystal structure. It was tested on zeolite mixtures and here applied to the investigated samples to check its effectiveness for this kind of compounds.

PROGRAM DESCRIPTION

The program is available for Microsoft Windows, Linux and Unix platforms; it is free of charge for Academic Institutions at the website http://www.ic.cnr.it./
Some technical details and general remarks of the distributed version are summarized:

- user-friendly *Graphic Interface*
- user management of the *Quanto Data Bank*(collecting structure models in .pha files)
- reading *.CIF files* and writing *.pha files*
- maximum number of crystalline phases: *10*
- maximum number of counts: *10000*
- atomic scattering factors available (*up to Cf*)
- analytical peak shape functions: *Pearson VII, Pseudo-Voigt, Gaussian, Lorentzian*
- background: *Young* and *Chebishev polynomials, linear interpolation*
- preferred orientation correction: *March-Dollase model* (max 3 planes)
- microabsoprtion correction: *Brindley model*
- automatic definition of *peak range* (to avoid truncation peak tails effects)
- amorphous content estimation: *internal standard method*
- refinable parameters: Global (*zero-shift, background coefficients*); Phase Dependent (*profile shape, width and asymmetry; atomic fractional coordinates, isotropic thermal factor and occupancy*)
- Help on line available (*http://www.ic.cnr.it/Varie/quantohelp/*)
- Le Bail algorithm available

A graphic representation of the input/output QUANTO information is given in Fig. 1, together with the flow-chart of the automatic procedure

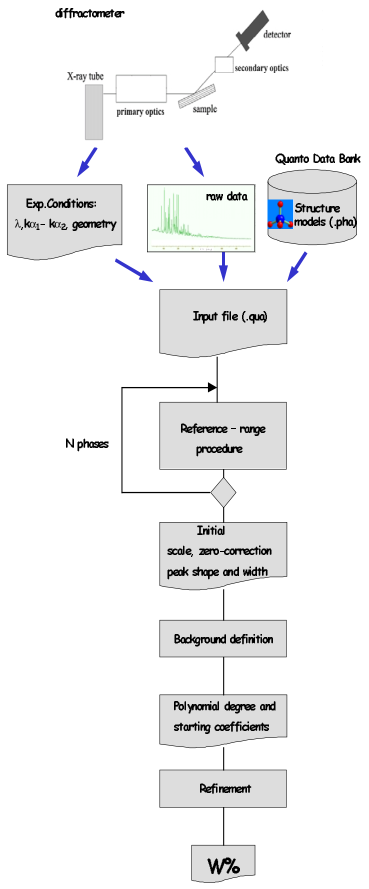

Fig. 1: *Schematic illustration of the minimal information required in input by the program (experimental conditions, raw data and crystal structure of phases) and the 3 main steps of the automatic procedure : 1) the reference range, to select and fit, for each phase, an isolated peak or a limited range of the whole pattern, to get initial values of peak shape and width; 2) automatic background definition; 3) Whole pattern refinement.*

APPLICATIONS

The investigated samples are binary mixtures of large and complex structures; their crystal model references and chemical details will not be given, because of the confidential nature of pharmaceutical compounds; they will be conventionally named *phase A* and *phase B*; some crystallographic information are given in the Table below.

	Unit Cell Content					Unit Cell Volume $(A°)^3$	Space Group
	Cl	*O*	*N*	*C*	*H*		
Phase A	4	48	4	172	280	4748.8	$P\,2_12_12_1$
Phase B	2	22	2	86	136	2226.0	$P\,2_1$

All datasets were collected with a Stoe diffractometer in transmission geometry, λ = 1.5406 Å, 2θ range 2-70°, step size of 0.02°.

All the investigated samples showed preferred orientations, with weak effects along (110) direction for *phase A* and stronger along (010) and (100) for *phase B*, respectively.

The automatic refinement procedure, as briefly described in Fig. 1, was carried out but taking care of the following conditions: a) cell parameters of *phase A* were kept fixed when it is in low concentration (Mix-1 and Mix-2) and the values refined by other datasets were adopted; b) preferred orientation corrections were refined (according to the March-Dollase model).

The estimated weight fractions of the test mixtures are shown in Table I, together with the profile agreement index R_{wp}, the Goodness of fit (GoF) and the absolute error percentage (Err) with respect to the known mixture composition. The plot of the final fit for Mix-3 is shown in Fig. 2. For most mixtures the absolute error is less than 1%; the largest errors refer to the mixtures with the highest concentration of *phase A* (Mix-7 and Mix-8). Indeed, the structural model of *phase A* revealed to be not properly suitable for reproducing the corresponding powder pattern, as highlighted by the pure phase profile fitting (not shown here) and confirmed by the increased R_{wp} of Mix-7 and Mix-8. We applied the method [5], referred in the introduction section, to test its effectiveness for this kind of compounds. We used the Le Bail algorithm implemented in QUANTO for extracting the reflection intensities from the *phase A* pattern; in successive runs we used the program feature of reading the external intensities file of the previous run and exploiting the available structural model to place the "observed" values on the absolute scale. The structural model of *phase B* was maintained to calculate the corresponding Bragg peak intensities. The procedure was applied automatically without including any preferred orientation correction for *phase A*. It is worthwhile noting that, the Wilson-plot technique for estimating absolute scale was also tested and proved to be not effective, in this case, because of the reduced 2θ range. The results for Mix-7 and Mix-8 are reported in Table II, confirming the applicability of the method to organic compounds.

Mixture	$\%w_{\mathbf{Known}}$ *phases* *A/B*	$\%\mathbf{w_Q}$	$\mathbf{R_{wp}}$ **Gof**	**Err%**
Mix-1	***3.39*** 96.61	3.04(52) 96.96(1)	5.26 3.47	0.35
Mix-2	***5.33*** 94.67	6.11(26) 93.89(2)	5.03 3.19	0.78
Mix-3	***10.09*** 89.91	10.05(24) 89.95(4)	5.91 4.27	0.04
Mix-4	***19.68*** 80.32	19.25(19) 80.75(5)	4.84 3.24	0.43
Mix-5	***48.09*** 51.91	46.92(16) 53.08(15)	4.50 2.81	1.17
Mix-6	***76.63*** 23.37	76.36(8) 23.64(28)	5.35 3.58	0.27
Mix-7	***87.28*** 12.72	85.19(4) 14.81(22)	6.50 4.73	2.09
Mix-8	***92.66*** 7.34	89.60(4) 10.40(26)	6.31 4.63	3.06

Table I: *QUANTO standard run results.*

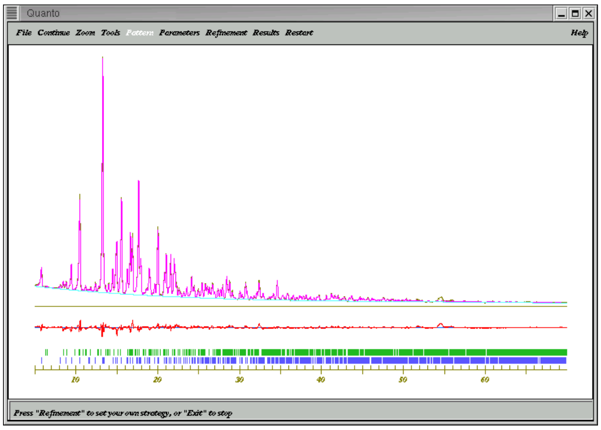

Press "Refinement" to set your own strategy, or "Exit" to stop

Fig. 2: *Final plot corresponding to the QUANTO standard run of Mix-3.*

Mixture	$\%w_{\mathbf{Known}}$ phases A/B	$\%w_{\mathbf{Q}}$	$\mathbf{R_{wp}}$ **Gof**	**Err%**
Mix-7	***87.28*** 12.72	89.03(4) 10.97(16)	5.99 3.37	1.75
Mix-8	***92.66*** 7.34	91.38(3) 8.62(20)	6.17 4.51	1.28

Table II: *QUANTO results when "observed" reflection intensities are used for phase A instead of those calculated from the structural model.*

References

[1] Altomare, A., Burla, M.C., Giacovazzo, C., Guagliardi, A., Moliterni, A.G.G., Polidori, P. & Rizzi, R. (2001). *J.Appl.Cryst.* **34**, 392-397

[2] Rietveld, H.M. (1969). *J.Appl.Cryst*. **2**, 65-71

[3] Hill, R.J. & Howard, C.J. (1987). *J.Appl.Cryst*. **20**, 467-474

[4] Bish, D.L., & Howard, S.A. (1988). *J.Appl.Cryst*. **21**, 86-91

[5] Giannini, C., Guagliardi A. & Millini, R. (2002) *J.Appl.Cryst*. **21**, 86-91

News from the
International Centre for Diffraction Data
(ICDD)

12 Campus Boulevard
Newtown Square, PA 19073-3273, U.S.A.
Phone: +610.325.9814
Fax: +610.325.9823

www.icdd.com
www.dxcicdd.com
www.ixas.org
E-mail: info@icdd.com

Ludo Frevel Crystallography Scholarship Recipients Named

The ICDD Ludo Frevel Crystallography Scholarship Committee selected six recipients for the 2003 Scholarship awards. These recipients were selected, on a competitive basis, from 34 commendable applications received by the ICDD Scholarship Committee. The recipients, along with their chosen field of research, are:

- *Kacey Claborn from The University of Washington, Seattle, Washington, USA with research involving, "Measurement of Optical Rotation in the Achiral Crystals of Pentaerythritol"*
- *Sean Dalrymple from The University of Calgary, Calgary, Alberta, Canada with exploration into "Flexible Hydrogen Bonded Networks via Second Sphere Coordination"*
- *Desire Fong from McGill University, Montreal, Quebec, Canada with major interest in "Substrate Binding Properties and Reaction Mechanism of an Aminoglycoside-Modifying Kinase"*
- *Erwann Jeanneau from The University of Rennes I, Rennes cedex, France with studies focusing on "Design of New Mixed Oxalates With Open-Framework Structures Based on MO_8 Building Units"*
- *Chong Lim from The University of Illinois at Urbana-Champaign, Urbana, Illinois, USA with research concerning "Crystallographic and Structural Studies of Cobalt Silicide Formation on Si(001)"*
- *Andrew Locock from The University of Notre Dame, South Bend, Indiana, USA, who's investigating "Crystal Structure and Synchrotron Radiation Study of Uranyl Oxysalts of Phosphate and Arsenate-Implications for Remediation"*

Each of these students received a check in the amount of $2,250 to assist in the continuation of studies in their selected fields of crystallographic research.

Scholarship awards are made possible by donations from both individuals and corporations. Since the program's inception in 1991, over $107,000 in scholarships have been awarded to 51 graduate students. As a reflection of the international scope of this award, students representing ten different countries have benefited from these scholarships.

X-ray Clinics

In pursuing its dynamic commitment to education, the ICDD recently held its annual training clinics in XRF and XRD at its headquarters in Newtown Square, Pennsylvania. These week-long clinics, held in late April and early June, offer both novices and professionals in the field of X-ray analysis an opportunity to learn techniques from the experts as well as the opportunity to discuss field experiences with peers.

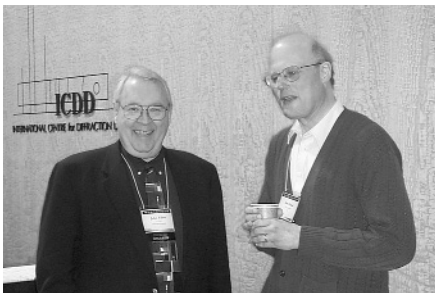

Clinic Instructors. Left to right: John Faber and Jim Kaduk.

The instructors for the XRF Clinic included: John Anzelmo of Anzelmo & Associates; Larry Arias of Bruker AXS, Inc.; Gene Bertin, Emeritus, RCA Labs; Richard Bostwick of SPEX CertiPrep, Inc.; Larry Creasy of Titanium Metals Corp.; Tim Fawcett of ICDD; Al Martin of Rigaku/MSC, Inc.; and Mary Ann Zaitz of IBM Microelectronics.

The instructors for the XRD Clinic included: Tom Blanton, Eastman Kodak Company; C. M. Foris, DuPont Central Research & Development; Richard Hamilton, Emeritus, Air Products and Chemicals, Inc.; James A. Kaduk, BP Amoco, Mark Rodriguez, Sandia National Laboratory; Susan Quick and Earle Ryba, both from The Pennsylvania State University; Bernie Squires, Rigaku/MSC, Inc.; and Harlan Clark, John Faber, Tim Fawcett, Suri Kabekkodu, Frank McClune, Fangling Needham, Chuck Weth, all from the ICDD.

The ICDD wishes to thank Bruker AXS, Inc., McCrone Microscopes and Accessories, Osmic, Inc., Oxford Instruments, PANalytical, Inc. and

Rigaku/MSC, Inc. for their assistance in providing X-ray instruments and equipment for use during the courses. Through these generous donations, the clinic curriculums were reinforced by providing hands-on experiences to the attendees.

ICDD Annual Spring Meetings

ICDD held its annual spring meetings during the week of 17-21 March 2003. For the first time in the ICDD's history, a new meeting format was introduced to maximize member interactions. A Plenary session, a poster session, and a tour of historical Philadelphia were added to the typical schedule of committee, subcommittee, and task group meetings.

A major announcement, delivered by Cam Hubbard, ICDD's Chairman, launched the meetings. In pursuing ICDD's long-term goal of supporting total pattern analysis, Dr. Hubbard announced a new collaborative agreement that was recently negotiated with Material Phases Data Systems (MPDS), distributors of the Linus Pauling File (LPF). This agreement will result in the incorporation of inorganic structural data (S-entry) from the LPF into the PDF-4 relational database, including atomic coordinates, crystallographic, and bibliographic data. Including this select LPF data will add new materials to the PDF database as well as provide complimentary atomic, crystallographic and bibliographic data to existing material sets. With integrated software, PDF-4 database users will be able to identify unknown materials and then quantitate the components by either the Reference Intensity Ratio (RIR) method or Rietveld method. The first collaboration product, scheduled to be released in 2005, will include the first 100,000 atomic coordinate data sets, visualization software, and enhanced digital pattern calculation in the PDF-4 database.

A meet & greet with Ben Franklin was a highlight of ICDD's tour of historical Philadelphia. Left to right: Tim Fawcett, Ben Franklin, Cam Hubbard.

Several awards, recognizing the contributions of the Editors and Consulting Editors to the various PDF products, were announced at the Annual Meeting of Members and presented to those in attendance. In addition, ICDD's Editor-in-Chief, Frank McClune, was named a Distinguished Fellow in recognition of his 34 years of diligent service.

Cam Hubbard presents an award to Frank McClune, recognizing his contributions and those of the entire ICDD staff, to the PDF.

New Student Online Subscription Rates

Published by the ICDD, *Powder Diffraction* is a quarterly journal devoted to the use of the powder method for materials characterization. With feature articles covering a wide range of applications, from mineral analysis to epitactic growth of thin films to advances in application software, this journal offers a wide range of practical applications. The ICDD is introducing a new annual student rate of $35.00 for online subscriptions.

PDF-4 Product Highlights

Did you know…

Combined, today's PDF-4/Full File and PDF-4/Organics features:

- Nearly 280,000 material data sets! (with patterns)
- 34 million d-spacings
- 513,000 literature citations from 1,602 journals

The PDF-4 product line offers total pattern analysis with unprecedented power to do full data mining with Boolean searches of all data fields. Learn more about the PDF-4 family of products by visiting the ICDD web site for an online overview.

ICDD, the ICDD logo & PDF are registered in the U.S. Patent and Trademark Office.

Further Information

To learn more about the ICDD, its products and services, please visit our web sites: www.icdd.com and www.dxcicdd.com.

WHAT'S ON

The following web-site contains an up-to-date and semi-exhaustive list of conference and workshops in crystallography and related areas. http://www.iucr.org/cww-top/mtg.date.html

26 – 31 July 2003
American Crystallographic Association Annual Meeting, ACA 2003
Northern Kentucky Convention Center, Cincinnati, Ohio, USA
http://www.hwi.buffalo.edu/ACA/
E-mail: jeanette.krause@uc.edu

4 – 6 August 2003
Polarised Neutrons and Synchrotron X-rays for Magnetism - PNSXM
Venice International University, San Servolo, Venice, Italy
http://venice.infm.it/
E-mail: massimo.altarelli@elettra.trieste.it

4 – 8 August 2003
52nd Annual Denver X-ray Conference
Denver Marriott Tech Center Hotel, Denver, Colorado, USA
http://www.dxcicdd.com/
E-mail: dxc@icdd.com

10 – 13 August 2003
AsCA'03/Crystal-23 : Asian Crystallographic Association and the Society for Crystallographers in Australia and New Zealand (SCANZ)
Cable Beach Club resort, Broome, Western Australia, Australia
http://www.crystal.uwa.edu.au/CrystalsDownUnder/
E-mail: srh@crystal.uwa.edu.au

24 – 30 August 2003
21st European Crystallographic Meeting
International Conference Center, Durban, South Africa
http://www.ecm21-africa.co.za/index.html
E-mail: jboeyens@postino.up.ac.za

8 – 13 September 2003
Aperiodic-2003
Universidade Federal de Minas Gerais (UFMG), Belo Horizonte, Brazil.
http://agora.grude.ufmg.br/aperiodic2003

8 – 18 September 2003
8th Oxford School on Neutron Scattering
Univ. of Oxford, Mansfield College, Oxford, UK.
http://www.isis.rl.ac.uk/conferences/osns2003/
E-mail: C.C.Wilson@rl.ac.uk

1 – 4 September 2003
XIX Conference in Applied Crystallography
Campanile Hotel, Krakow, Poland
http://www.us.edu.pl/uniwersytet/konferencje/2003/cac/index.php
E-mail: dana @us.edu.pl

4 – 7 September 2003
Summer School on Polycrystalline Structure Determination by Direct Methods
Campanile Hotel, Krakow, Poland
http://www.us.edu.pl/uniwersytet/konferencje/2003/cac
E-mail: dana @us.edu.pl

7 – 9 September 2003
MECA-SENS, Stress Evaluation By Neutron and Synchrotron Radiation
Crawford House, Manchester, UK
http://www.mecasens.org/
E-mail: admin@mecasens.org

14 – 19 September 2003
Structure Solution from Powder Diffraction Data - SSPD'03
Congress Center Academia, Stara Lesna, Slovak Republic
http://www.sspd-03.sav.sk/
E-mail: Lubomir.Smrcok@savba.sk

Clinics at ICDD, Newton Square, Pennsylvania, USA.
26 – 30 April 2004
Practical X-ray Fluorescence Spectrometry
Covering basics of X-ray spectra, instrumentation design, methods of qualitative and quantitative analysis, specimen preparation, review of mathematical matrix correction procedures, applications for both wavelength and energy dispersive spectrometry and new developments in XRF.
7 – 11 June 2004
Fundamentals of X-ray Powder Diffraction
Covering instrumentation, specimen preparation, data acquisition, and qualitative phase analysis.
14 – 18 June 2004
Advanced Methods in X-ray Powder Diffraction
Emphasizing computer-based methods of data collection and interpretation, both for qualitative and quantitative phase analysis.
http://www.icdd.com/education/clinics/
E-mail: clinics@icdd.com

9 – 20 June 2004
Diversity amidst Similarity: a Multidisciplinary Approach to Polymorphs, Solvates and Phase Relationships: the 35th crystallographic course at the Ettore Majorana Centre
http://www.crystalerice.org/Erice2004/Diversity.htm
E-mail: Yoel@bgumail.bgu.ac.il

2 – 6 August 2004
The 53rd Denver X-ray Conference
Sheraton Steamboat Resort, Steamboat Springs, Colorado, USA
http://www.dxcicdd.com/04/
E-mail: flaherty@icdd.com
2 – 5 September 2004

EPDIC-9
Prague, Czech Republic
http://www.xray.cz/epdic/
E-mail: kuzel@karlov.mff.cuni.cz

23 – 31, August 2005
IUCr XX Congress and General Assembly of the International Union of Crystallography
Congress Citidal, Florence, Italy
http://www.iucr2005.it

1 – 4 September 2006
EPDIC-10
Geneva, Switzerland
E-mail: Radovan.Cerny@cryst.unige.ch

13 – 15 September 2006
European Congress on Residual Stresses,ECRS7
TU Berlin, Germany
http://www.ecrs7.de/
E-mail: Walter.Reimers@TU-Berlin.de

How to receive the IUCr CPD Newsletter

If you wish to be added to the mailing list for the Newsletter of the IUCr Commission on Powder Diffraction or have changed address, please contact the Chairman:
Robert Dinnebier (r.dinnebier@fkf.mpg.de).

The Newsletter can also be downloaded in electronic format, as a .pdf file, from the CPD web-site.

Companies

If you would like to advertise in this twice-yearly newsletter, please contact Robert Dinnebier
e-mail: r.dinnebier@fkf.mpg.de
Telephone: +49-711-689-1503
Fax: +49-711-689-1502

Call for contributions to the next CPD Newsletter (No 30)

The next issue of the CPD Newsletter will be edited by *Dr. C.R. Hubbard*, to appear in December 2003. Cam will greatly appreciate contributions from readers on matters of interest to the powder diffraction community, e.g. meeting reports, future meetings, developments in instruments, techniques, and news of general interest. Please contact him for sending articles and suggestions. Software developments can be directly addressed to *Lachlan Cranswick* or to the Editor of Newsletter No 30 (addresses are given below).

Dr C. R. Hubbard
Diffraction and Thermophysical Properties Group, MS 6064, Bldg 4515, High Temperature Materials Laboratory, Metals & Ceramics Division, Oak Ridge National Laboratory, Oak Ridge, TN 37831-6064
Telephone: 865-574-4472 | Fax: 865-574-3940
e-mail: hubbardcr@ornl.gov

Dr Lachlan M. D. Cranswick
Neutron Program for Materials Research (NPMR), National Research Council (NRC),
Building 459, Station 18, Chalk River Laboratories, Chalk River, Ontario, Canada, K0J 1J0
Telephone: (613) 584-8811 Fax: (613) 584-4040
e-mail: l.m.d.cranswick@dl.ac.uk
WWW: http://neutron.nrc-cnrc.gc.ca/

JUNE 2003 EDITION
OUT NOW!

No Internet access? No problem

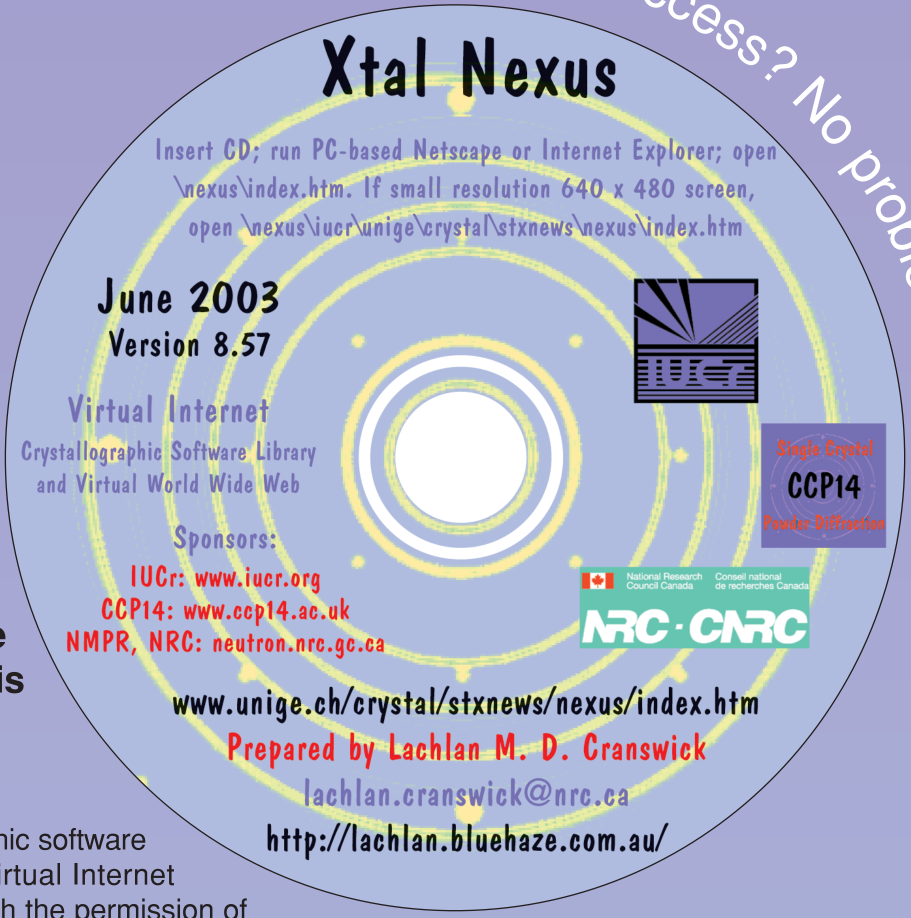

If you're working in the developing world and have limited or no access to the Internet, then the free Xtal Nexus CD-ROM is here to help.

Packed with a host of crystallographic software packages and resources, these virtual Internet CD-ROMs have been produced with the permission of software and website custodians. The organizer of the Nexus project, the IUCr Committee on Electronic Publishing, Dissemination and Storage of Information, invites academics and students using single-crystal, powder diffraction and other crystallographic analysis methods in developing countries that are isolated from the Internet to register their interest. The CD-ROMs are free of charge and available while stocks last.

The CD-ROM is sponsored by the IUCr, the EPSRC-funded Collaborative Computational Project No. 14 (CCP14) for Single Crystal and Powder Diffraction, and the Neutron Program for Materials Research of the National Research Council of Canada.

Contents

Multiple software packages and suites relevant to single-crystal, powder diffraction, crystallographic structure validation and crystallographic teaching, including

- single-crystal structure solution and refinement suites for PC
- crystallographic structure visualization programs
- powder diffraction pattern visualization, peak profiling and indexing software
- powder diffraction structure solution
- classic and modern crystallographic program source code
- Rietveld refinement packages
- structure validation and checking software
- powder pattern simulation and journal-quality structure plotting and photorealistic rendering programs
- educational websites dealing with crystallographic teaching
- webpage-based tutorials on how to use many of the programs within the CD-ROM
- part of the IUCr website including IUCr Commissions.

Send your request for a free Xtal Nexus CD-ROM (preferably via e-mail or by conventional mail) to

Lachlan M. D. Cranswick
NPMR, NRC
Building 459, Station 18
Chalk River Laboratories, Chalk River
Ontario, Canada, K0J 1J0

E-mail: lachlan.cranswick@nrc.gc.ca
Tel: +1 (613) 584-8811 ext. 3719
Fax: +1 (613) 584-4040
WWW: http://neutron.nrc.ca/

The CD-ROMs, and regular updates, will be sent by airmail.